

# The macro-eco-evolutionary interplay between dispersal, competition, and landscape structure in generating biodiversity

## Supplementary Materials

Hagen O      Viana SD      Wiegand T      Chase JM      Onstein RE

### Environment

We simulated 5 million years of environmental dynamics on four islands (A, B, C, and D), inspired by a realistic theoretical isolated island system in the Southern Hemisphere with a total area of 60x60 km<sup>2</sup> (cell area = 1 km<sup>2</sup> and timestep = 10,000 years), leading to 501 timesteps (Animation 1). We considered dynamic topography, minimum and maximum temperature variations combined with sea level changes, which intensified during the Quaternary (~last 2.6 Ma) with a periodicity of 100 ky (i.e., 10 timesteps) (Pillans, Chappell, and Naish 1998). This approximates Earth's eccentricity with a conservative periodicity (Shepard et al. 2018) and reflects interactions among global climate dynamics and changes in incoming solar radiation, likely influencing ecological and evolutionary patterns. We approximated empirical mean temperature and sea levels (Westerhold et al. 2020; Hoffmann and Sgrò 2011).

Temperature and sea level oscillated with similar periodicity and intensity, so that lower temperature periods matched with the periods of lowest sea levels (Figure 1 in the main article). Given the location on Earth, i.e., the Southern Hemisphere, the northern sides of each island were 2°C warmer than the southern sides and were smoothed with a focal function of mean 3x3 sites (raster package). We derived  $T_{min}$  and  $T_{max}$  fluctuations over time by decreasing 0.01°C for each meter increase in altitude (lapse rate 0.01°C/m). Minimum and maximum temperatures were drawn from site mean temperatures by respectively subtracting and adding absolute values from a normal distribution with mean = 0 and standard deviation  $SD = \frac{E_i}{\max(E)}$ . This means that the distance between  $T_{min}$  and  $T_{max}$  increases as site elevation  $E_i$  (m) increases. The lowest available elevation was -115 m, and the highest elevation was 803 m above sea level at the final timestep (i.e., 0 m). This resulted in temperature ranges of 0 to 5°C (Animation 1, Figure 2).

In all our simulations, we penalized connectivity through a cost multiplier of geographical distance, similarly to (Hagen et al. 2021). We used a cost of four (4) for unsuitable sites (i.e.,

below sea level) and 1 for suitable sites, with an additional 0.1 per 100 m slope difference between source and destination sites. Empirical evidence suggests that for high elevation species, greater elevation changes represent greater dispersal barriers, as mountain peaks are often embedded in a low elevation matrix, creating an island-like system (Vasconcelos et al. 2020). By choosing a strong matrix resistance of four, we emphasized the effects of topography, geodynamics, and sea-level changes.

Our simulations started with three islands (A, B, and C), which did not change in topography, and ended with four islands (A, B, C, and D) (Figure 1). Island A and B had their connectivity periodically increased due to a shallow land bridge that enhanced connectivity between these islands when sea levels were low (Figure 1, Figure 3, Figure 4), while island C remained relatively isolated regardless of sea level changes. Island D began appearing around 1.5 Ma due to topographic and sea level changes.

## Eco-evolutionary models

We build three models:

1. **M0** assumes fixed dispersal and competitive traits for all species within a simulation ( $n=2000$ ).
2. **ME** relaxes this assumption by allowing dispersal and competitive traits to evolve freely, resulting in divergent values over time between disconnected populations and different species ( $n=2000$ ).
3. **MET** introduces a linear trade-off between dispersal and competitive traits, ensuring that no super species (i.e.,  $d_i = 1, l_i = 1$ ) are possible ( $n=2000$ ).

In context, M0 serves as a reference model, facilitating the exploration of parameter ranges and sensitivity tests. The two alternative simulation scenarios, ME and MET, referred to as counterfactuals, investigate the effects of manipulating different components of the model. Specifically, these counterfactuals involve modifying the underlying biological model concerning the evolution and trade-offs between dispersal and competitive abilities. Consequently, species within a simulation not only diverge in their temperature optima  $T_i$  and niche width  $\omega_i$  (applicable for M0, ME, and MET), but also in dispersal  $d_i$  and competitive  $l_i$  traits (applicable for ME and MET). For each counterfactual, we conducted 2000 simulations with the same parameters for all models. This systematic exploration of alternative scenarios allowed us to assess the impact of specific model parameters on resulting biodiversity patterns.

## Initial conditions

All models (M0, ME, and MET) were initiated at 5 Ma with three species, each with populations distributed across the suitable sites of each island (i.e., sp1 on island A, sp2 on island B,

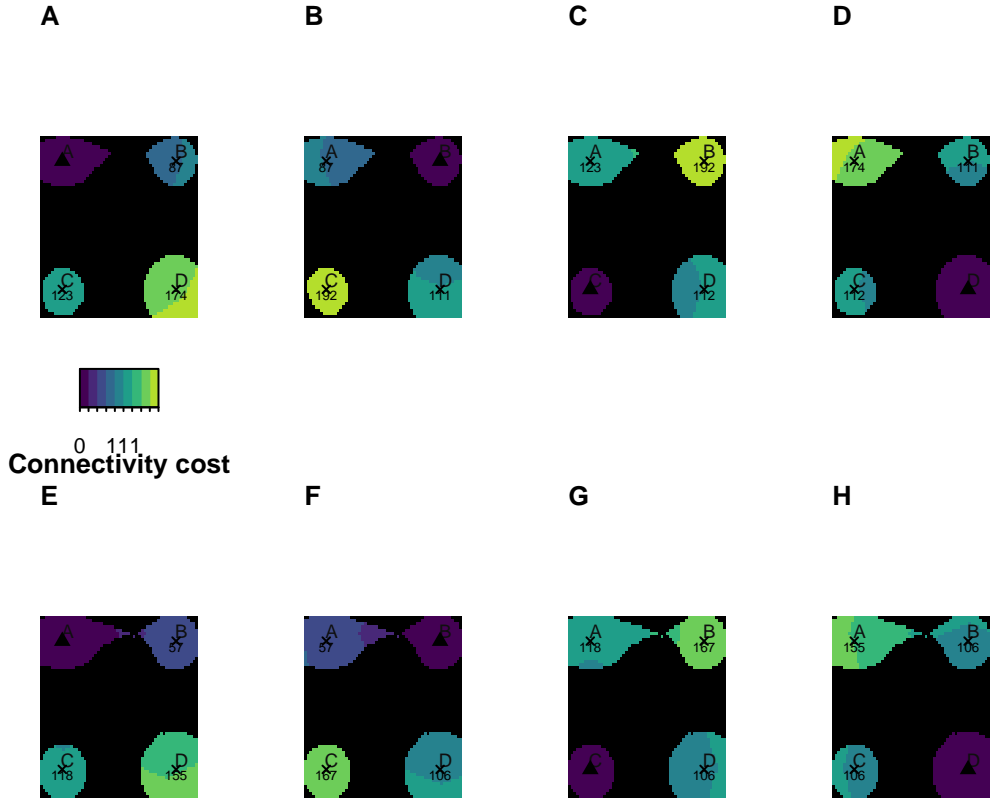


Figure 1: Connectivity costs in reference to the center of each island (i.e. A,B,C and D) for two timesteps, i.e. Present (0 Ma, resp. A,B,C and D) and for 130'000 years ago (0.13 Ma, resp. E,F,G and H). Note the changes in connectivity due to sea level changes between the present and the lowest seal level period (i.e. 0.13 Ma).

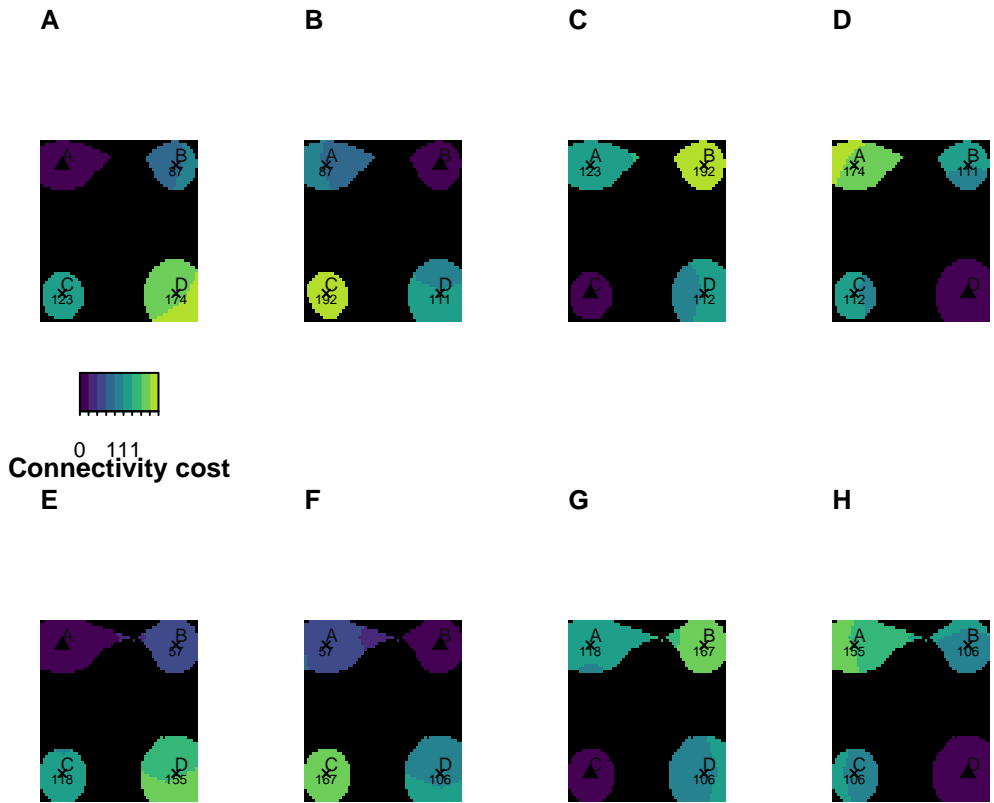


Figure 2: Connectivity costs in reference to the center of each island (i.e. A,B,C and D) for two timesteps, i.e. Present (0 Ma, resp. A,B,C and D) and for 130'000 years ago (0.13 Ma, resp. E,F,G and H). Note the changes in connectivity due to sea level changes between the present and the lowest seal level period (i.e. 0.13 Ma).

and sp3 on island C). Initial populations had a thermal range  $\omega_i = 0.4$  and a thermal optimum equal to the local mean temperature  $T_i = T_{mean}$ .

We conducted a full factorial experiment ranging from extreme dispersal and competitive abilities,  $d_i = [0-1]$  and  $l_i = [0.9-1]$ , with a fixed  $\Theta_s = 65$  (Figure 3). For the MET model, we imposed the trade-off assuming the same parameters as the other models, ensuring no initial species had inconsistently high values (i.e. physiologically implausible main Figure 2C). We randomized the seed at this stage so that each simulation could be reproduced.

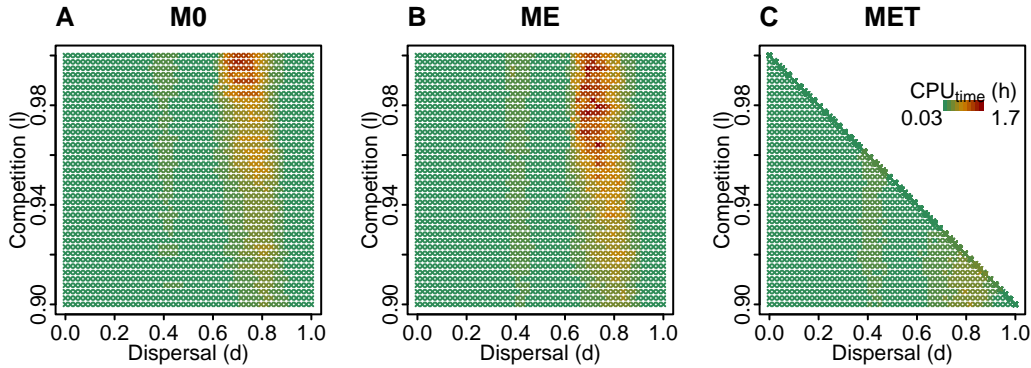


Figure 3: Initial competition and dispersal parameters for the main models and experiments. Colors show the CPU time per simulation ( $n=6000$ ).

## Dispersal

Frequencies of dispersal are given according to a Weibull function that has scale changed by  $d$  resulting in concentrated short range dispersal events for small  $d$  with increasingly larger and longer tails for larger  $d$  (Figure 4).

## Ecological equilibrium

Ecological equilibrium was assumed for every site and at every timestep. Environmental fitness was determined by considering the minimum and maximum temperatures. Population size  $N_i$  changes according to local site conditions (i.e.,  $T_{min}, T_{max}$  [9 to 26°C]) and the evolving species temperature optimum  $T_i$  and thermal range  $\omega_i$ , based on the geometric mean of a Gaussian environmental function at minimum and maximum site temperatures (for an example, see Figure 5).

Relative growth rate decreases linearly with conspecific population size  $N_i$  in the site, with a conspecific interaction coefficient  $\alpha_{ff}$  and a heterospecific interaction coefficient  $\alpha_{fh}$ . The conspecific interaction coefficient was fixed for all simulations (i.e.,  $\alpha_{ff} = 0.2$ ), as our focus was on components of interspecific competition, modulated through the heterospecific tolerance

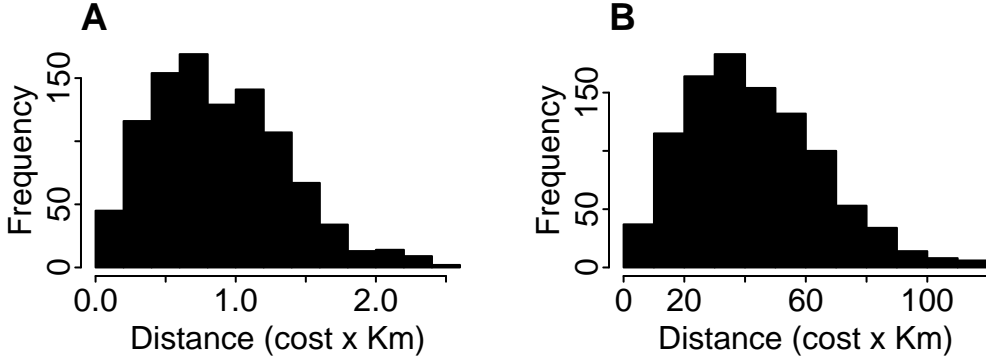


Figure 4: Histogram showing two extreme frequencies of 1000 dispersal events in a weibull distribution with shape of 2 and scale of 1 (A) and 50 (B). Note the difference of the x axis scales.

trait ( $l$ ). For an example, see the interactions between three (3) and thirteen (13) species through ODE (i.e., 30 interactions) in our Lotka-Volterra model type (Figure 6 AB and C, respectively).

### Equilibrium equations

We want to estimate the equilibrium of our Lotka-Volterra model that describes the dynamics of a focal species  $f$  in a given site, depending on other heterospecific species  $k$  :

$$\frac{dN_f}{dt} \frac{1}{N_f} = r_f - \alpha_{ff} N_f - \alpha_{fh} \sum_{k \neq f} N_k \quad (1)$$

with parameters  $r_f$ ,  $\alpha_{ff}$  and  $\alpha_{fh}$ . We first estimate the carrying capacity of a local population of species  $f$  (that is the equilibrium for the case  $\alpha_{fh} = 0$ ), that is given by  $N_f = r_f / \alpha_{ff}$  and by inserting the site-condition dependency of the maximal per capita growth rate  $r_f$  from equation 2 we obtain

$$K_f = \frac{r_f}{\alpha_{ff}} = \frac{g}{\alpha_{ff}} \times \sqrt{n_f(T_{min}) \times n_f(T_{max})} \quad (2)$$

The total population size of all species in the site is given by  $J = \sum_{i=1}^S N_i$  where  $S$  is the total number of species in the site. Assuming zero-sum dynamics, which emerges if there is density dependence at the individual scale (e.g., through crowding competition), the number of heterospecifics at the site is given in good approximation by  $\sum_{i \neq f} N_i = J - N_f$ . Thus, equation 1 in equilibrium simplifies to

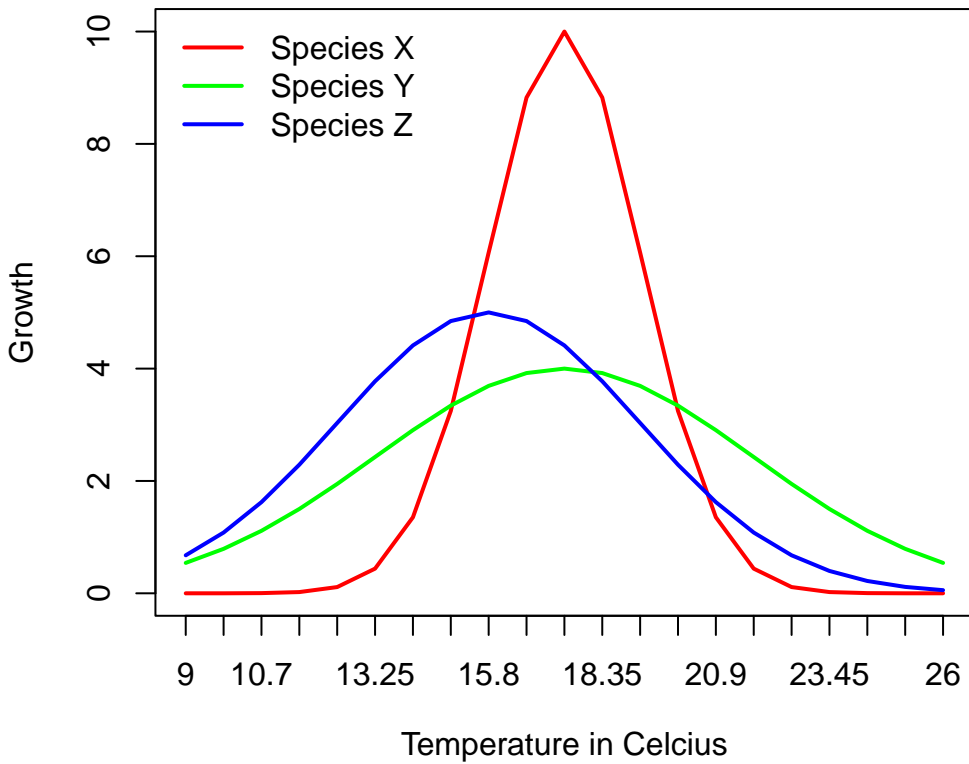


Figure 5: Population growth across a temperature gradient in °C for three different species with varying thermal optimum ( $T$ ) and thermal range ( $\omega$ ) traits. Species X (dark red) has  $T=18^\circ\text{C}$  and  $\omega=0.1$ ; Species Y (green) has  $T=18$  and  $\omega=0.25$ ; Species Z (blue) has  $T=16$  and  $\omega=0.2$ . Temperature-dependent growth is applied a constant and equal rate to all simulations. Maximal growth is proportional to the geometric mean of the fitness of the focal species at the minimal and maximal temperature in the site.

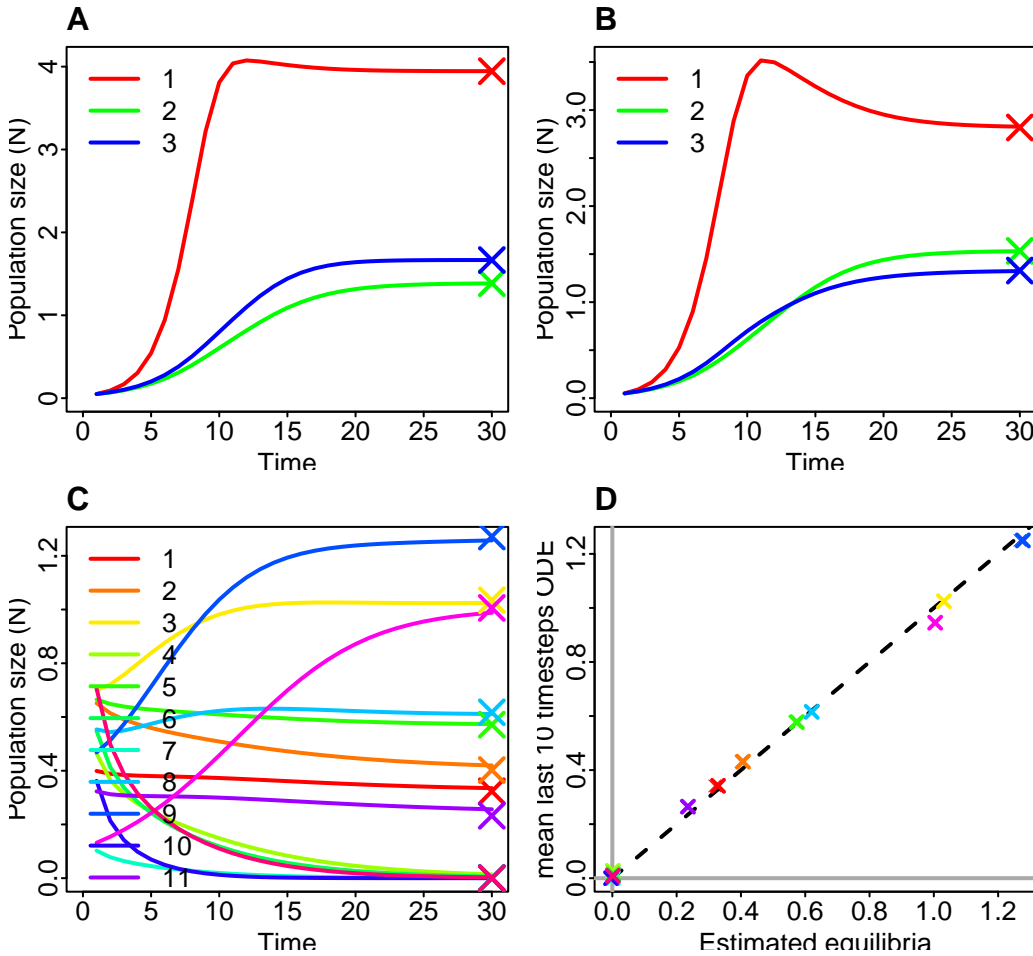


Figure 6: Local dynamics within 10'000 years showing population size changes for different communities (ABC) and comparison of mean last 10 timesteps of the ODE against estimated equilibria (D). Crosses show the estimated ecological equilibria. (A) Species 1 and 2 have a thermal optimum closer to the thermal optimum between site min and maximal temperatures than species 3. Moreover, species 1, 2 and 3 have thermal range of  $\omega_1 = 0.1, \omega_2 = 0.25, \omega_3 = 0.2$  and same heterospecific tolerance ( $l=0.98$ ). (B) we change heterospecific tolerance to ( $l_1 = 0.9, l_2 = 0.98, l_3 = 0.96$ ). (C) Random community of 13 species. (D) Comparison of mean last 10 timesteps of ODE of community in (C) against estimated equilibria; grey lines show zero lines and dashed line show the 1-1 line. Note that we use here only 30 interactions though time and we increase in precision by increasing the number of interactions (ODE timesteps) and decreasing the number of coexisting species.

$$0 = r_f - \alpha_{ff}N_f^* + \alpha_{fh}N_f^* - \alpha_{fh}J \quad (3)$$

which leads to  $r_f - \alpha_{fh}J = (\alpha_{ff} - \alpha_{fh})N_f^*$ , which yields the equilibrium

$$N_f^* = \frac{r_f - \alpha_{fh}J}{\alpha_{ff} - \alpha_{fh}} \quad (4)$$

Thus, besides the condition that  $\alpha_{ff} > \alpha_{fh}$  (i.e. the conspecific interaction coefficient is larger than the heterospecific interaction coefficient), feasibility (i.e., a positive equilibrium  $N_f^*$ ) requires that

$$\alpha_{fh}J < r_f \quad (5)$$

which also means that heterospecific competition must be sufficiently small to allow population growth at low populations sizes (this is the so called invasion criterion). Note that we obtain from equation 5, for small abundances of the focal species f the per-capita population growth rate  $\frac{dN_f}{dt} \frac{1}{N_f} = r_f - \alpha_{fh}J$ , which is positive if equation 5 is satisfied. As explained in detail in Wiegand et al. (2021), the total population size J in one site at equilibrium can be then be estimated as

$$J = \frac{\sum_{f=1}^S \frac{\alpha_{ff}K_f}{\alpha_{ff} - \alpha_{fh}}}{(1 + \sum_{f=1}^S \frac{\alpha_{fh}}{\alpha_{ff} - \alpha_{fh}})} \quad (6)$$

In the special case where the interaction coefficients are the same for all species (as in our M0 model), we can derive a more detailed condition for the per capita population growth rates  $r_f = \alpha_{ff}K_f$  to obtain positive abundances. In this case the community size J of the community in equilibrium can be estimated as

$$J = \frac{S \frac{1}{\alpha_{ff}\alpha_{fh}}}{(1 + S \frac{\alpha_{fh}}{\alpha_{ff} - \alpha_{fh}})} \frac{1}{S} \sum_{f=1}^S r_f \quad (7)$$

and with  $\bar{r}_f = \frac{1}{S} \sum_{f=1}^S r_f$  being the community average maximal per capita population growth rate we find together with equation 4 the feasibility condition.

$$\frac{r_f}{\bar{r}_f} > \frac{S\alpha_{fh}}{\alpha_{ff} + \alpha_{fh}(S-1)} = \mu \quad (8)$$

The factor  $\mu$  is always smaller than one and particularly small if the number of species (S) and the heterospecific interaction coefficient  $\alpha_{fh}$  are small. It approaches a value of one if the species richness S becomes large and/or if heterospecific competition  $\alpha_{fh}$  approaches the

strength of conspecific competition  $\alpha_{ff}$ . Equation 8 defines a minimum value for the growth rate  $r_f$  to allow for a positive equilibrium. Equation 8 thus tells us that a species will go extinct in a given site (i.e. having a negative equilibrium abundance) if its maximal per capita population growth rate  $r_f$  is too small, compared to the average per capita population growth rate  $\bar{r}_f$  of all species at the site. Importantly, the environmental conditions, leading to lower growth rate  $r_f$ , can be poorer if there are fewer species at the site and/or if heterospecific competition is weaker.

To estimate equilibrium in the context of competition dynamics, we implement an iterative approach. Firstly, all species in a site are checked to determine if  $a_{ff} > \bar{a}_{ff}$  (condition 1, eq. 4). If not, the species is removed from consideration as conspecifics compete weaker than heterospecifics. Next, the carrying capacity ( $J^*$ ) is estimated based on the values of  $K_f, a_{ff}, a_{fh}$  for each species  $f$  (eq. 6). Then, all species are checked again to see if the product of the intraspecific competition coefficient and carrying capacity is greater than the product of the interspecific competition coefficient  $a_{ff}K > a_{fh}J^*$  (condition 2, eq. 4). Species that do not meet this condition, indicating a too low carrying capacity, are removed, and the estimation process returns estimating  $J^*$  (eq. 6). This is repeated until all remaining species satisfy the condition 2. Finally, the equilibrium of each species  $N_f^*$  is estimated using equations 4 and 6 (Figure 6).

## Summary statistics

We conducted several statistics using custom and code from several R-packages [Kembel et al. (2010)](Bortolussi et al. 2006)(Castiglione et al. 2021), specifically,  $\log_{10}(\bar{\alpha})$ : Log 10 of mean alpha diversity (all sites) at final timestep.  $\overline{occup}$   $Km^2$ : Mean regional occupancy calculated in Km<sup>2</sup> according to the mean number of sites occupied by all species through time. *Occupancychange*: Proportion of occupancy change during the simulation.  $\frac{Slope\ dispersal}{T_{start}/T_{end}}$ : Rate of change in dispersal trait over time.  $Dispersal(d)_{t_{start}}$ : Dispersal trait value at the initial timestep.  $\phi$ : Speciation threshold or time of isolation until reproductive isolation occurs.  $l_{t_{start}}$ : Competition trait value at the initial timestep. *Extinction prop.*: Proportion of extinction events in a simulation over final gamma diversity. *Speciation prop.*: Proportion of speciation events in a simulation over final gamma diversity.  $\gamma$ : Final gamma diversity, or final regional taxonomic richness (number of species alive at the last timestep). *Turnover*: Turnover between speciation and extinction. *Speciation invar.*: Temporal speciation invariability. *Extinction invar.*: Temporal extinction invariability. *Turnover invar.*: Temporal turnover invariability.  $\bar{N}_{5\% t_{end}}$ : Mean population size of its 5% quantile at final timestep.  $\bar{N}_{50\% t_{end}}$ : Mean population size at final timestep.  $\bar{N}_{95\% t_{end}}$ : Mean population size of its 95% quantile at final timestep.  $\bar{PD}_\alpha$ : The Mean Faith's Phylogenetic Diversity at the site level.  $\bar{\alpha}$ : Mean alpha diversity of the entire archipelago.  $\beta\%$ : Proportional species turnover.  $\beta W$ : Whittaker beta diversity. *Zeta zeta*: Proportion of species that are common to all assemblages. *Eta eta*: Proportion of species that are not unique to an assemblage nor common

to all assemblages. *Theta theta*: Species that are unique to an assemblage.  $PD_S$ : Standardized value of the unrooted Phylogenetic Diversity measure for species.  $MPD_S$ : Standardized value of the Mean Pairwise Distance measure.  $MNTD_S$ : Standardized value of the mean nearest taxon distance measure.  $CD_{X-Y}$ : Standardized Community Distance between two locations. *Mode d*: Number of modes at the dispersal trait distribution at final timestep.  $\bar{d}_{50\% t_{end}}$ : Mean dispersal trait at final timestep.  $\bar{T}_{50\% t_{end}}$ : Mean thermal optimum trait at final timestep.  $\bar{\omega}_{50\% t_{end}}$ : Mean thermal range trait at final timestep.  $\bar{l}_{50\% t_{end}}$ : Mean tolerance to other species trait at final timestep. *Spread d t<sub>end</sub>*: The range between the lowest and highest dispersal trait values at the final timestep.  $\beta_{max \text{ split}}$ : The complete phylogenetic beta value derived from the Maximum Likelihood estimation within the Beta-splitting model. Additional recorded values include: *Finished*: Status of final simulation, if OK, simulation was finished. *CPU time (h)*: CPU time in hours for simulation.

## M0

M0 diversity statistics reflected our expectations on general patterns of diversity, such as the highest speciation rates at intermediate diversity levels (Figure 7). This indicates that peaks of  $\gamma$  diversity relate to the spatial structure of our landscape. We found that all speciation events in simulations with dispersal  $d_i < 0.1$  occurred within islands and mostly during the dynamic phase (Figure 16 A). Speciation within islands was only observed in M0, as dispersal in ME and MET quickly evolved beyond the critical threshold. We also observed qualitative changes in speciation events for intermediate dispersal  $d_i = [0.15 - 0.55]$ , which began involving speciation events between islands C and D (Figure 16 C).

Investigating spatial dynamics for M0 during 4.5-0 Ma (Figure 17 A-D) shows that mean occupancy increases with dispersal, while changes leave scale signatures and show that proportional change (i.e.,  $\frac{(increase-decrease)}{total\ occupancy}$ ) decreases with competition. In contrast, neutral models have a higher proportional increase/decrease ratio. Moreover, we can see that this signature was stronger during the dynamic stage of these simulations (Figure 17 I-L).

Inspecting the community distances between all the islands, there is a clear effect of increased community diversity with island distance and dispersal ability (Figure 14). As expected, competition tends to decrease community distance overall, where communities reach maximum diversity. The combination of community distances between islands A, B, C, and D is depicted for M0 in Figure 15. Each line corresponds to simulations with the same competitive value. Community distance represents the standardized value of community distance, akin to the beta diversity version of the Mean Pairwise Distance (MPD), which provides the average phylogenetic distance between two communities.

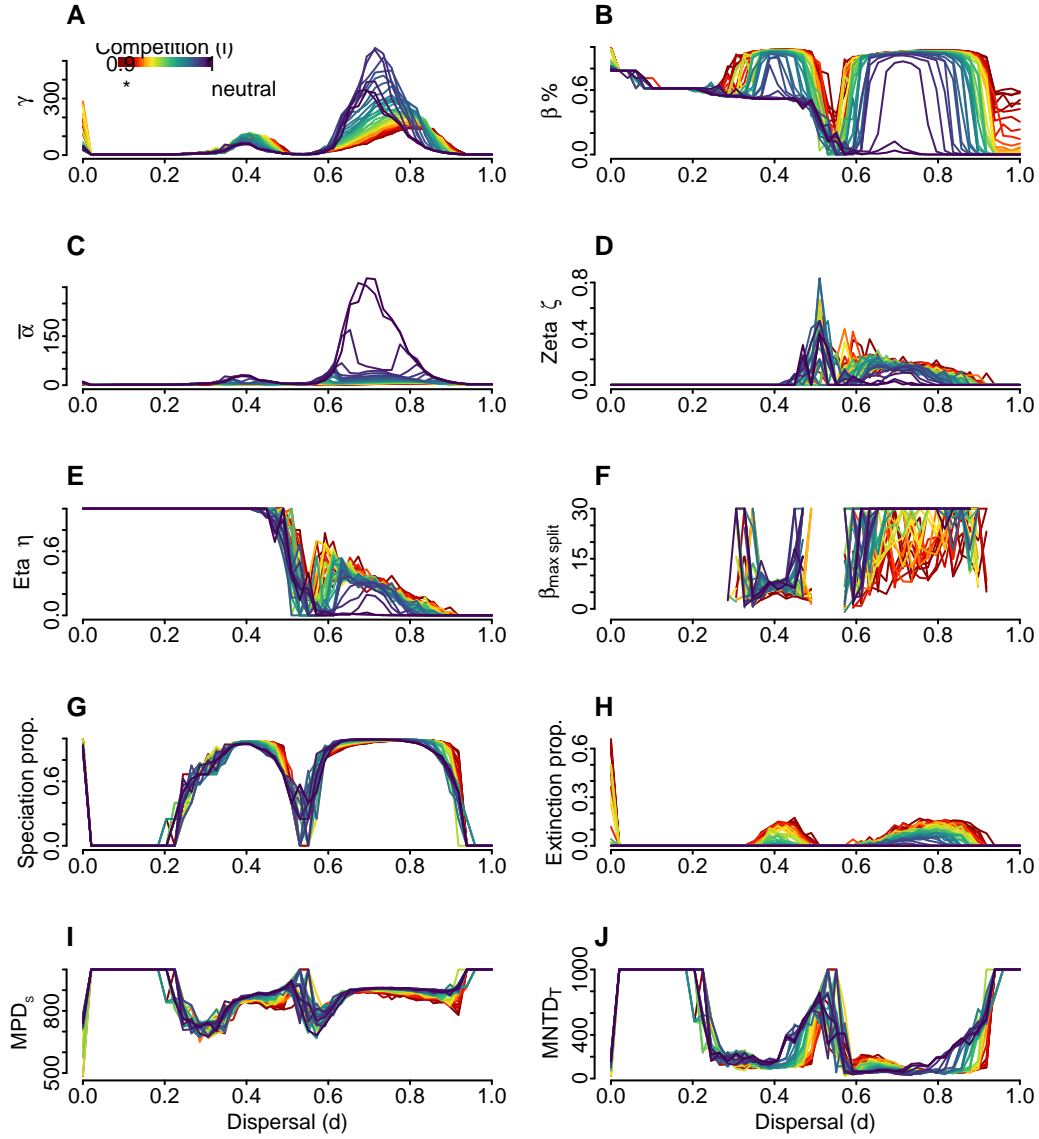


Figure 7: Summary statistics for M0 through dispersal. Each line corresponds to simulation within a same competitive value along dispersal ability at the initial timestep. (A) Final gamma diversity, or final regional taxonomic richness (number of species alive at the last timestep). (B) Proportional species turnover, i.e.  $1 - \text{mean}(\alpha/\gamma)$  quantifies what proportion of the species diversity in the dataset that is not contained in an average site (C) Mean alpha diversity of the entire archipelago. (D) Proportion of species that are common to all assemblages. Zeta diversity sensu Hui and McGeoch (2014). (E) Proportion of species that are not unique to an assemblage nor common to all assemblages. (F) The complete phylogenetic beta value derived from the Maximum Likelihood estimation within the Beta-splitting model. This is computed using the `maxlik.betasplit` function from the `apTreeshape` package. (G) Proportion of speciation events in a simulation over final gamma diversity. (H) Proportion of extinction events in a simulation over final gamma diversity. (I) Standardized value of the Mean Pairwise Distance measure on the archipelago, calculated using the `mpd` function from the `picante` package. (J) Standardized value of the mean nearest taxon distance measure for the entire archipelago.

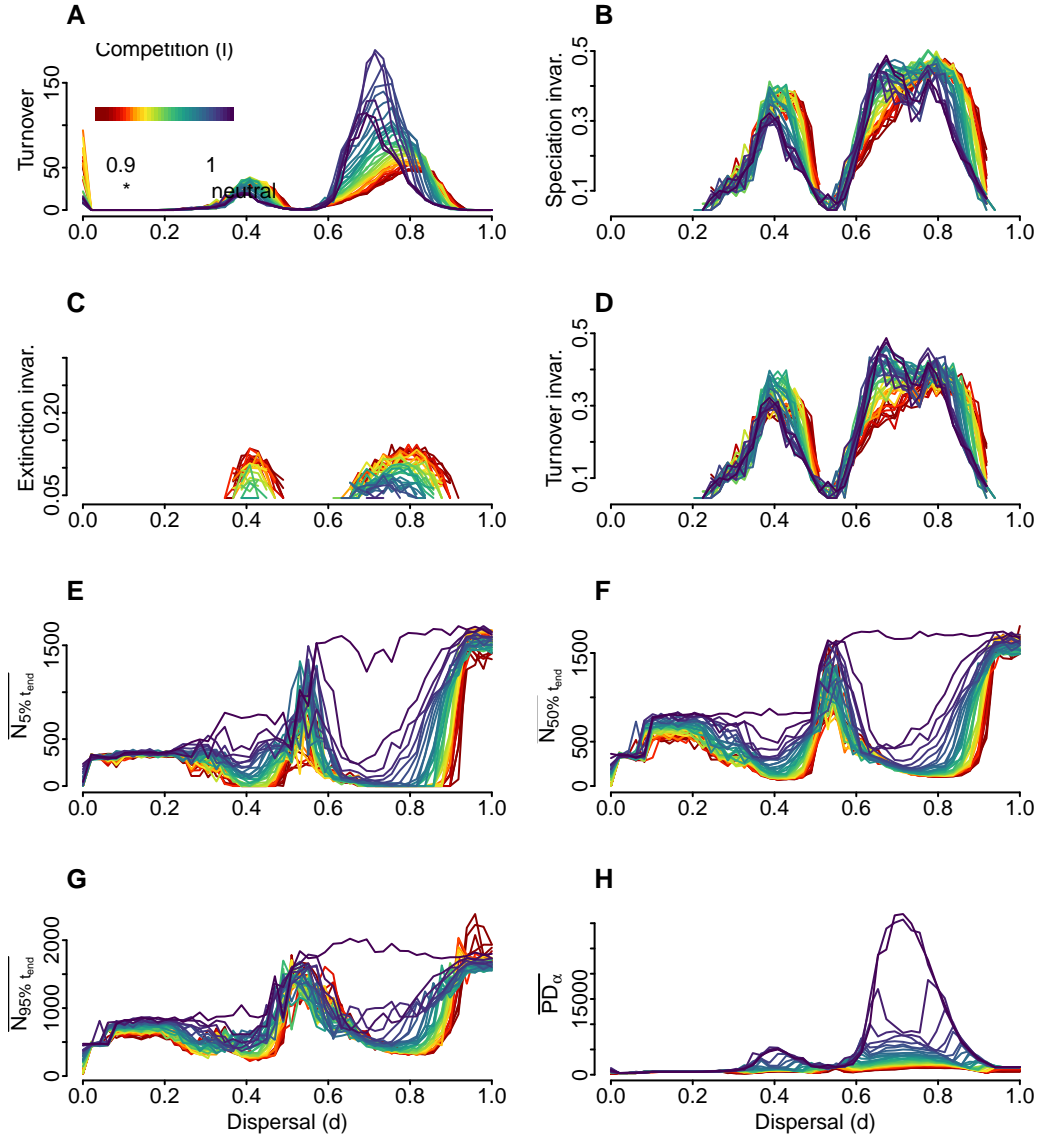


Figure 8: Additional summary statistics for M0 though initial dispersal values. Each line corresponds to simulations within a same competitive value, along dispersal ability. (A) Turnover between speciation and extinction. I.e. the sum of speciation - extinction for all timesteps divided by the number of initial species. (B) Temporal speciation invariability, also referred to as temporal stability of speciation events. (C) Temporal extinction invariability, also referred to as temporal stability of extinction events. (D) Temporal turnover invariability, also referred to as temporal turnover stability. (E) Mean population size of its 5% quantile at final timestep. (F) Mean population size at final timestep. (G) Mean population size of its 95% quantile at final timestep. (H) The Mean Faith's Phylogenetic Diversity (PD) at the site level, quantifies the total branch lengths and was calculated with the function PD from the picante package.

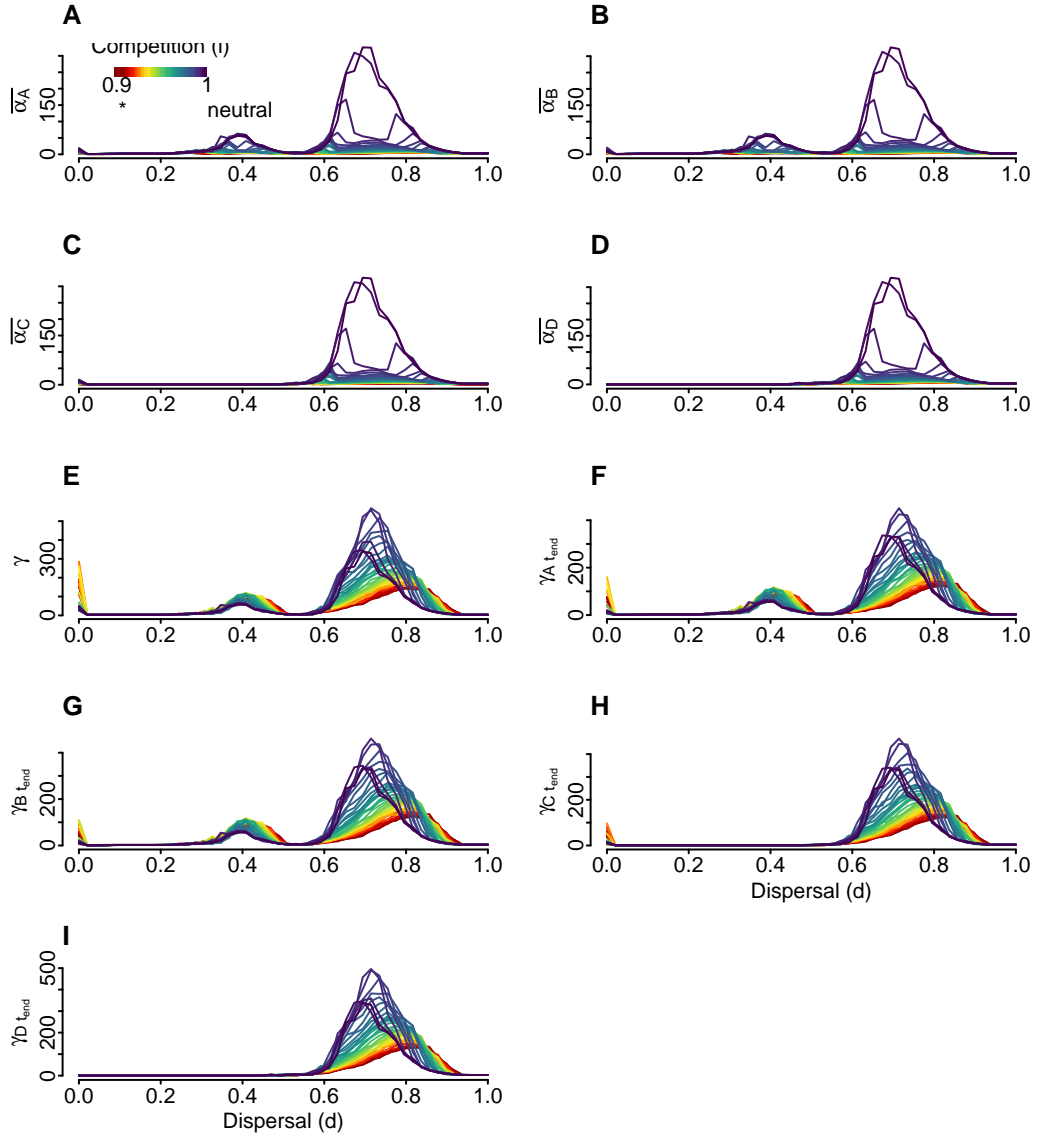


Figure 9: Additional summary statistics for M0 though initial dispersal values. Each line corresponds to simulations within a same competitive value, along dispersal ability. (A) Mean alpha diversity of sites on island A. (B) Mean alpha diversity of sites on island B. (C) Mean alpha diversity of sites on island C. (D) Mean alpha diversity of sites on island D. (E) Final gamma diversity, or final regional taxonomic richness (number of species alive at the last timestep). (F) Final gamma diversity of island A, or final regional taxonomic richness (number of species alive at the last timestep). (G) Final gamma diversity of island B. (H) Final gamma diversity of island C. (I) Final gamma diversity of island D.

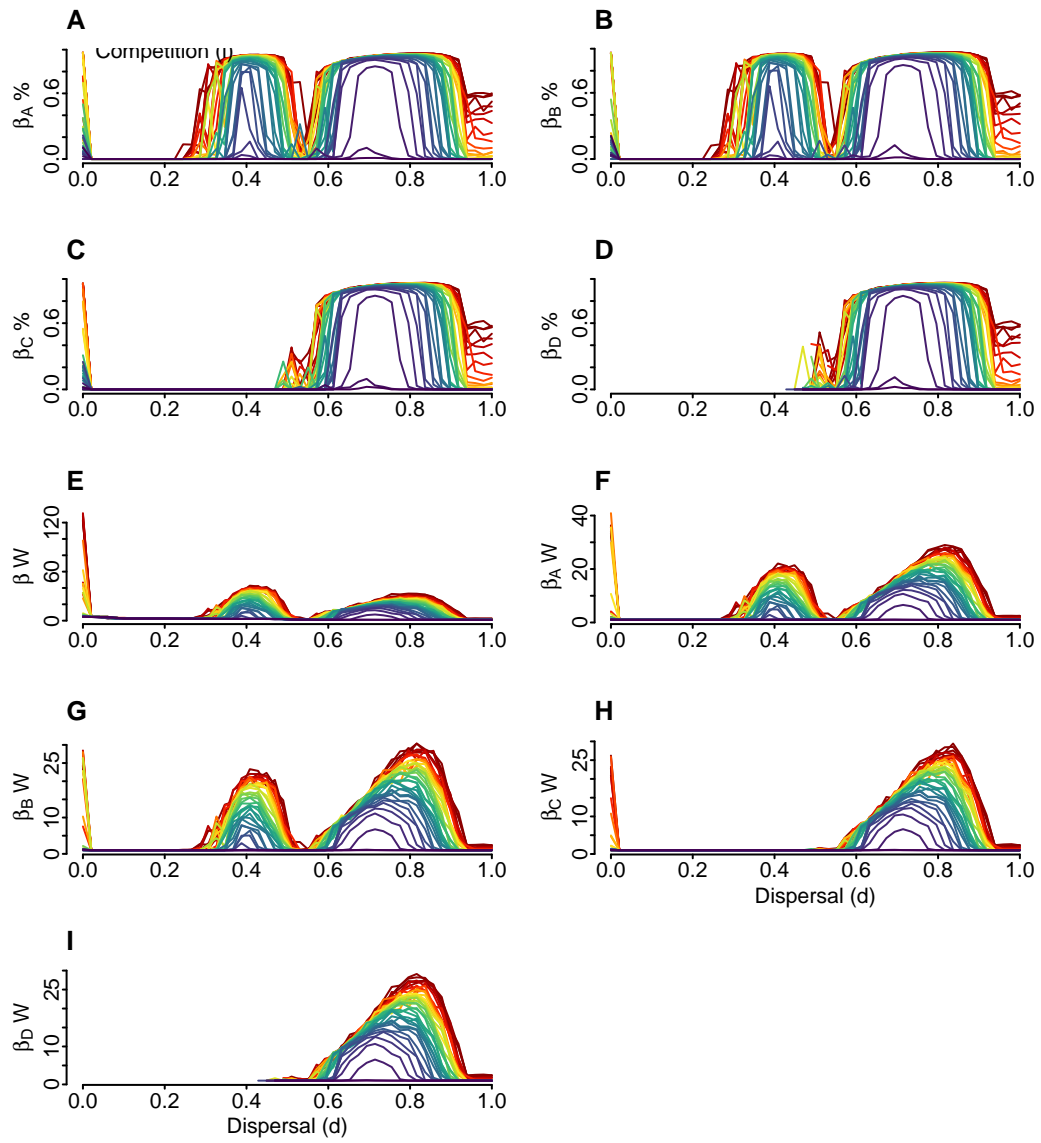


Figure 10: Additional summary statistics for M0 though initial dispersal values. Each line corresponds to simulations within a same competitive value, along dispersal ability. (A) Proportional species turnover in island A. (B) Proportional species turnover in island B. (C) Proportional species turnover in island C. (D) Proportional species turnover in island D. (E) Whittaker beta diversity, i.e. gamma/mean(alpha), how many subunits there would be if the total species diversity of the mean species diversity per subunit remained the same, but the subunits shared no species. (F) Whittaker beta diversity of island A. (G) Whittaker beta diversity of island B. (H) Whittaker beta diversity of island C. (I) Whittaker beta diversity of island D.

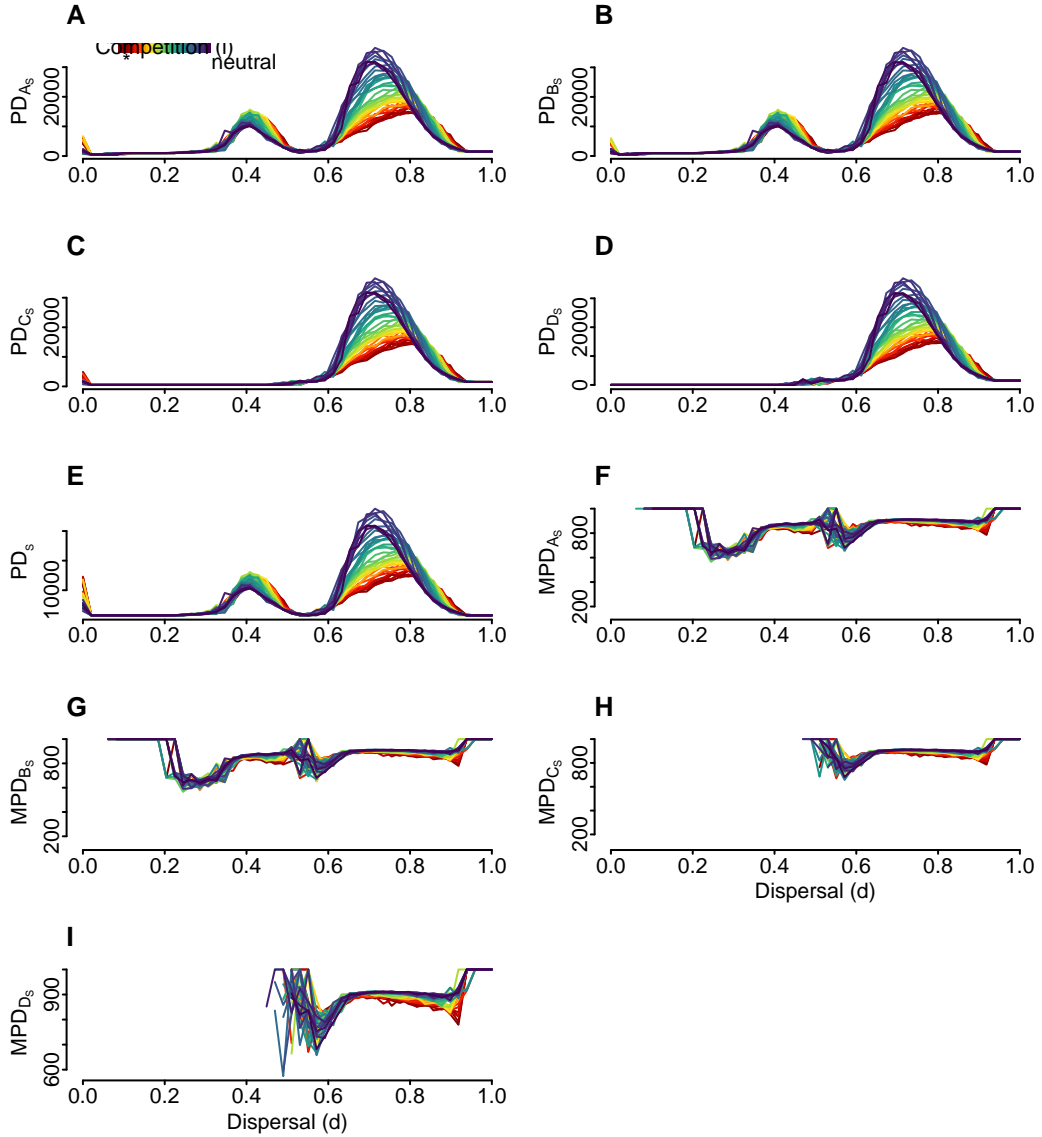


Figure 11: Additional summary statistics for M0 though initial dispersal values. Each line corresponds to simulations within a same competitive value, along dispersal ability. (A) Standardized value of the unrooted Phylogenetic Diversity measure for species in island A. (B) Standardized value of the unrooted Phylogenetic Diversity measure for species in island B. (C) Standardized value of the unrooted Phylogenetic Diversity measure for species in island C. (D) Standardized value of the unrooted Phylogenetic Diversity measure for species in island D. (E) Standardized value of the unrooted Phylogenetic Diversity measure for species on the archipelago, calculated using the `pd` function from the `picante` package. (F) Standardized value of the Mean Pairwise Distance measure in island A. (G) Standardized value of the Mean Pairwise Distance measure in island B. (H) Standardized value of the Mean Pairwise Distance measure in island C. (I) Standardized value of the Mean Pairwise Distance measure in island D.

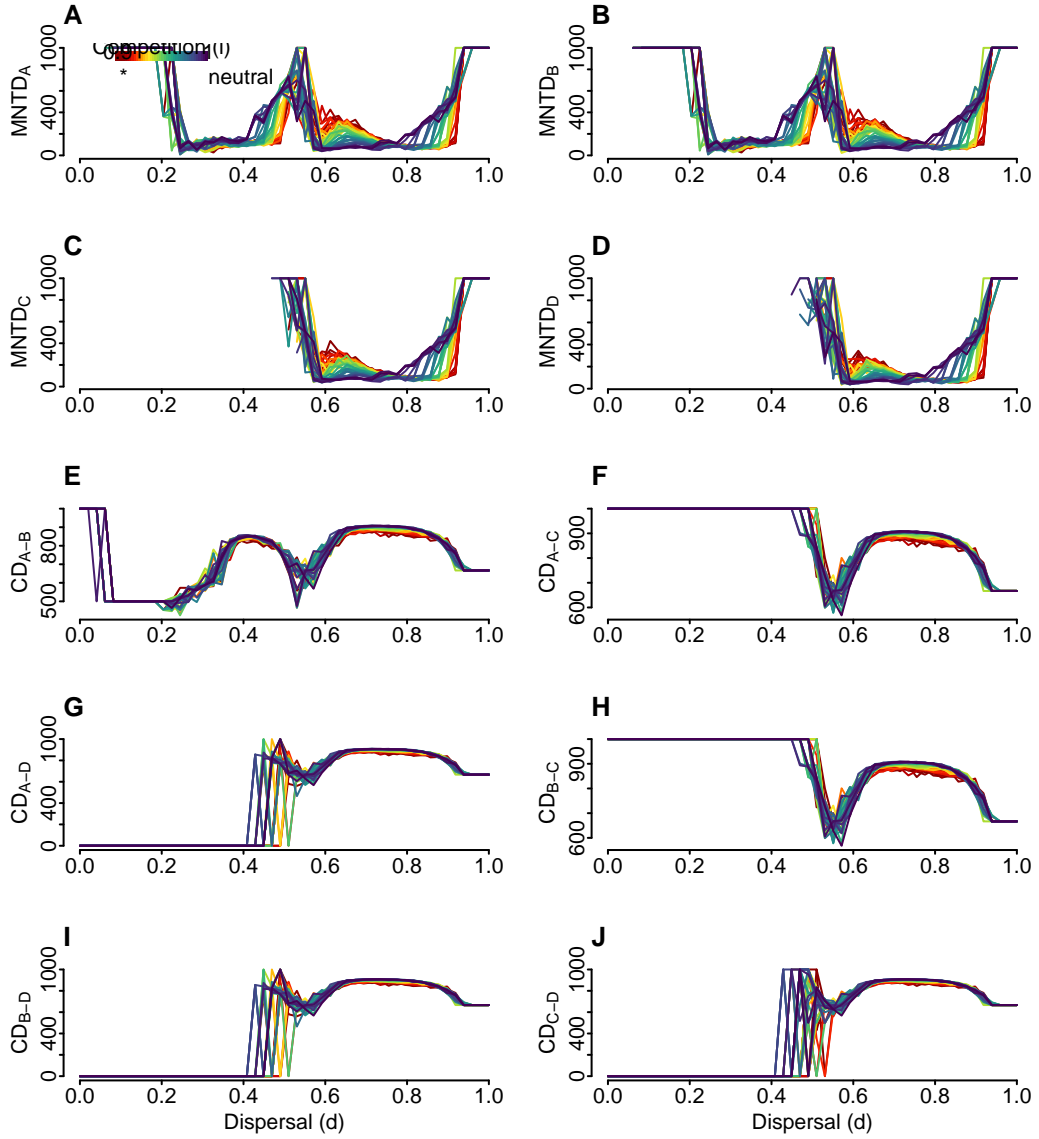


Figure 12: Additional summary statistics for M0 though initial dispersal values. Each line corresponds to simulations within a same competitive value, along dispersal ability. (A) Standardized value of the mean nearest taxon distance measure for the island A. (B) Standardized value of the mean nearest taxon distance measure for the island B. (C) Standardized value of the mean nearest taxon distance measure for the island C. (D) Standardized value of the mean nearest taxon distance measure for the island D. (E) Standardized Community Distance between island A and B. It is the beta diversity version of Mean Pairwise Distance (MPD), giving the average phylogenetic distance between two communities. (F) Standardized Community Distance between island A and C. (G) Standardized Community Distance between island A and D. (H) Standardized Community Distance between island B and C. (I) Standardized Community Distance between island B and D. (J) Standardized Community Distance between island C and D.

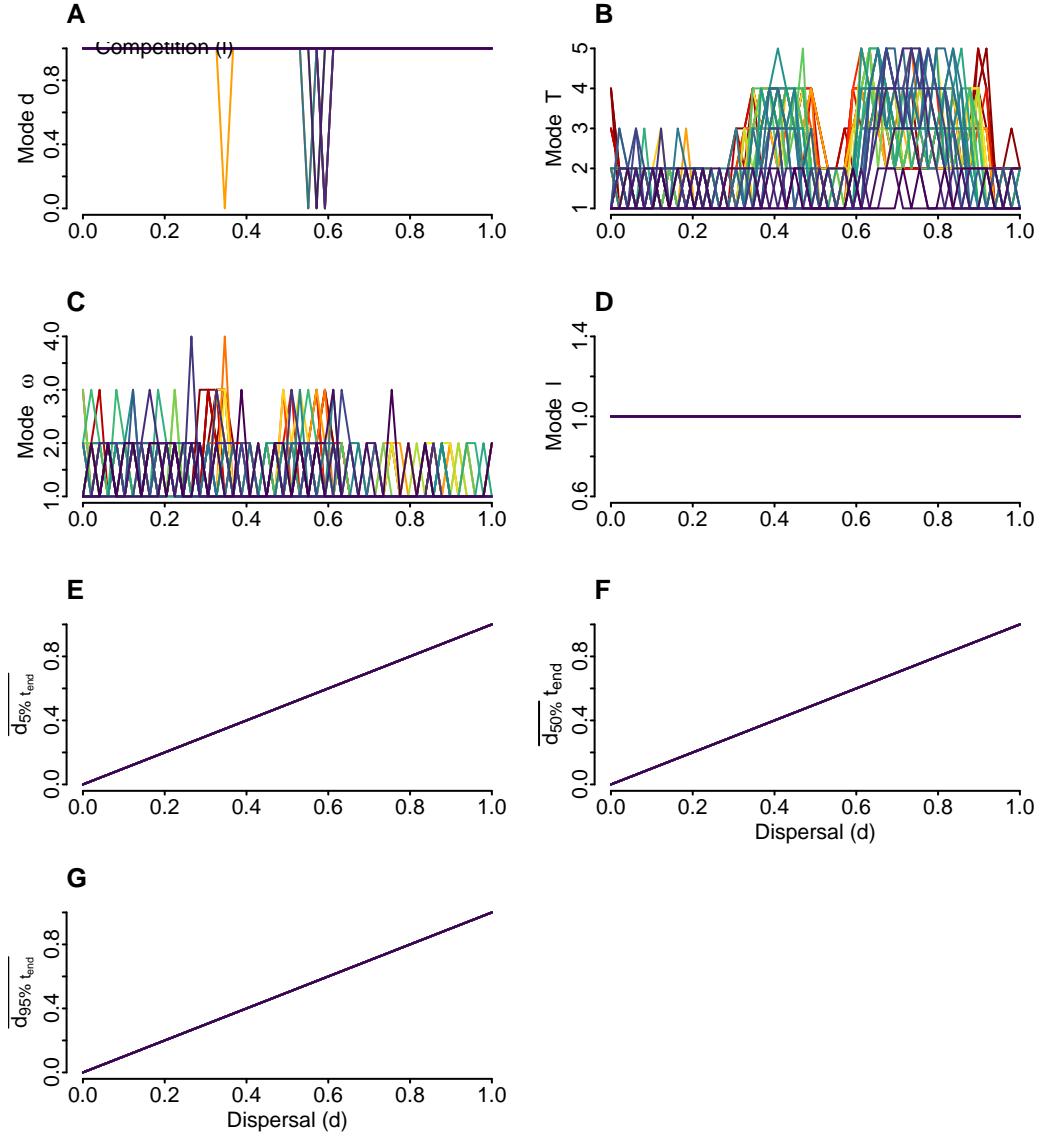


Figure 13: Additional summary statistics for M0 though initial dispersal values. Each line corresponds to simulations within a same competitive value, along dispersal ability. (A) Number of modes at the dispersal trait distribution at final timestep, i.e. no modes (such as in a uniform distribution), or more. Calculated with the function ‘Mode’ from package LaplacesDemon. (B) Number of modes at the thermal optimum distribution at final timestep. (C) Number of modes at the thermal range trait distribution at final timestep. (D) Number of modes at the competition trait (i.e. tolerance to other species) distribution at final timestep. (E) Mean dispersal trait of its 5% quantile at final timestep. (F) Mean dispersal trait at final timestep. (G) Mean dispersal trait of its 95% quantile at final timestep.

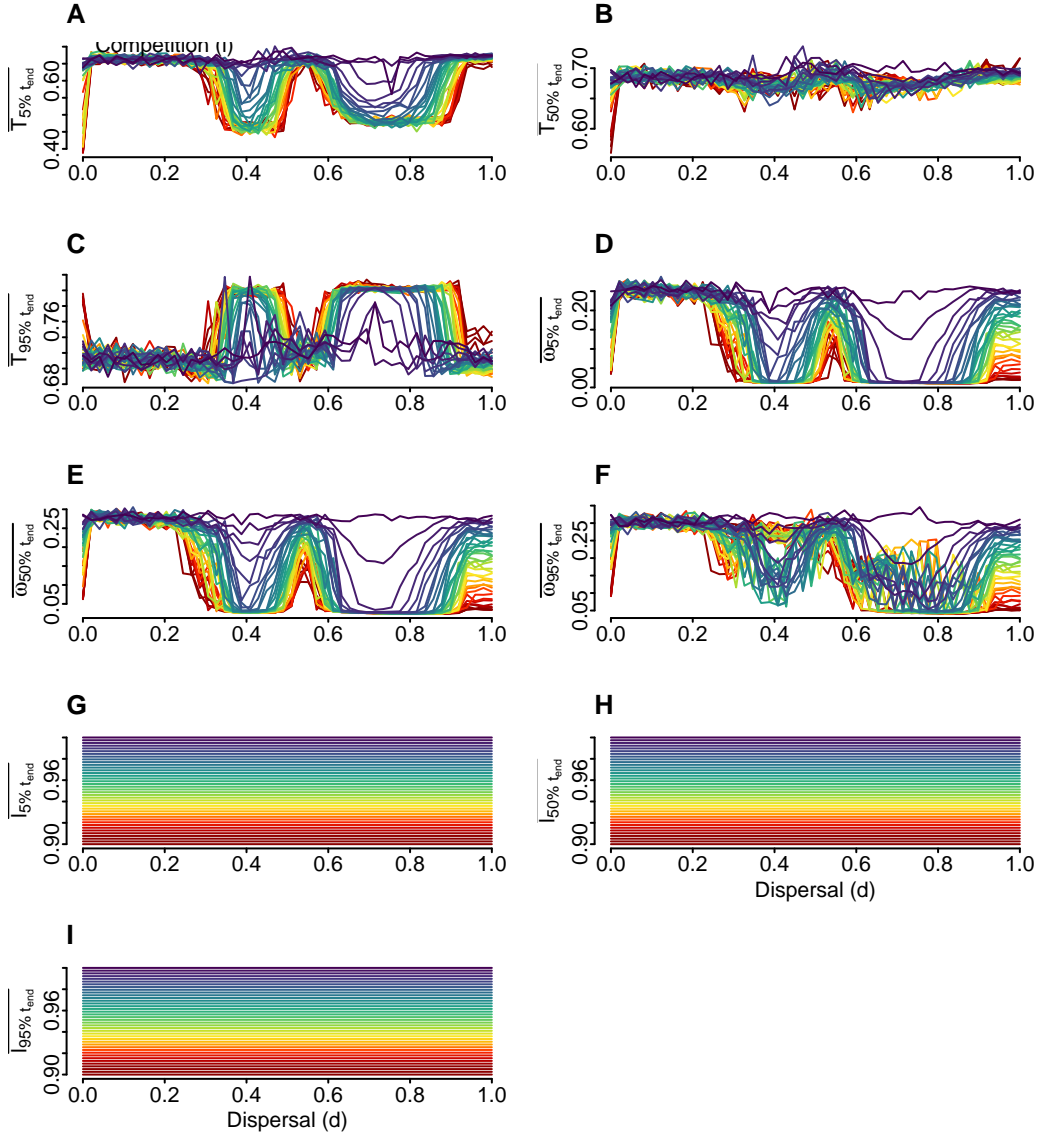


Figure 14: Additional summary statistics for M0 though initial dispersal values. Each line corresponds to simulations within a same competitive value, along dispersal ability. (A) Mean thermal optimum of its 5% quantile at final timestep. (B) Mean thermal optimum at final timestep. (C) Mean thermal optimum of its 95% quantile at final timestep. (D) Mean thermal range trait of its 5% quantile at final timestep. (E) Mean thermal range trait at final timestep. (F) Mean thermal range trait of its 95% quantile at final timestep. (G) Mean tolerance to other species trait of its 5% quantile at final timestep. (H) Mean tolerance to other species trait at final timestep. (I) Mean tolerance to other species trait of its 95% quantile at final timestep.

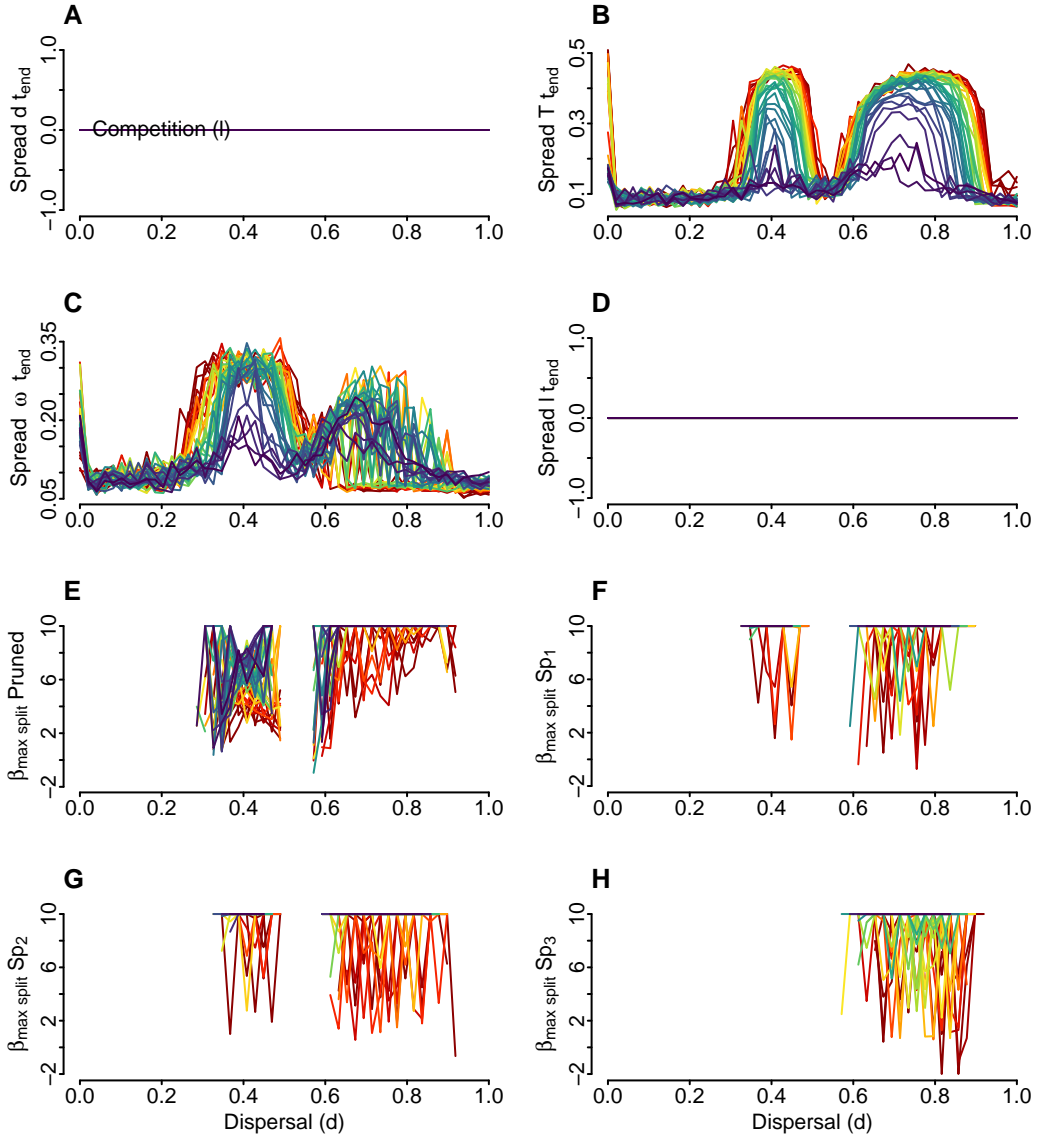


Figure 15: Additional summary statistics for M0 though initial dispersal values. Each line corresponds to simulations within a same competitive value, along dispersal ability. (A) The range between the lowest and highest dispersal trait values at the final timestep. (B) The range between the lowest and highest thermal optimum values at the final timestep. (C) The range between the lowest and highest thermal range trait values at the final timestep. (D) The range between the lowest and highest tolerance to other species trait values at the final timestep. (E) The pruned phylogeny beta value, excluding extinct branches, derived from the Maximum Likelihood estimation within the Beta-splitting model. (F) The pruned phylogeny beta value of species 1, excluding extinct branches. (G) The pruned phylogeny beta value of species 2, excluding extinct branches. (H) The pruned phylogeny beta value of species 3, excluding extinct branches.

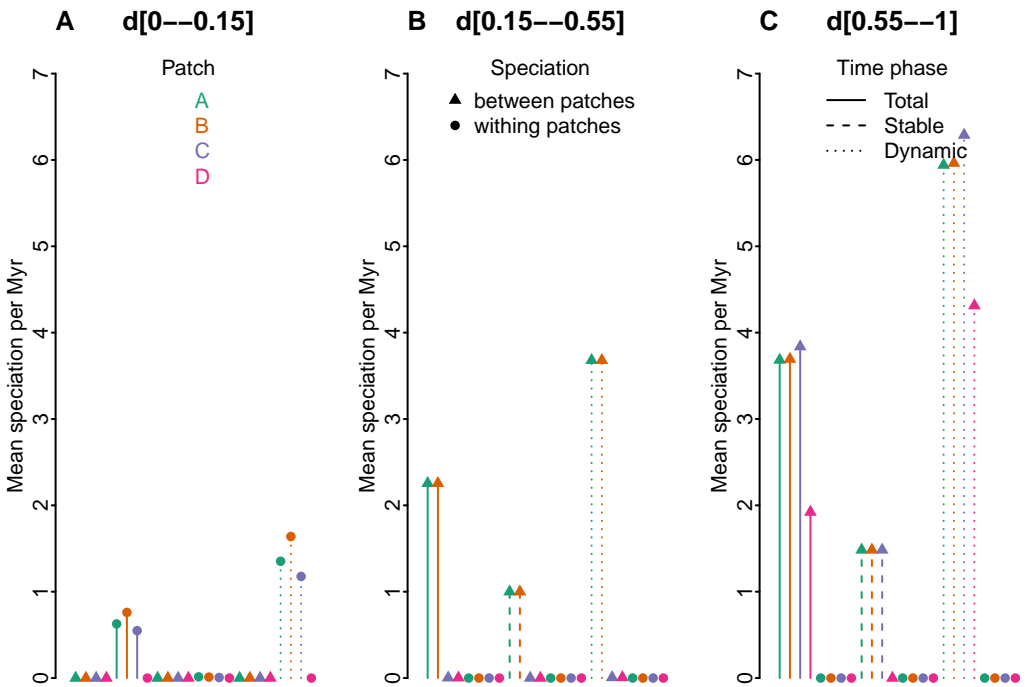


Figure 16: Mean speciation percentage for M0 with dispersal (A) smaller than, 0.15; (B) between 0.15 and 0.55; and (C) bigger than 0.55. We show for each island (in different colors) and each phase (i.e. Total 4.5-0Ma, Stable 4.5-2.5Ma, Dynamic 2-0Ma) for speciation events between or within islands (respectively triangles and circles).

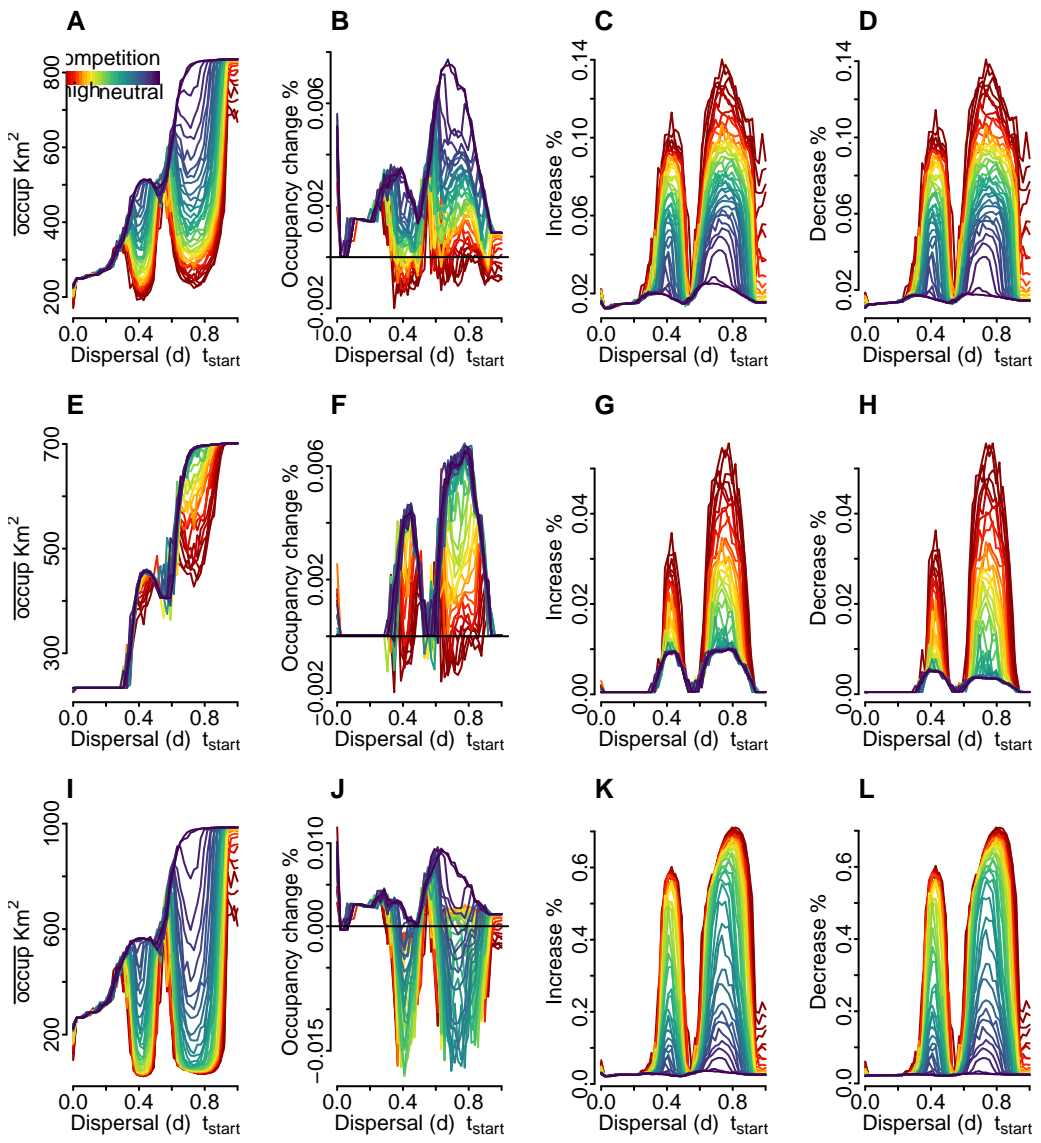


Figure 17: Spatial dynamics of M0 from 4.5 to 0 Ma (A-D), Stability from 4.5 to 2.5 Ma (E-H), and Dynamism from 2 to 0 Ma (I-L). Figures show the mean occupancy, proportional occupancy, and changes in isolated proportional increase and decrease of the number of occupied sites per species.

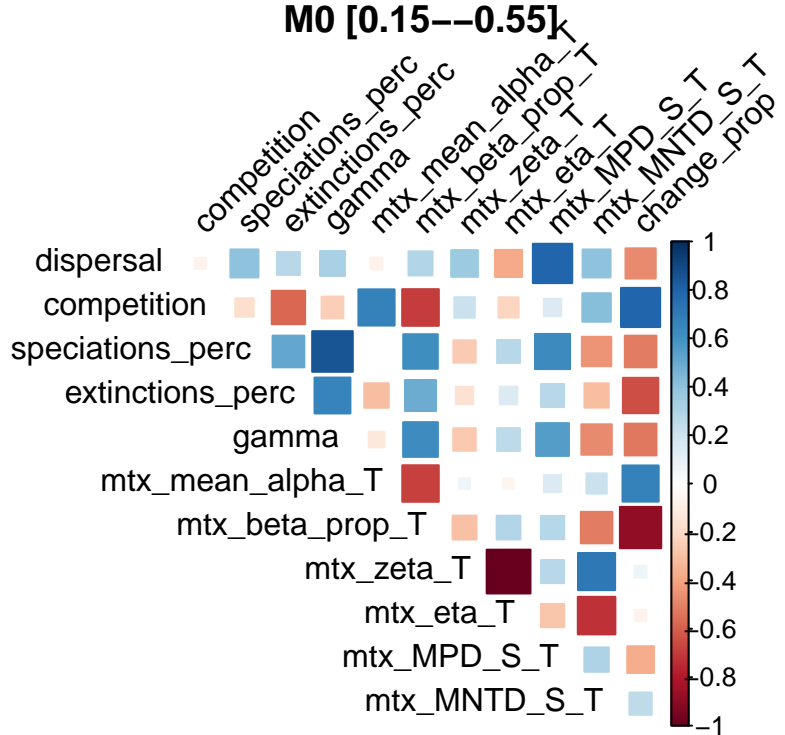
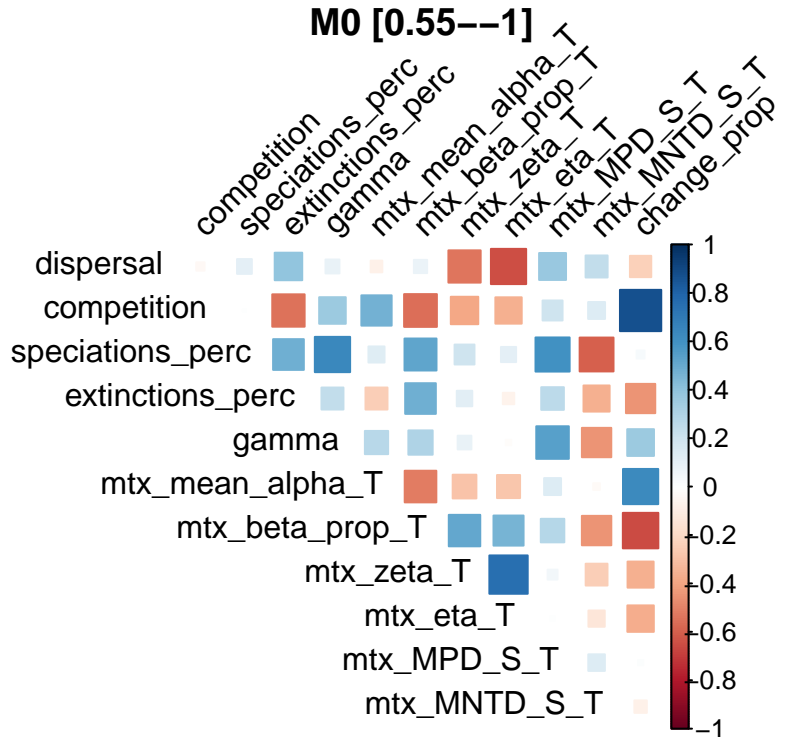
**A****B**

Figure 18: Correlations for hand-picked summary statistics for M0 for different intervals of dispersal distance 0.15-0.55 (A) and 0.55-1 (B).

## ME

Figure Figure 19 captures the evolving spatial patterns and occupancy dynamics of species from 4.5 million years ago (Ma) to the present. This visualization portrays a period of stability between 4.5 and 2.5 Ma, followed by a phase of significant change from 2 to 0 Ma, elucidating the evolutionary trajectory of species occupancy over millennia.

Figure Figure 20 delves into the intricate correlations between selected summary statistics across various dispersal distance intervals. This analysis sheds light on the complex interplay between dispersal, competition, and landscape structure.

Furthermore, Figure 21, along with Figure 22, Figure 23, Figure 24, Figure 25, Figure 26, Figure 27, Figure 28 and Figure 29 present multiple statistical summaries along initial dispersal trait values. The depiction of competition is nuanced, with simulation regimes delineated by unique lines within the same initial competitive grouping, offering a comprehensive overview of the dispersal, competitive, and landscape structure behind biodiversity dynamics.

## MET

Figure Figure 30 captures the evolving spatial patterns and occupancy dynamics of species from 4.5 million years ago (Ma) to the present. This visualization portrays a period of stability between 4.5 and 2.5 Ma, followed by a phase of significant change from 2 to 0 Ma, elucidating the evolutionary trajectory of species occupancy over millennia.

Figure Figure 31 delves into the intricate correlations between selected summary statistics across various dispersal distance intervals. This analysis sheds light on the complex interplay between dispersal, competition, and landscape in molding the geographical distribution of species.

Furthermore, Figure 32, along with Figure 33, Figure 34, Figure 35, Figure 36, Figure 37, Figure 38, Figure 39 and Figure 40 present multiple statistical summaries along initial dispersal trait values. The depiction of competition is nuanced, with simulations regimes delineated by unique lines within the same initial competitive grouping, offering a comprehensive overview of the dispersal, competitive and landscape structure behind biodiversity dynamics.

## Models Comparison

The correlation coefficients between the summary statistics and the mean final trait values for each model (M0, ME, MET) show how traits and species numbers are interrelated and vary across models ( Figure 41 ). M0 Model had a positive correlation (0.35) between final richness  $\gamma$  and dispersal, indicating that an increase in dispersal trait values is associated with a higher number of species. The number of species and thermal range trait ( $\omega$ ) had negative correlation (-0.56), suggesting that wider temperature tolerance is associated with a

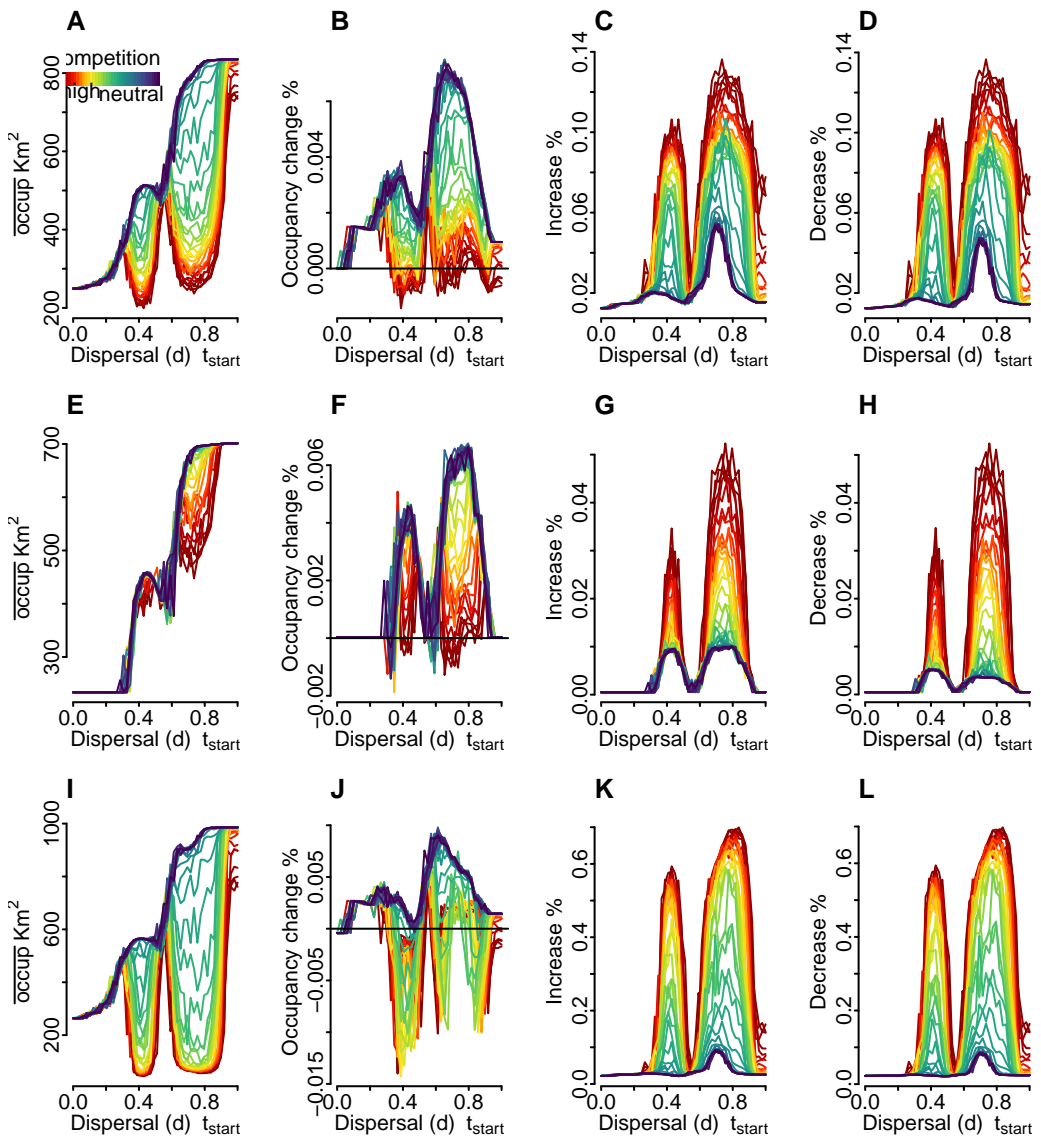


Figure 19: Spatial dynamics of ME from 4.5 to 0 Ma (A-D), Stability from 4.5 to 2.5 Ma (E-H), and Dynamism from 2 to 0 Ma (I-L). Figures show the mean occupancy, proportional occupancy, and changes in isolated proportional increase and decrease of the number of occupied sites per species.

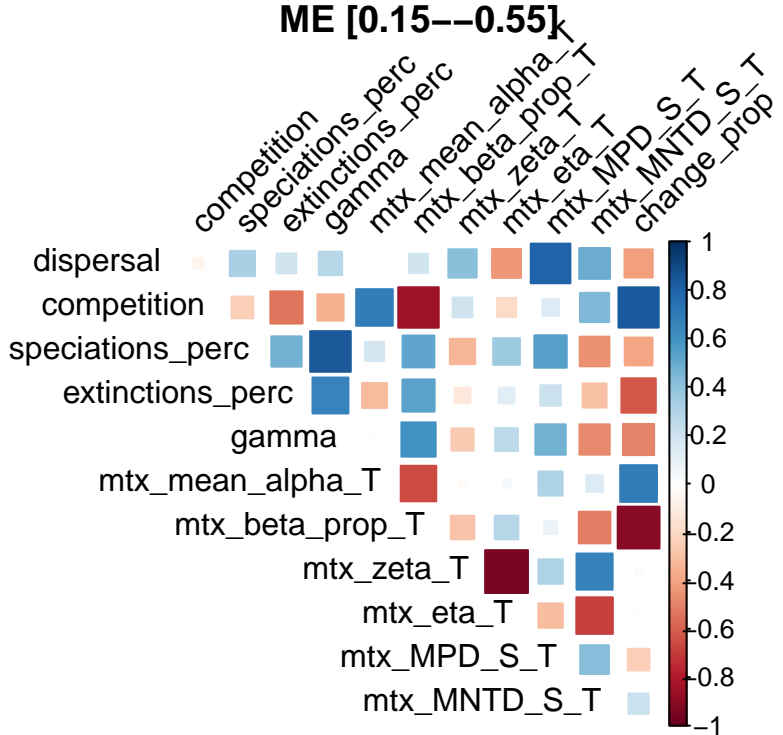
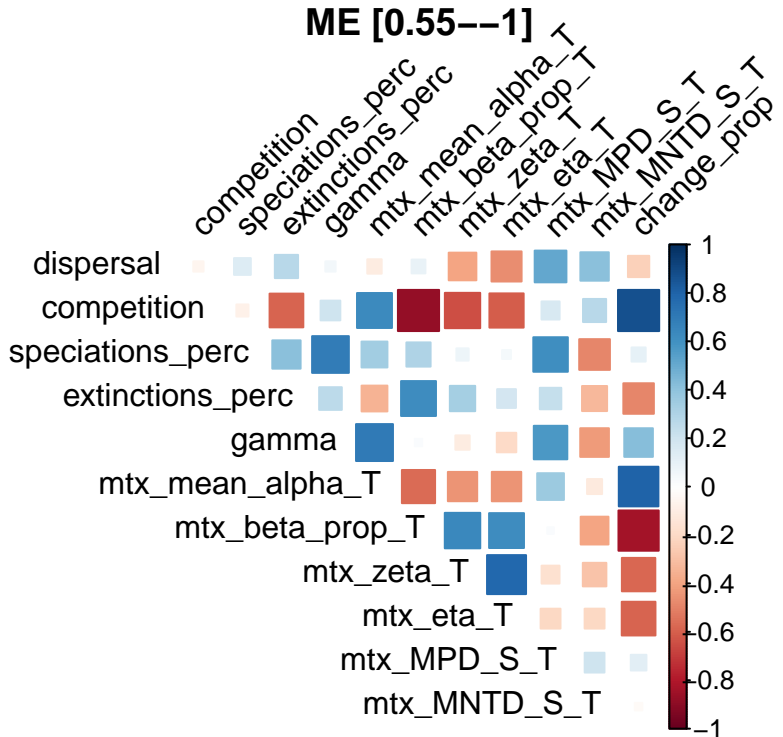
**A****B**

Figure 20: Correlations for hand-picked summary statistics for ME for different intervals of dispersal distance 0.15-0.55 (A) and 0.55-1 (B).

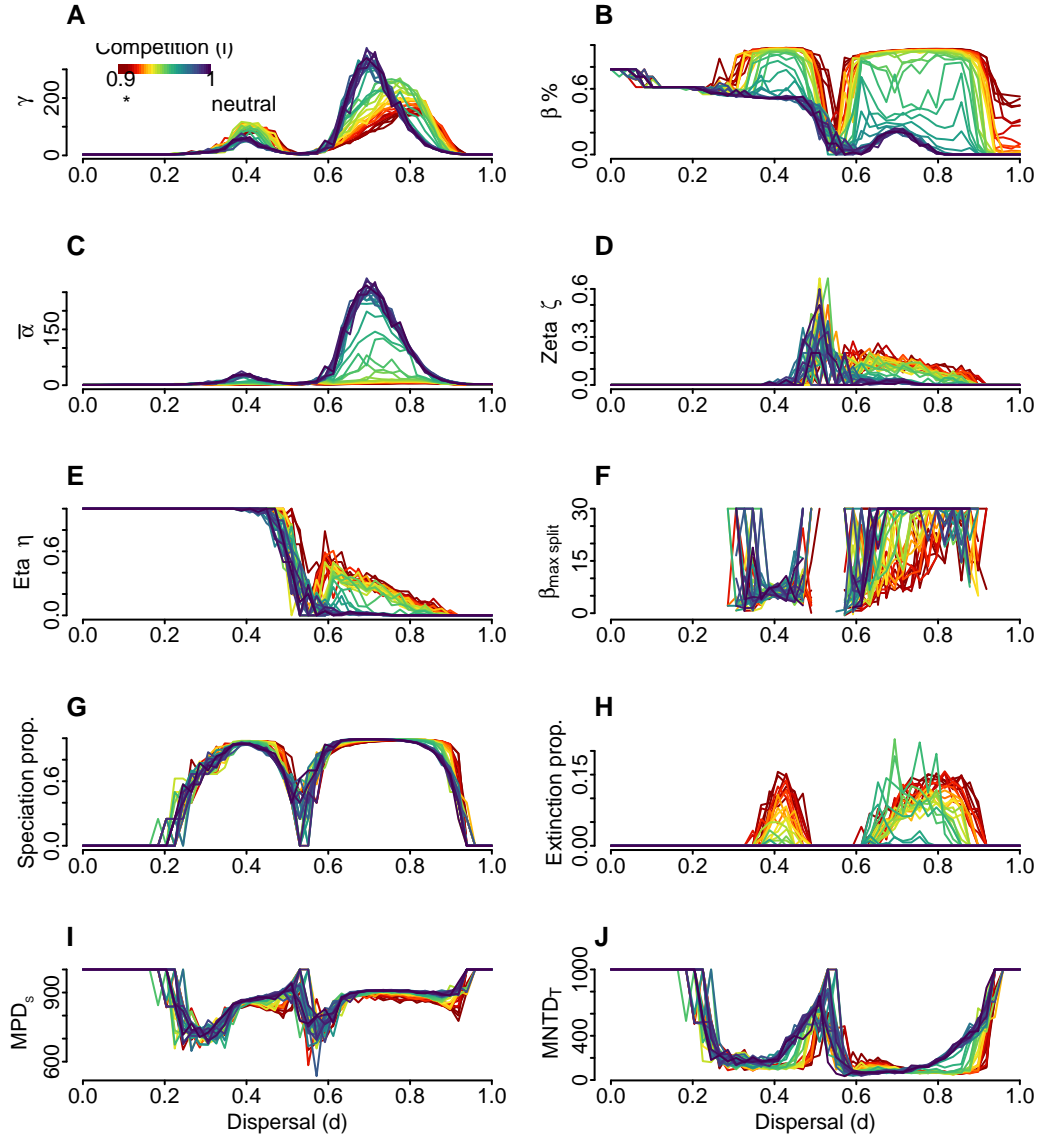


Figure 21: Summary statistics for ME through dispersal. Each line corresponds to simulation within a same competitive value along dispersal ability at the initial timestep. (A) Final gamma diversity, or final regional taxonomic richness (number of species alive at the last timestep). (B) Proportional species turnover, i.e.  $1 - \text{mean}(\alpha/\gamma)$  quantifies what proportion of the species diversity in the dataset that is not contained in an average site (C) Mean alpha diversity of the entire archipelago. (D) Proportion of species that are common to all assemblages. Zeta diversity sensu Hui and McGeoch (2014). (E) Proportion of species that are not unique to an assemblage nor common to all assemblages. (F) The complete phylogenetic beta value derived from the Maximum Likelihood estimation within the Beta-splitting model. This is computed using the `maxlik.betasplit` function from the `apTreeshape` package. (G) Proportion of speciation events in a simulation over final gamma diversity. (H) Proportion of extinction events in a simulation over final gamma diversity. (I) Standardized value of the Mean Pairwise Distance measure on the archipelago, calculated using the `mpd` function from the `picante` package. (J) Standardized value of the mean nearest taxon distance measure for the entire archipelago.

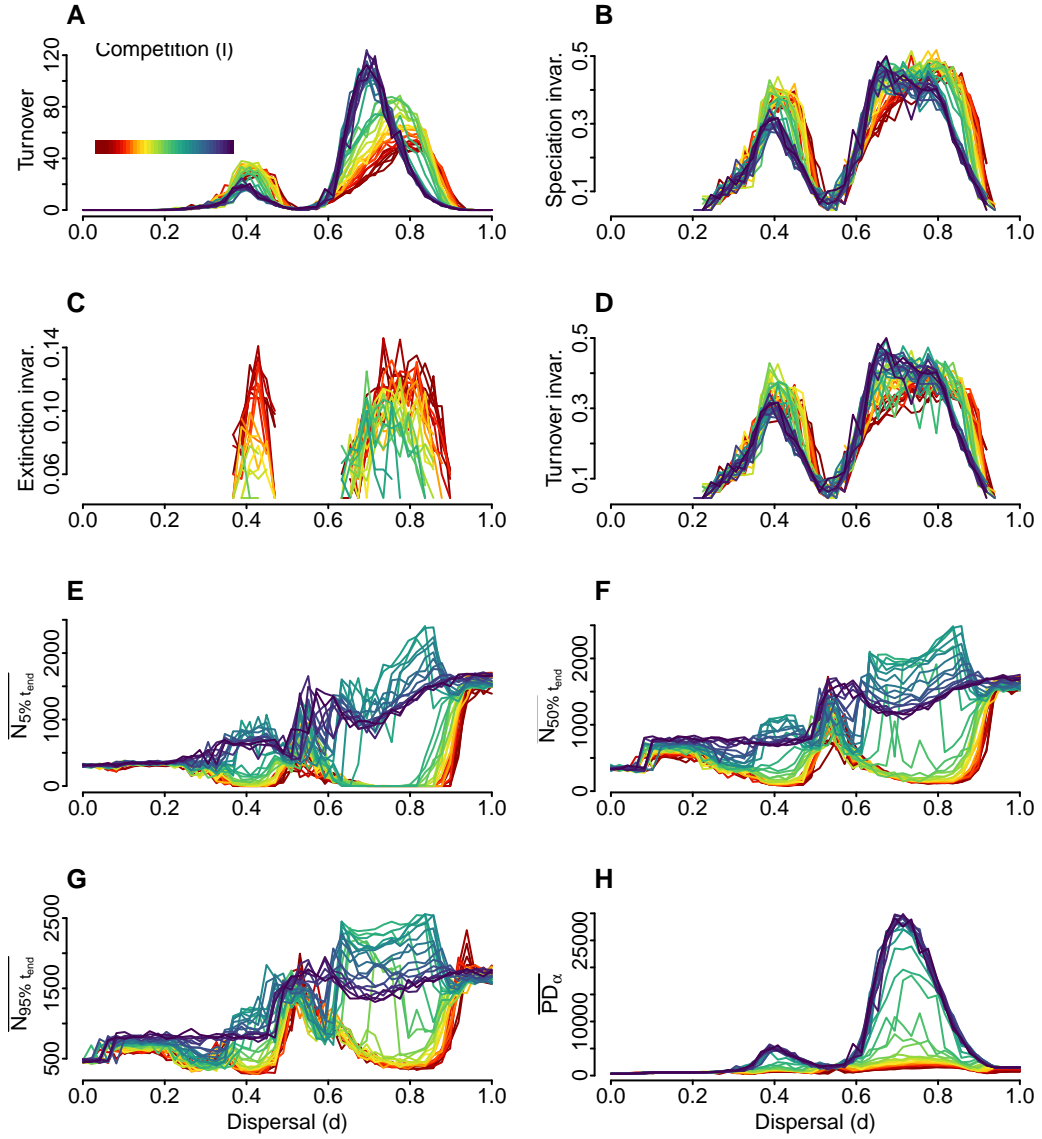


Figure 22: Additional summary statistics for ME though initial dispersal values. Each line corresponds to simulations within a same competitive value, along dispersal ability. (A) Turnover between speciation and extinction. I.e. the sum of speciation - extinction for all timesteps divided by the number of initial species. (B) Temporal speciation invariability, also refered to as temporal stability of speciation events. (C) Temporal extinction invariability, also refered to as temporal stability of extinction events. (D) Temporal turnover invariability, also referred to as temporal turnover stability. (E) Mean population size of its 5% quantile at final timestep. (F) Mean population size at final timestep. (G) Mean population size of its 95% quantile at final timestep. (H) The Mean Faith's Phylogenetic Diversity (PD) at the site level, quantifies the total branch lengths and was calculates with the function PD from the picante pacakge.

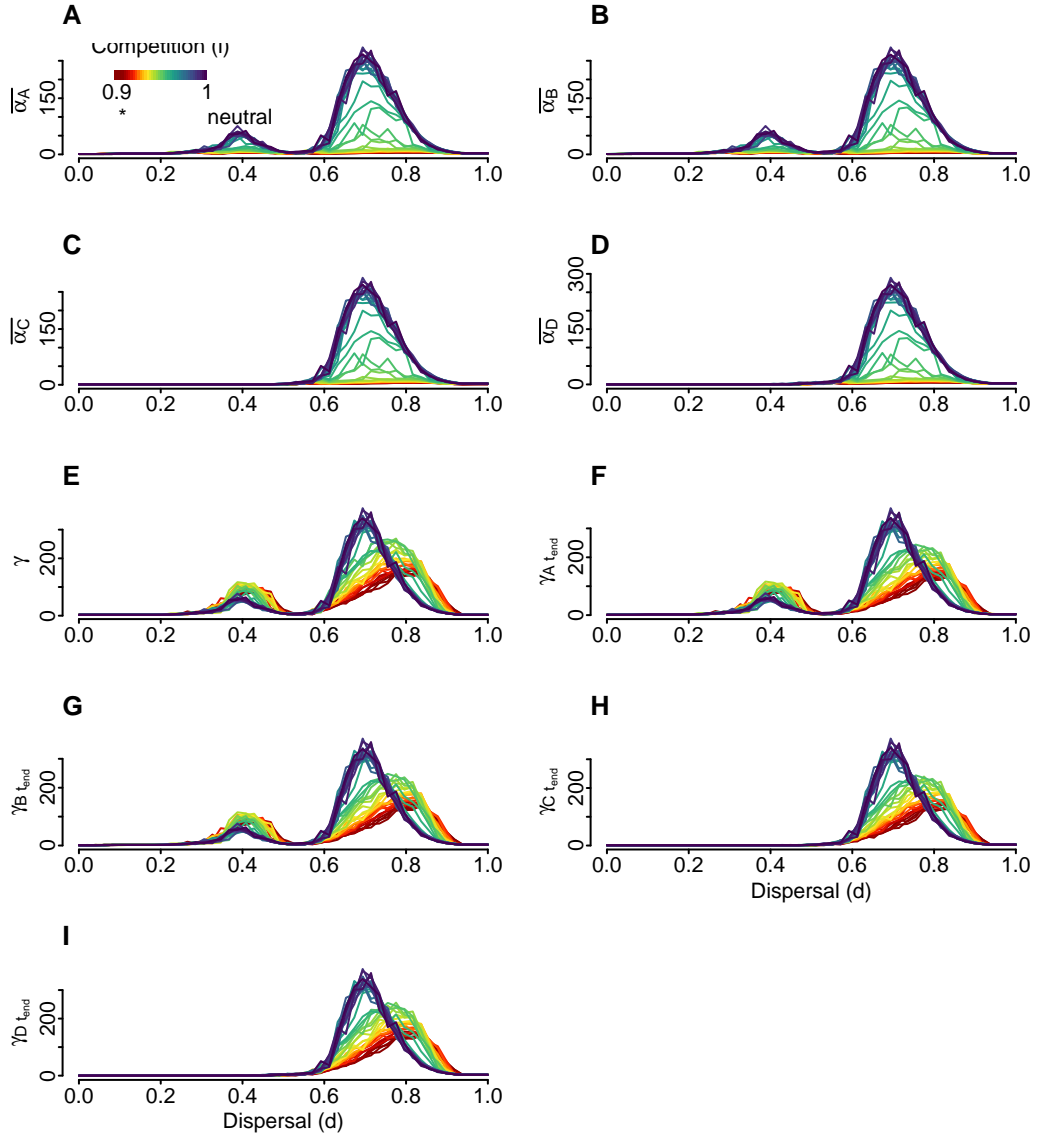


Figure 23: Additional summary statistics for ME though initial dispersal values. Each line corresponds to simulations within a same competitive value, along dispersal ability. (A) Mean alpha diversity of sites on island A. (B) Mean alpha diversity of sites on island B. (C) Mean alpha diversity of sites on island C. (D) Mean alpha diversity of sites on island D. (E) Final gamma diversity, or final regional taxonomic richness (number of species alive at the last timestep). (F) Final gamma diversity of island A, or final regional taxonomic richness (number of species alive at the last timestep). (G) Final gamma diversity of island B. (H) Final gamma diversity of island C. (I) Final gamma diversity of island D.

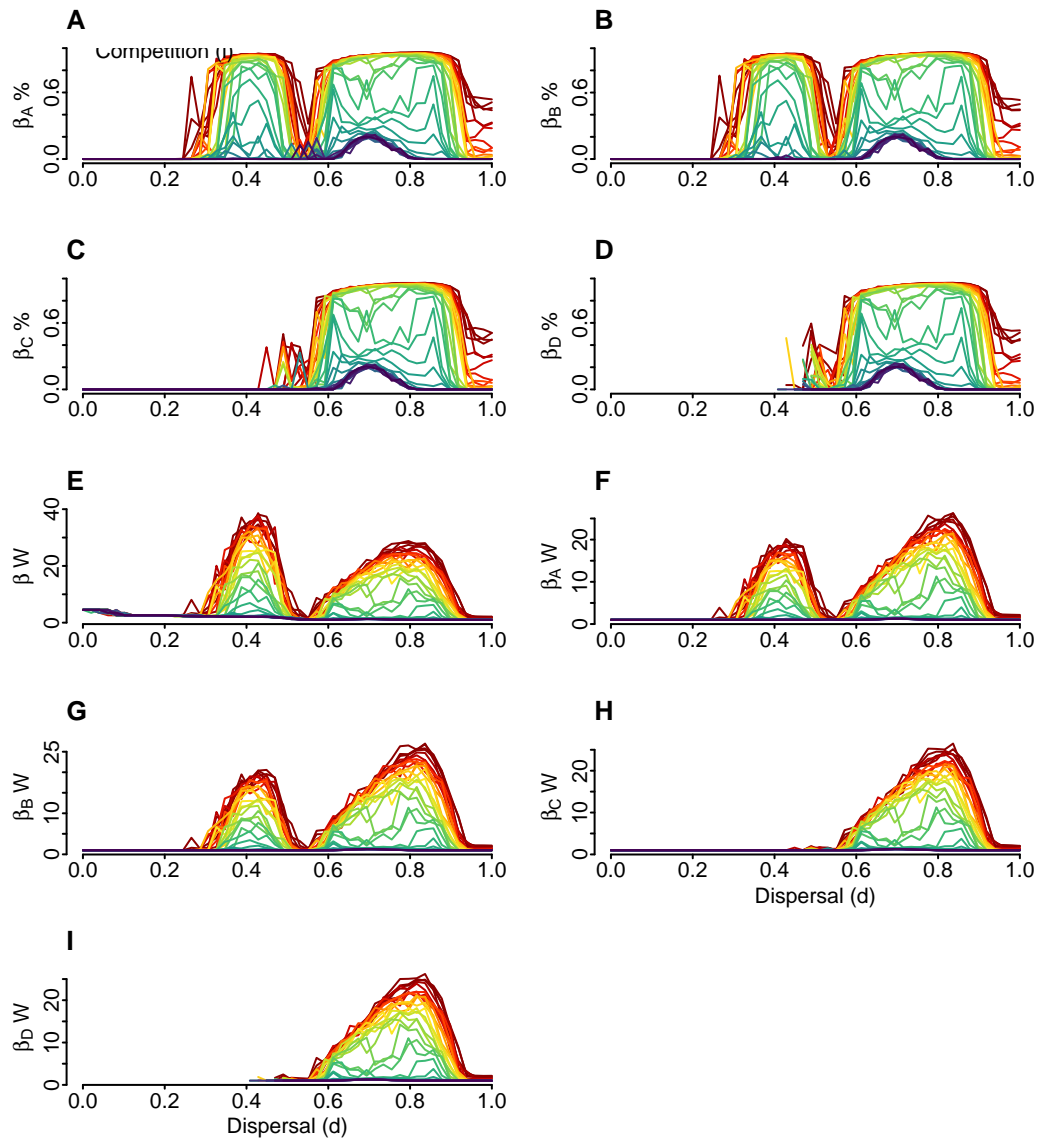


Figure 24: Additional summary statistics for ME though initial dispersal values. Each line corresponds to simulations within a same competitive value, along dispersal ability. (A) Proportional species turnover in island A. (B) Proportional species turnover in island B. (C) Proportional species turnover in island C. (D) Proportional species turnover in island D. (E) Whittaker beta diversity, i.e. gamma/mean(alpha), how many subunits there would be if the total species diversity of the mean species diversity per subunit remained the same, but the subunits shared no species. (F) Whittaker beta diversity of island A. (G) Whittaker beta diversity of island B. (H) Whittaker beta diversity of island C. (I) Whittaker beta diversity of island D.

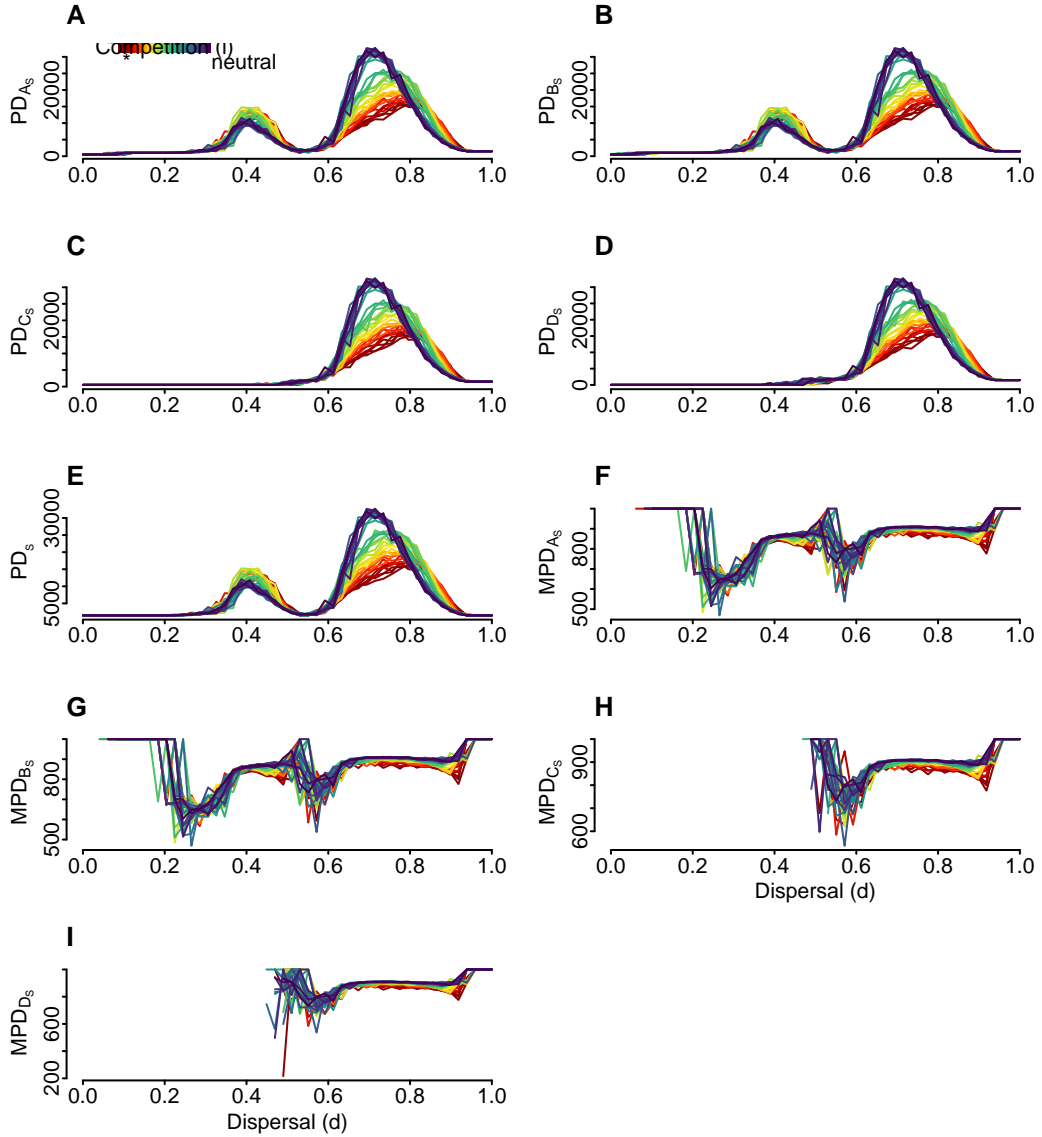


Figure 25: Additional summary statistics for ME though initial dispersal values. Each line corresponds to simulations within a same competitive value, along dispersal ability. (A) Standardized value of the unrooted Phylogenetic Diversity measure for species in island A. (B) Standardized value of the unrooted Phylogenetic Diversity measure for species in island B. (C) Standardized value of the unrooted Phylogenetic Diversity measure for species in island C. (D) Standardized value of the unrooted Phylogenetic Diversity measure for species in island D. (E) Standardized value of the unrooted Phylogenetic Diversity measure for species on the arquipelago, calculated using the `pd` function from the `picante` package. (F) Standardized value of the Mean Pairwise Distance measure in island A. (G) Standardized value of the Mean Pairwise Distance measure in island B. (H) Standardized value of the Mean Pairwise Distance measure in island C. (I) Standardized value of the Mean Pairwise Distance measure in island D.

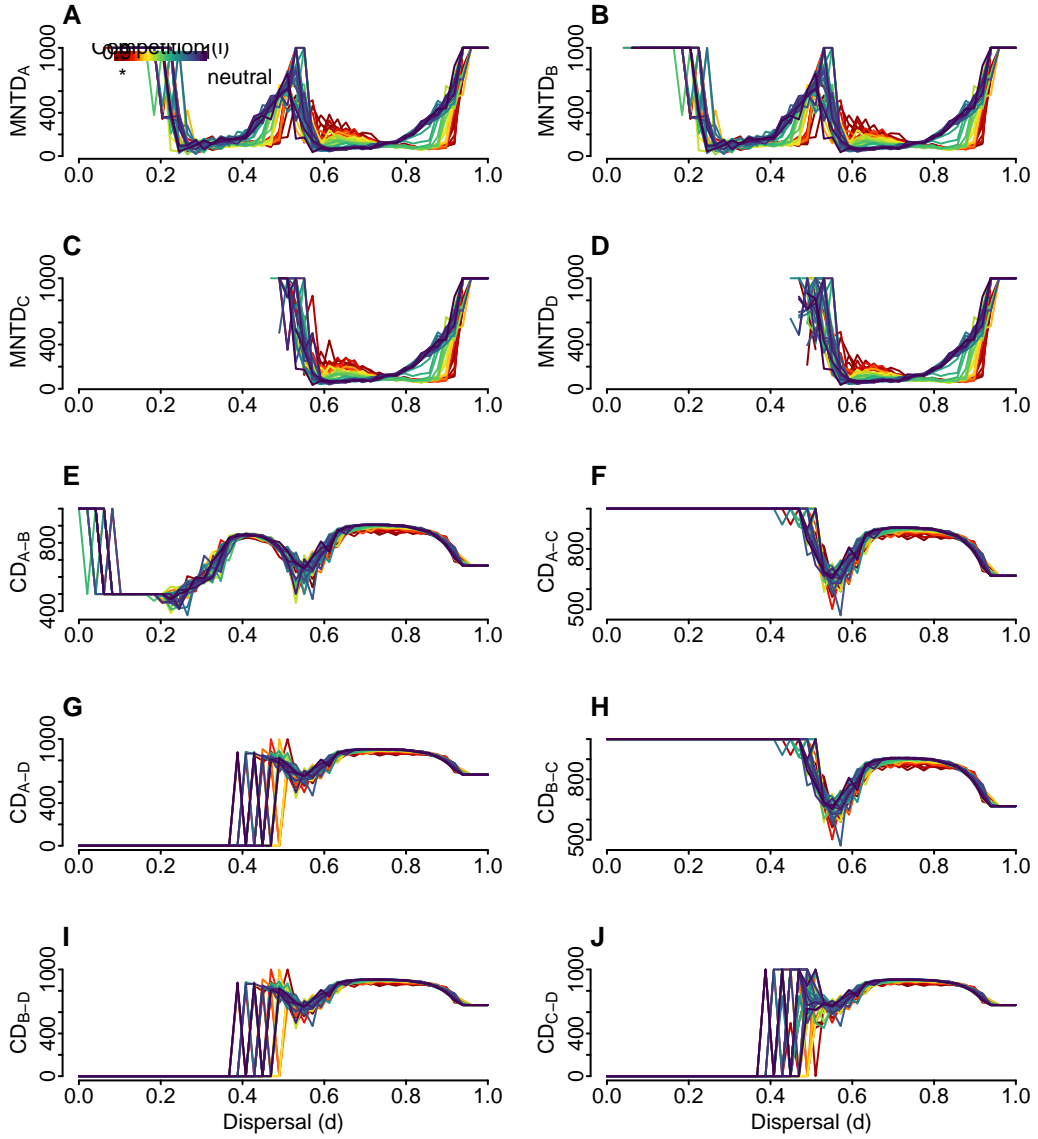


Figure 26: Additional summary statistics for ME though initial dispersal values. Each line corresponds to simulations within a same competitive value, along dispersal ability. (A) Standardized value of the mean nearest taxon distance measure for the island A. (B) Standardized value of the mean nearest taxon distance measure for the island B. (C) Standardized value of the mean nearest taxon distance measure for the island C. (D) Standardized value of the mean nearest taxon distance measure for the island D. (E) Standardized Community Distance between island A and B. It is the beta diversity version of Mean Pairwise Distance (MPD), giving the average phylogenetic distance between two communities. (F) Standardized Community Distance between island A and C. (G) Standardized Community Distance between island A and D. (H) Standardized Community Distance between island B and C. (I) Standardized Community Distance between island B and D. (J) Standardized Community Distance between island C and D.

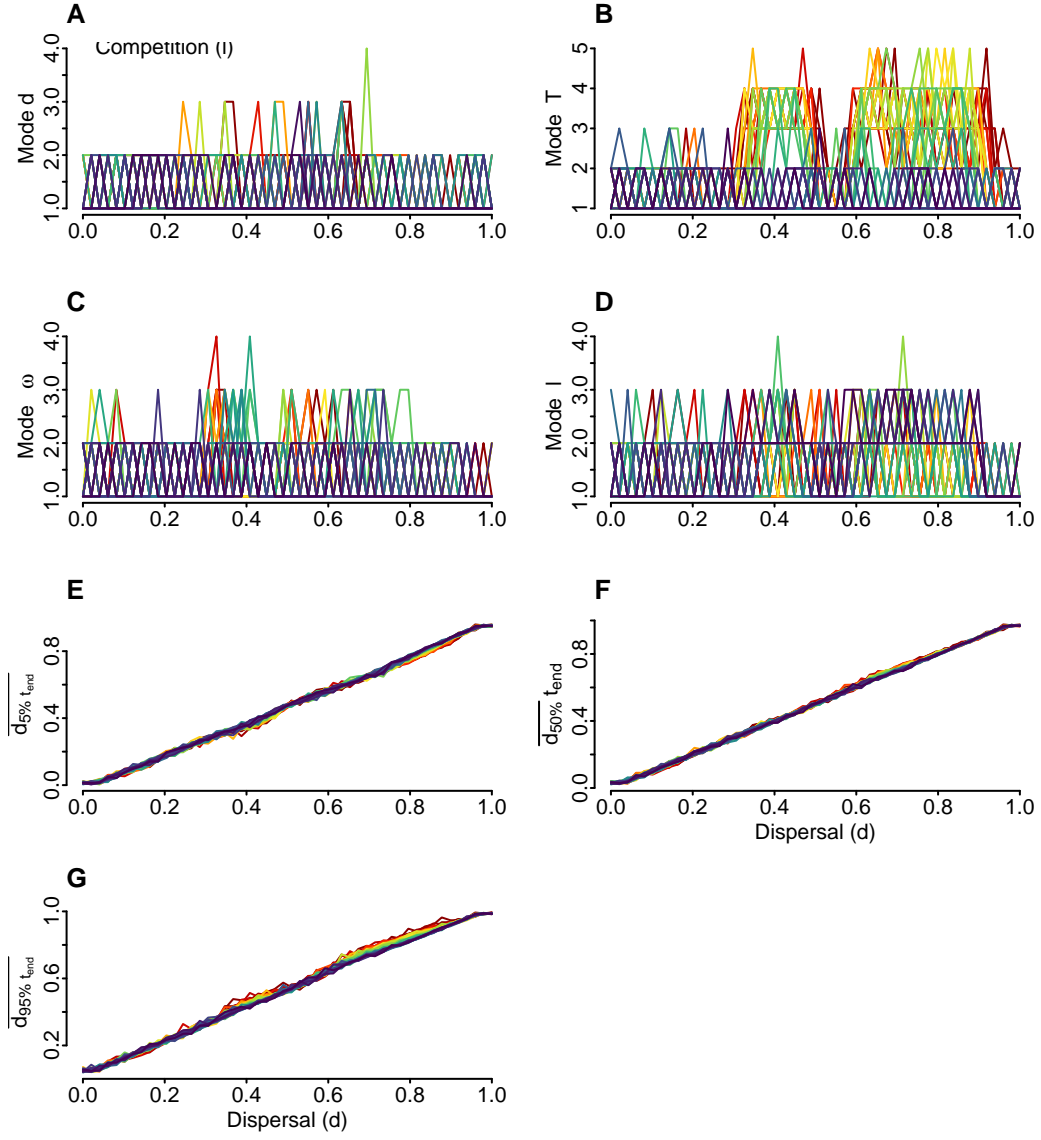


Figure 27: Additional summary statistics for ME though initial dispersal values. Each line corresponds to simulations within a same competitive value, along dispersal ability. (A) Number of modes at the dispersal trait distribution at final timestep, i.e. no modes (such as in a uniform distribution), or more. Calculated with the function ‘Mode’ from package LaplacesDemon. (B) Number of modes at the thermal optimum distribution at final timestep. (C) Number of modes at the thermal range trait distribution at final timestep. (D) Number of modes at the competition trait (i.e. tolerance to other species) distribution at final timestep. (E) Mean dispersal trait of its 5% quantile at final timestep. (F) Mean dispersal trait at final timestep. (G) Mean dispersal trait of its 95% quantile at final timestep.

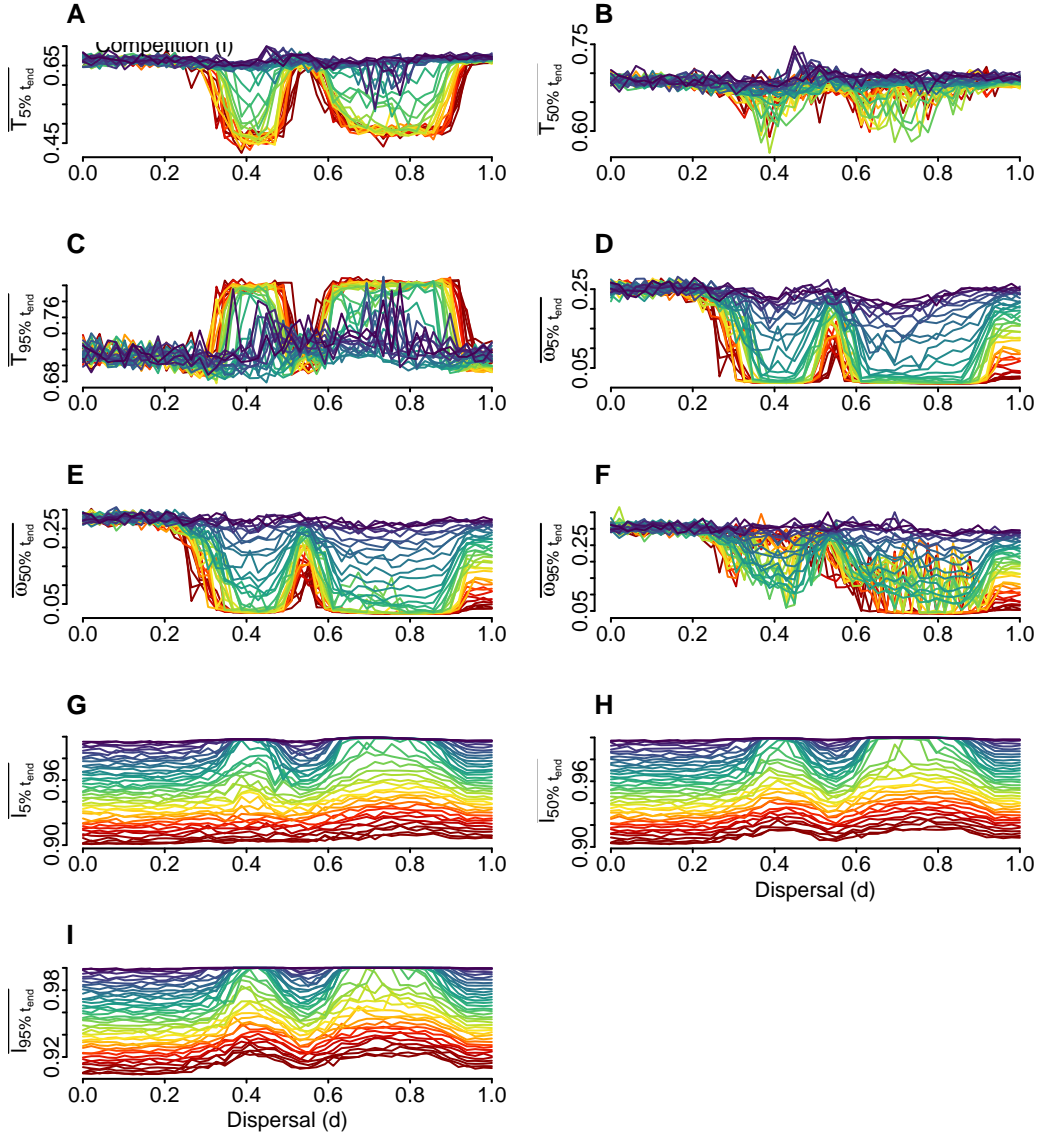


Figure 28: Additional summary statistics for ME though initial dispersal values. Each line corresponds to simulations within a same competitive value, along dispersal ability. (A) Mean thermal optimum of its 5% quantile at final timestep. (B) Mean thermal optimum at final timestep. (C) Mean thermal optimum of its 95% quantile at final timestep. (D) Mean thermal range trait of its 5% quantile at final timestep. (E) Mean thermal range trait at final timestep. (F) Mean thermal range trait of its 95% quantile at final timestep. (G) Mean tolerance to other species trait of its 5% quantile at final timestep. (H) Mean tolerance to other species trait at final timestep. (I) Mean tolerance to other species trait of its 95% quantile at final timestep.

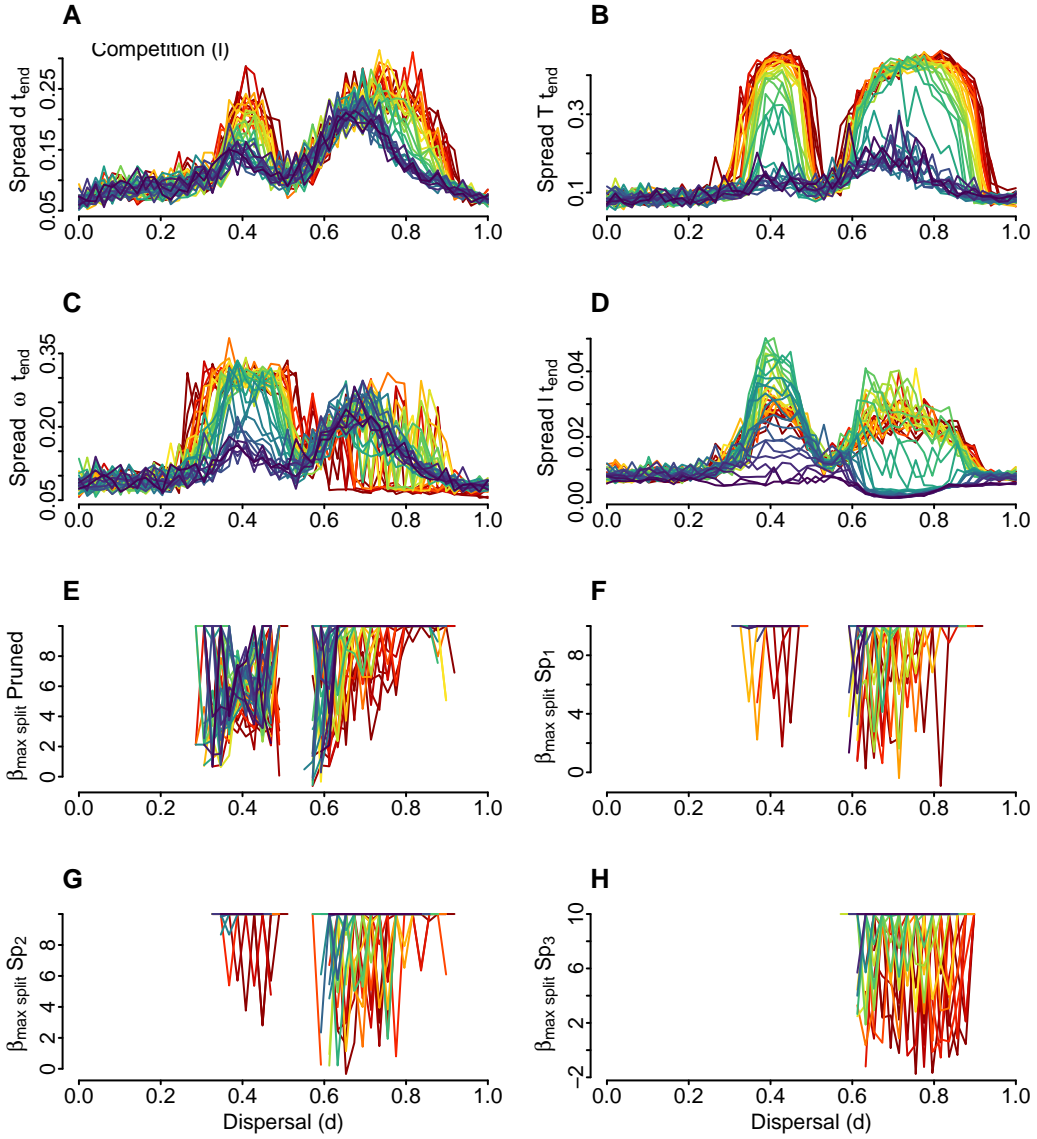


Figure 29: Additional summary statistics for ME though initial dispersal values. Each line corresponds to simulations within a same competitive value, along dispersal ability. (A) The range between the lowest and highest dispersal trait values at the final timestep. (B) The range between the lowest and highest thermal optimum values at the final timestep. (C) The range between the lowest and highest thermal range trait values at the final timestep. (D) The range between the lowest and highest tolerance to other species trait values at the final timestep. (E) The pruned phylogeny beta value, excluding extinct branches, derived from the Maximum Likelihood estimation within the Beta-splitting model. (F) The pruned phylogeny beta value of species 1, excluding extinct branches. (G) The pruned phylogeny beta value of species 2, excluding extinct branches. (H) The pruned phylogeny beta value of species 3, excluding extinct branches.

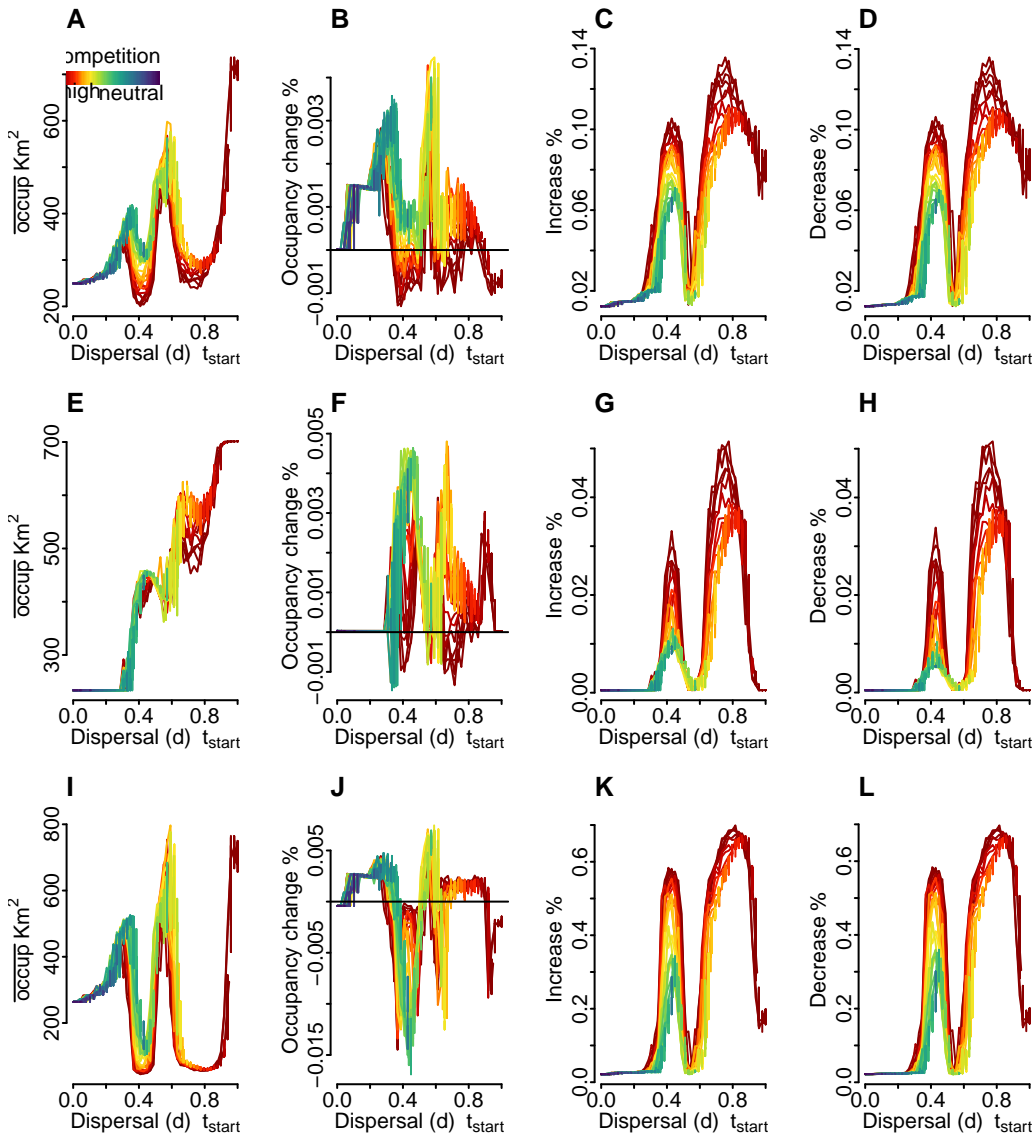


Figure 30: Spatial dynamics of MET from 4.5 to 0 Ma (A-D), Stability from 4.5 to 2.5 Ma (E-H), and Dynamism from 2 to 0 Ma (I-L). Figures show the mean occupancy, proportional occupancy, and changes in isolated proportional increase and decrease of the number of occupied sites per species.

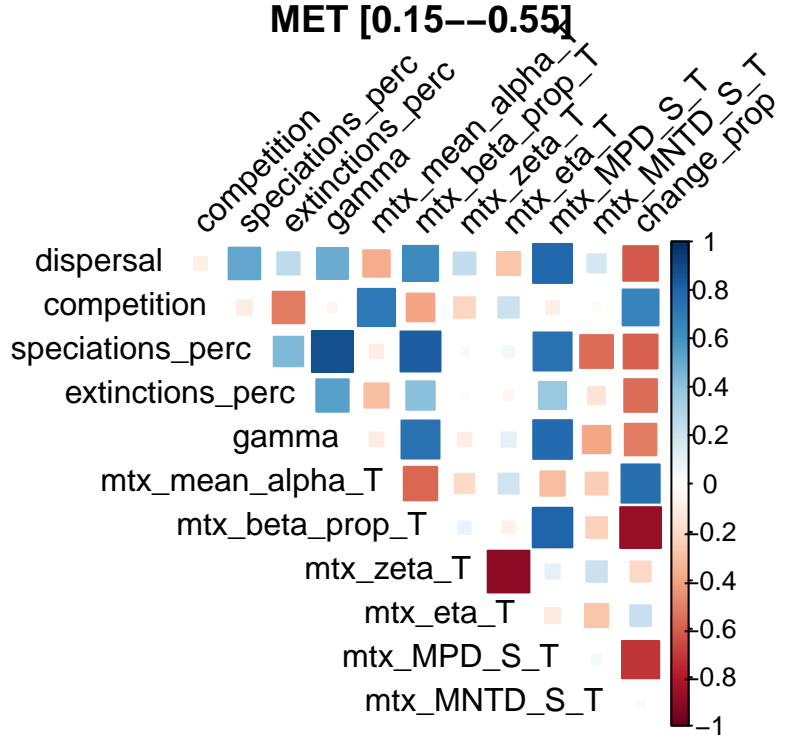
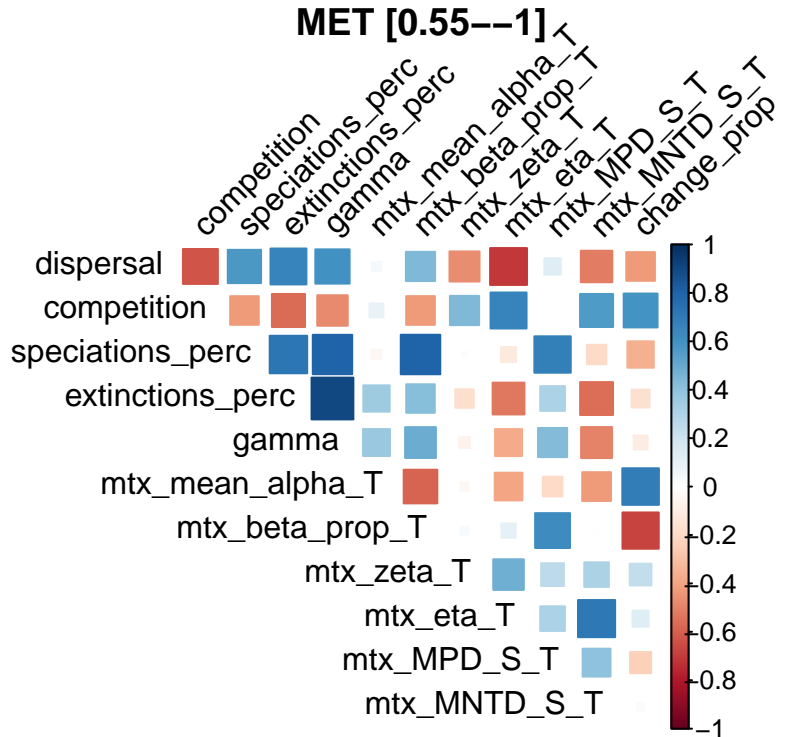
**A****B**

Figure 31: Correlations for hand-picked summary statistics for MET for different intervals of dispersal distance 0.15-0.55 (A) and 0.55-1 (B).

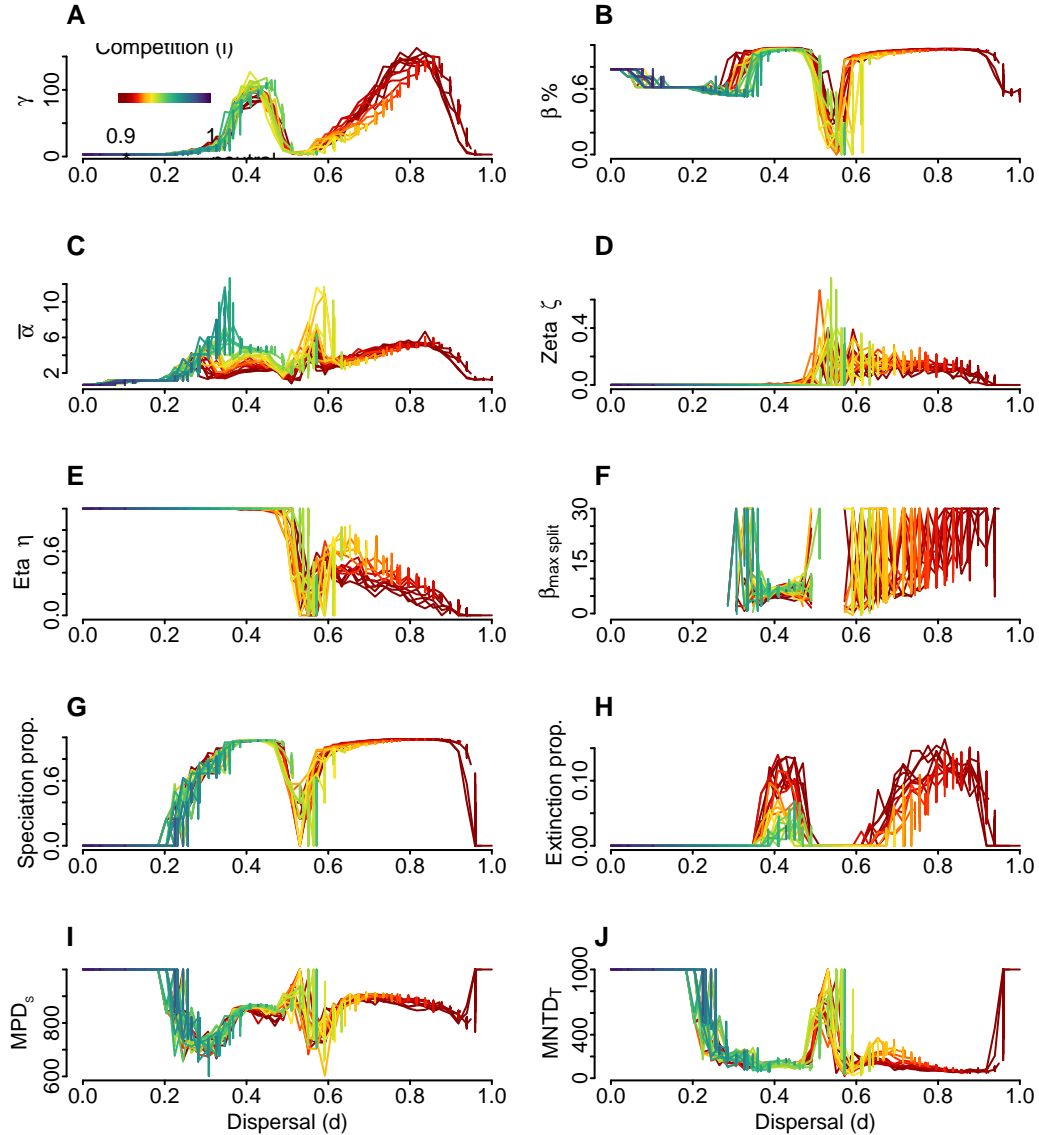


Figure 32: Summary statistics for ME through dispersal. Each line corresponds to simulation within a same competitive value along dispersal ability at the initial timestep. (A) Final gamma diversity, or final regional taxonomic richness (number of species alive at the last timestep). (B) Proportional species turnover, i.e.  $1 - \text{mean}(\alpha/\gamma)$  quantifies what proportion of the species diversity in the dataset that is not contained in an average site (C) Mean alpha diversity of the entire archipelago. (D) Proportion of species that are common to all assemblages. Zeta diversity sensu Hui and McGeoch (2014). (E) Proportion of species that are not unique to an assemblage nor common to all assemblages. (F) The complete phylogenetic beta value derived from the Maximum Likelihood estimation within the Beta-splitting model. This is computed using the `maxlik.betasplit` function from the `apTreeshape` package. (G) Proportion of speciation events in a simulation over final gamma diversity. (H) Proportion of extinction events in a simulation over final gamma diversity. (I) Standardized value of the Mean Pairwise Distance measure on the archipelago, calculated using the `mpd` function from the `picante` package. (J) Standardized value of the mean nearest taxon distance measure for the entire archipelago.

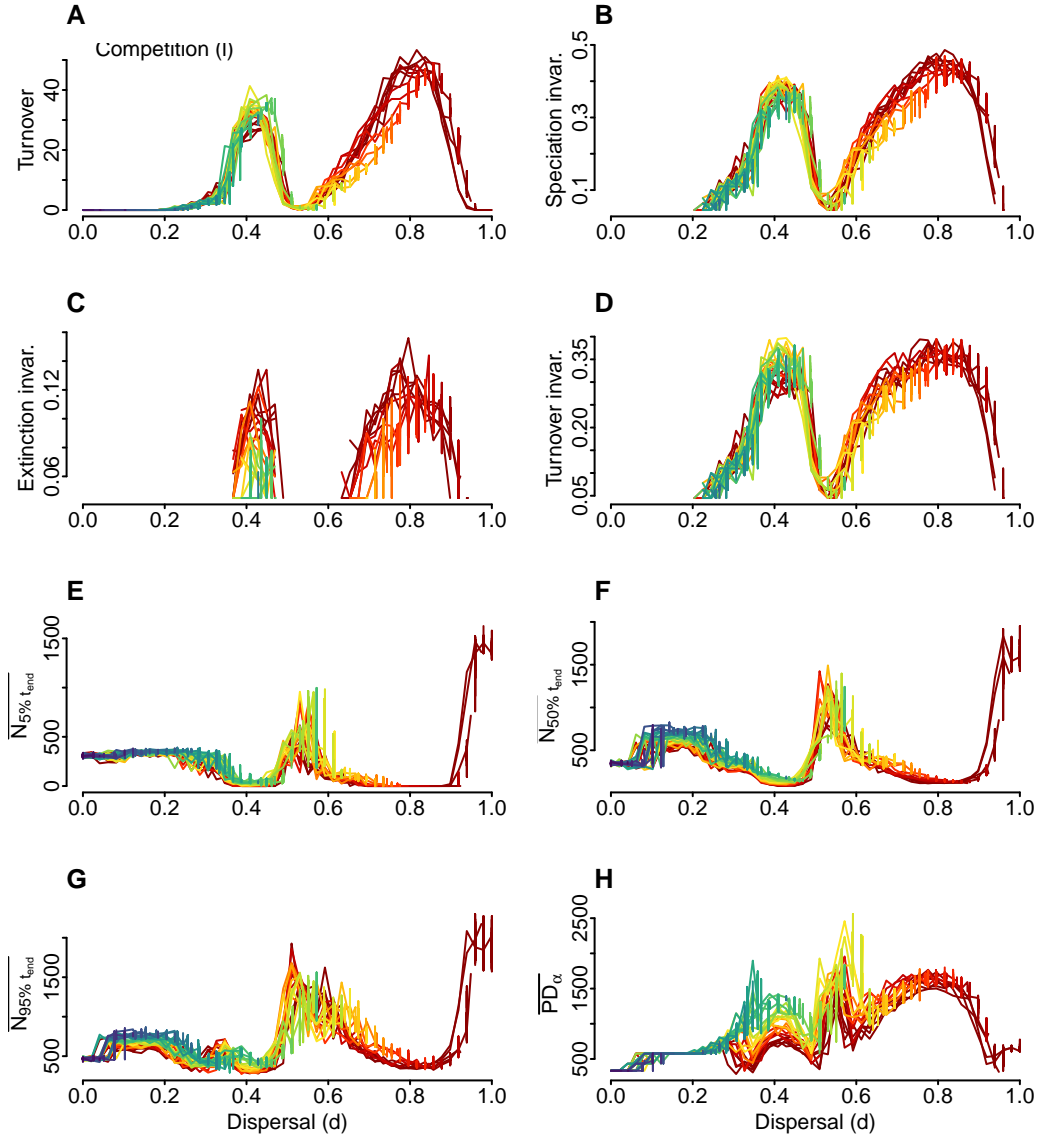


Figure 33: Additional summary statistics for MET through initial dispersal values. Each line corresponds to simulations within a same competitive value, along dispersal ability. (A) Turnover between speciation and extinction. I.e. the sum of speciation - extinction for all timesteps divided by the number of initial species. (B) Temporal speciation invariability, also referred to as temporal stability of speciation events. (C) Temporal extinction invariability, also referred to as temporal stability of extinction events. (D) Temporal turnover invariability, also referred to as temporal turnover stability. (E) Mean population size of its 5% quantile at final timestep. (F) Mean population size at final timestep. (G) Mean population size of its 95% quantile at final timestep. (H) The Mean Faith's Phylogenetic Diversity (PD) at the site level, quantifies the total branch lengths and was calculated with the function PD from the picante package.

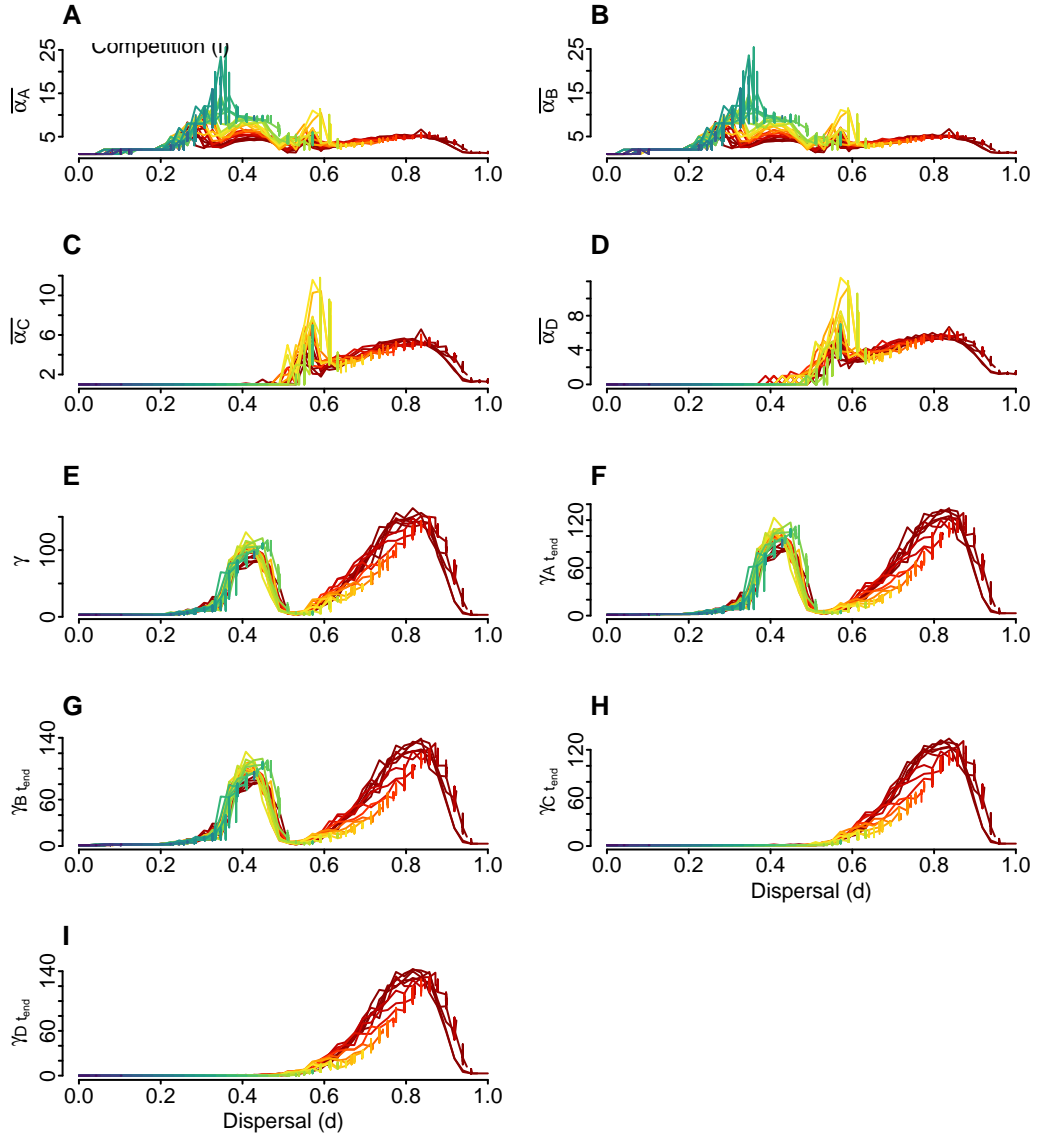


Figure 34: Additional summary statistics for MET though initial dispersal values. Each line corresponds to simulations within a same competitive value, along dispersal ability. (A) Mean alpha diversity of sites on island A. (B) Mean alpha diversity of sites on island B. (C) Mean alpha diversity of sites on island C. (D) Mean alpha diversity of sites on island D. (E) Final gamma diversity, or final regional taxonomic richness (number of species alive at the last timestep). (F) Final gamma diversity of island A, or final regional taxonomic richness (number of species alive at the last timestep). (G) Final gamma diversity of island B. (H) Final gamma diversity of island C. (I) Final gamma diversity of island D.

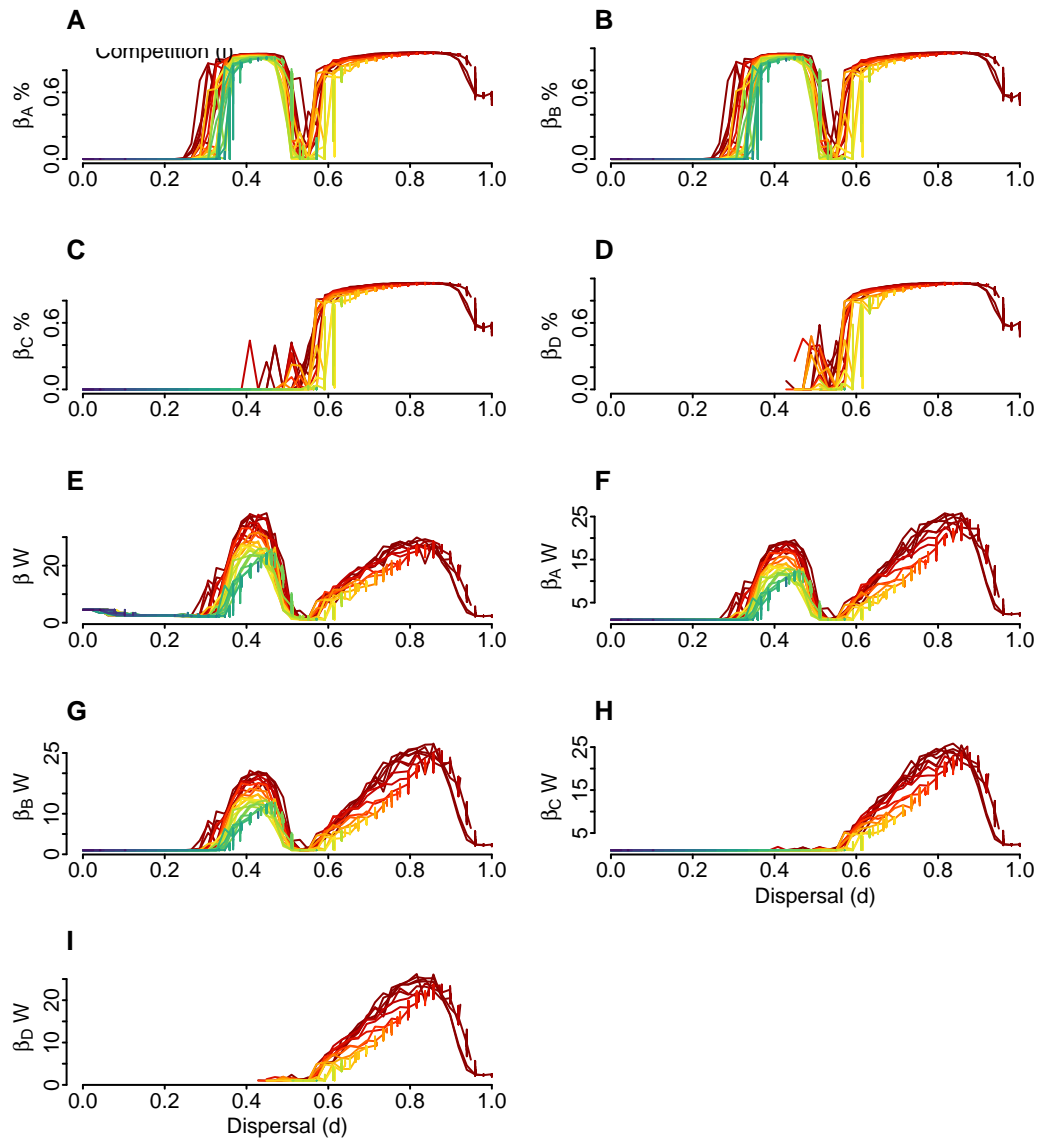


Figure 35: Additional summary statistics for MET though initial dispersal values. Each line corresponds to simulations within a same competitive value, along dispersal ability. (A) Proportional species turnover in island A. (B) Proportional species turnover in island B. (C) Proportional species turnover in island C. (D) Proportional species turnover in island D. (E) Whittaker beta diversity, i.e. gamma/mean(alpha), how many subunits there would be if the total species diversity of the mean species diversity per subunit remained the same, but the subunits shared no species. (F) Whittaker beta diversity of island A. (G) Whittaker beta diversity of island B. (H) Whittaker beta diversity of island C. (I) Whittaker beta diversity of island D.

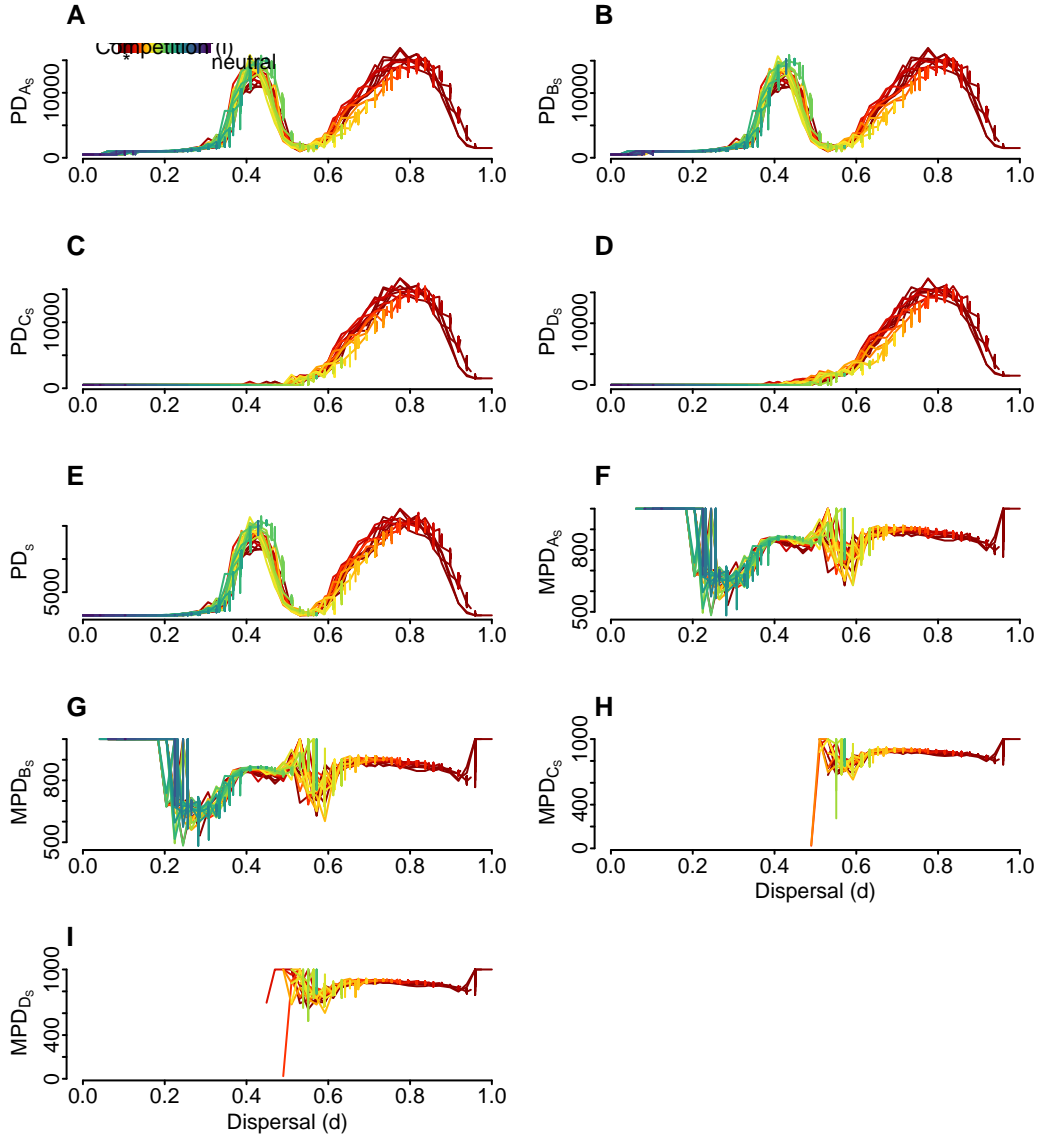


Figure 36: Additional summary statistics for MET through initial dispersal values. Each line corresponds to simulations within a same competitive value, along dispersal ability. (A) Standardized value of the unrooted Phylogenetic Diversity measure for species in island A. (B) Standardized value of the unrooted Phylogenetic Diversity measure for species in island B. (C) Standardized value of the unrooted Phylogenetic Diversity measure for species in island C. (D) Standardized value of the unrooted Phylogenetic Diversity measure for species in island D. (E) Standardized value of the unrooted Phylogenetic Diversity measure for species on the archipelago, calculated using the `pd` function from the `picante` package. (F) Standardized value of the Mean Pairwise Distance measure in island A. (G) Standardized value of the Mean Pairwise Distance measure in island B. (H) Standardized value of the Mean Pairwise Distance measure in island C. (I) Standardized value of the Mean Pairwise Distance measure in island D.

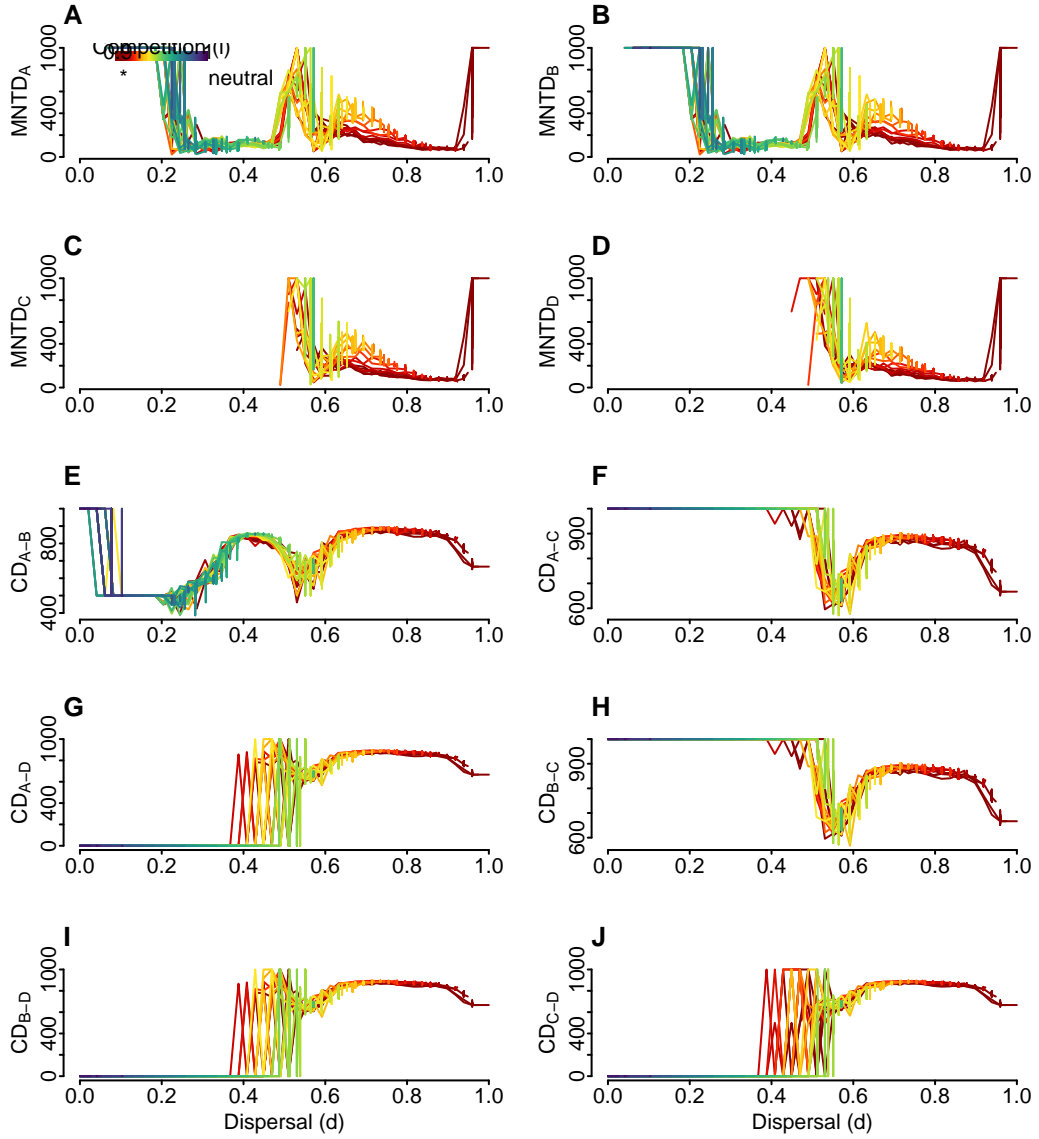


Figure 37: Additional summary statistics for MET through initial dispersal values. Each line corresponds to simulations within a same competitive value, along dispersal ability. (A) Standardized value of the mean nearest taxon distance measure for the island A. (B) Standardized value of the mean nearest taxon distance measure for the island B. (C) Standardized value of the mean nearest taxon distance measure for the island C. (D) Standardized value of the mean nearest taxon distance measure for the island D. (E) Standardized Community Distance between island A and B. It is the beta diversity version of Mean Pairwise Distance (MPD), giving the average phylogenetic distance between two communities. (F) Standardized Community Distance between island A and C. (G) Standardized Community Distance between island A and D. (H) Standardized Community Distance between island B and C. (I) Standardized Community Distance between island B and D. (J) Standardized Community Distance between island C and D.

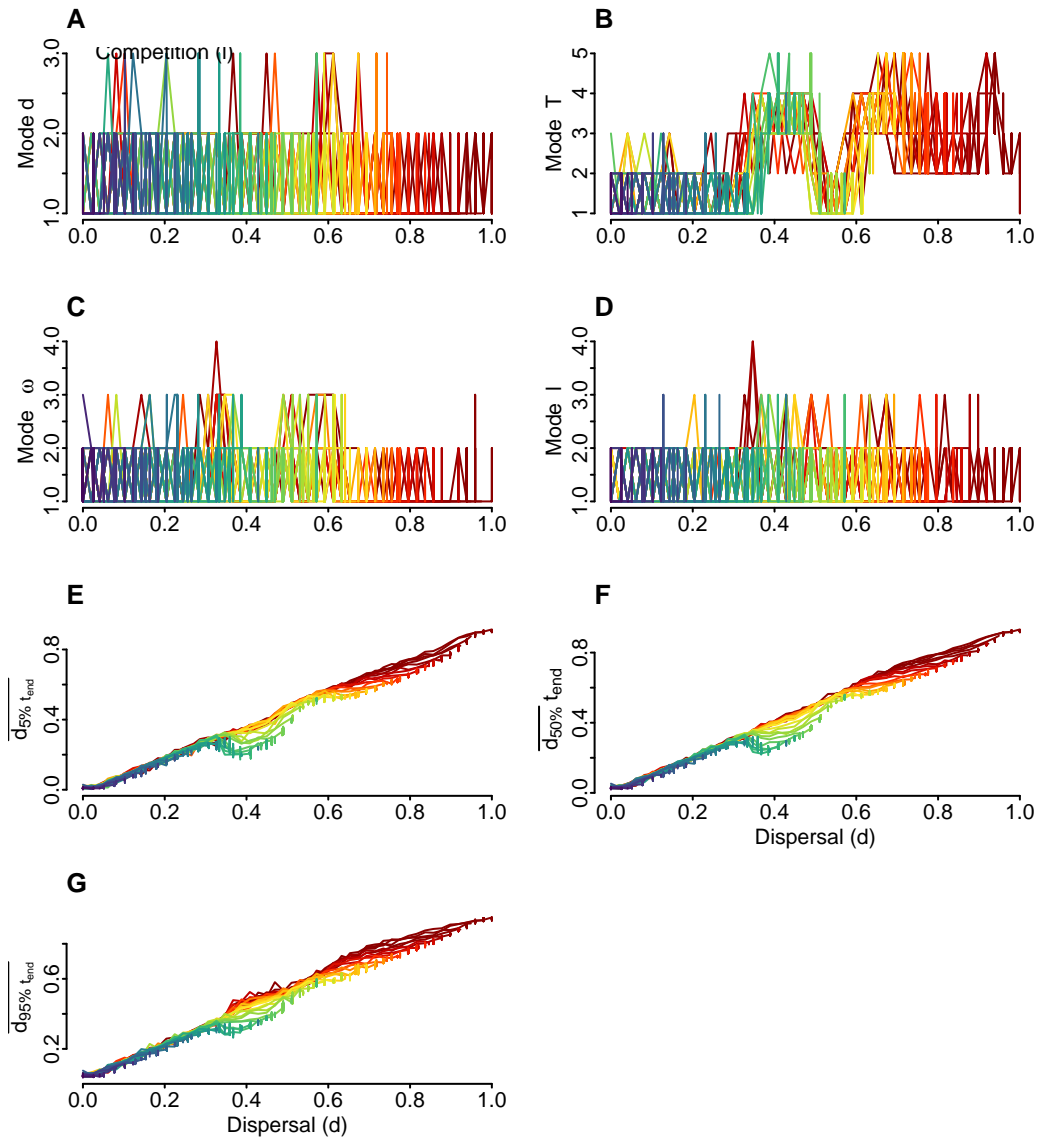


Figure 38: Additional summary statistics for MET through initial dispersal values. Each line corresponds to simulations within a same competitive value, along dispersal ability. (A) Number of modes at the dispersal trait distribution at final timestep, i.e. no modes (such as in a uniform distribution), or more. Calculated with the function ‘Mode’ from package LaplacesDemon. (B) Number of modes at the thermal optimum distribution at final timestep. (C) Number of modes at the thermal range trait distribution at final timestep. (D) Number of modes at the competition trait (i.e. tolerance to other species) distribution at final timestep. (E) Mean dispersal trait of its 5% quantile at final timestep. (F) Mean dispersal trait at final timestep. (G) Mean dispersal trait of its 95% quantile at final timestep.

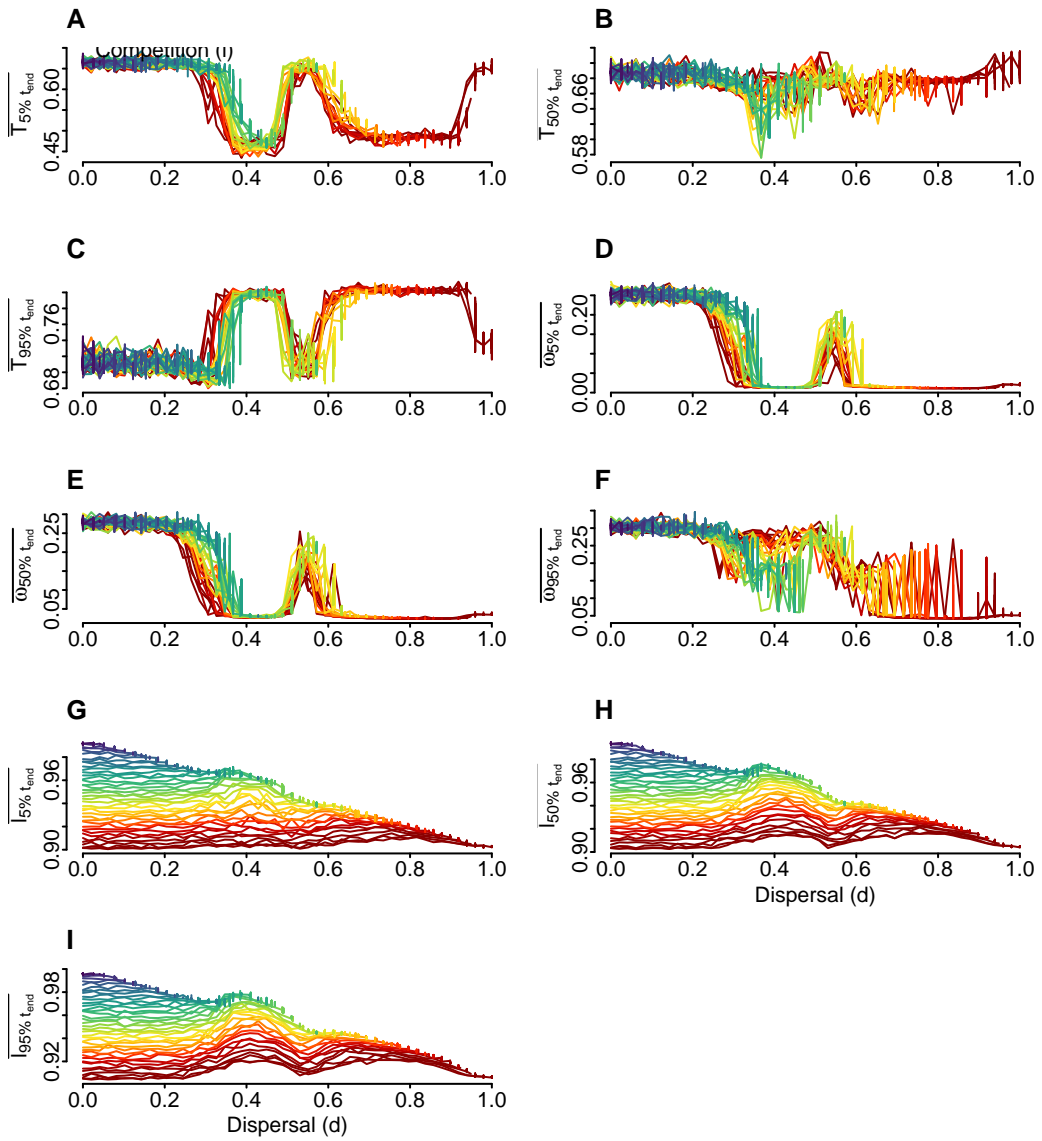


Figure 39: Additional summary statistics for MET through initial dispersal values. Each line corresponds to simulations within a same competitive value, along dispersal ability. (A) Mean thermal optimum of its 5% quantile at final timestep. (B) Mean thermal optimum at final timestep. (C) Mean thermal optimum of its 95% quantile at final timestep. (D) Mean thermal range trait of its 5% quantile at final timestep. (E) Mean thermal range trait at final timestep. (F) Mean thermal range trait of its 95% quantile at final timestep. (G) Mean tolerance to other species trait of its 5% quantile at final timestep. (H) Mean tolerance to other species trait at final timestep. (I) Mean tolerance to other species trait of its 95% quantile at final timestep.

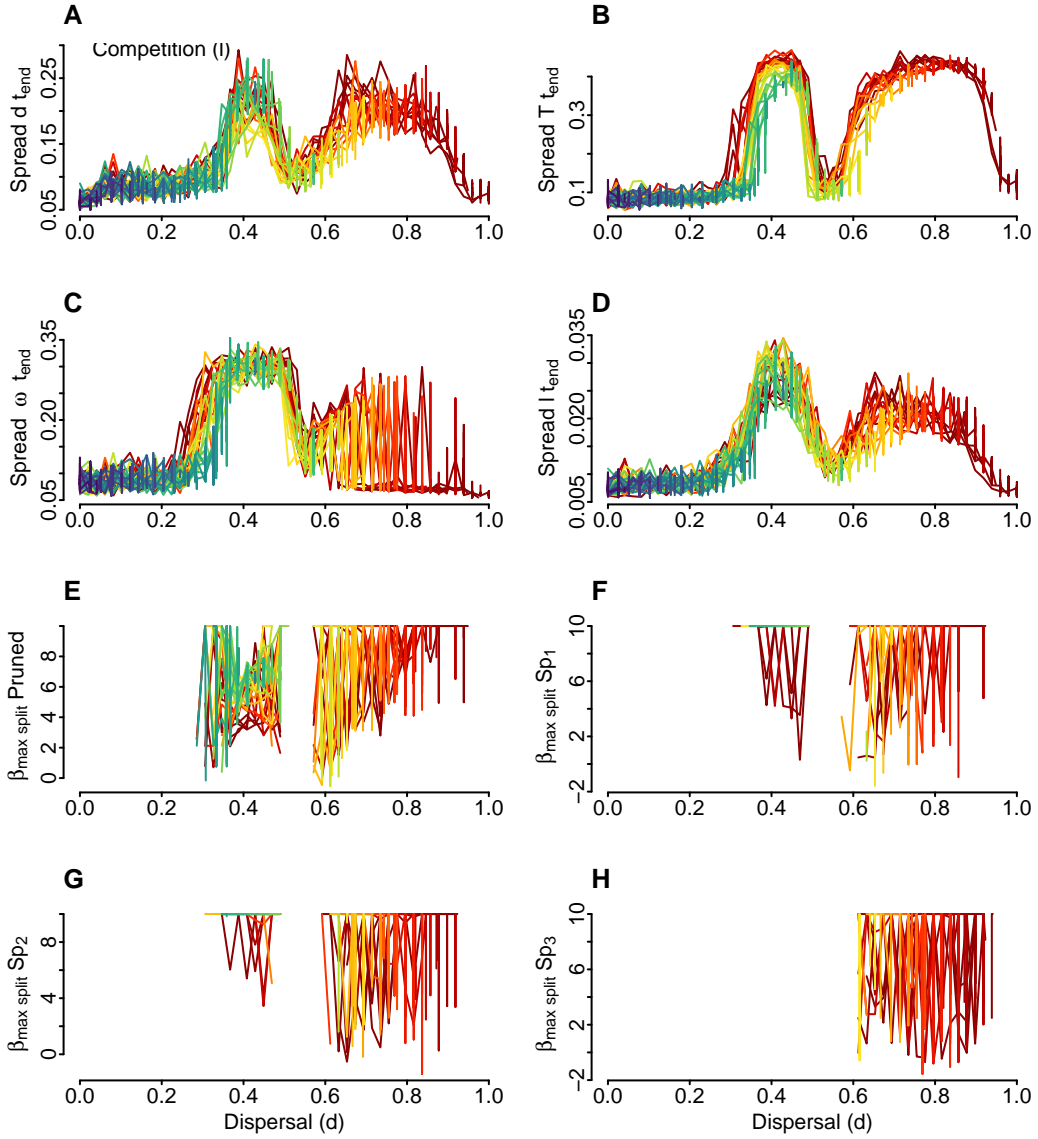


Figure 40: Additional summary statistics for MET though initial dispersal values. Each line corresponds to simulations within a same competitive value, along dispersal ability. (A) The range between the lowest and highest dispersal trait values at the final timestep. (B) The range between the lowest and highest thermal optimum values at the final timestep. (C) The range between the lowest and highest thermal range trait values at the final timestep. (D) The range between the lowest and highest tolerance to other species trait values at the final timestep. (E) The pruned phylogeny beta value, excluding extinct branches, derived from the Maximum Likelihood estimation within the Beta-splitting model. (F) The pruned phylogeny beta value of species 1, excluding extinct branches. (G) The pruned phylogeny beta value of species 2, excluding extinct branches. (H) The pruned phylogeny beta value of species 3, excluding extinct branches.

lower number of species. ME Model had number of species and dispersal similarly correlated as to M0, a positive correlation (0.40) is observed, reinforcing the idea that higher dispersal capabilities are beneficial for species richness. Number of Species and thermal range: Again, a negative correlation (-0.43) is found, consistent with the M0 model's findings. Number of Species and Dispersal in MET Model shows a stronger positive correlation (0.56) compared to M0 and ME, indicating the assumed trade-off. The number of species and thermal range shows a very strong negative correlation (-0.74), suggesting that in the MET model, the impact of temperature tolerance on species numbers is even more significant.

### Trait Changes

Figure 43 illustrates the variations in trait changes for the models M0, ME, and MET across different ecological parameters: dispersal, tolerance to other species, thermal range, and thermal optimum. Each model's (i.e. columns) shows the slope of trait change between the initial and final timesteps, highlighting how these traits evolve over time under different conditions and assumptions. The use of color gradients conveys the intensity of competition affecting these traits, with warmer colors indicating higher levels of competition. This visualization underscores the complex interplay between competition and trait adaptability in ecological models, highlighting how traits like dispersal capacity and temperature tolerance shift in response to environmental pressures and species interactions.

Figure 44 presents the final gamma richness in relation to various mean parameter values at the final timestep, including thermal range, dispersal, and heterospecific interaction coefficient, across the models M0, ME, and MET. The columns for each model demonstrate the impact of these parameters on biodiversity, utilizing color gradients to represent the strength of competition and dispersal. The analysis of these relationships stresses the critical roles that temperature tolerance, dispersal capabilities, and interactions with other species play in shaping community richness and diversity.

Figure 45 depicts the final gamma richness plotted against the mean trait changes, illustrating the slope between initial and final trait values for all species within the models M0, ME, and MET. Note the traits such as thermal range, dispersal, and heterospecific interaction coefficient, segmented by each model in separate columns. Two color gradients are used for the strength of competition and dispersal. This visualization showcases the linkage between trait adaptability and community richness, emphasizing the importance of assumptions to evolutionary responses to environmental and interspecific pressures in determining ecological outcomes.

### Further analysis

Additional, we explore the intricate dynamics of species interaction and environmental adaptation through a series of figures. Figure Figure 46 showcases the final mean dispersal trait ( $d$ ),

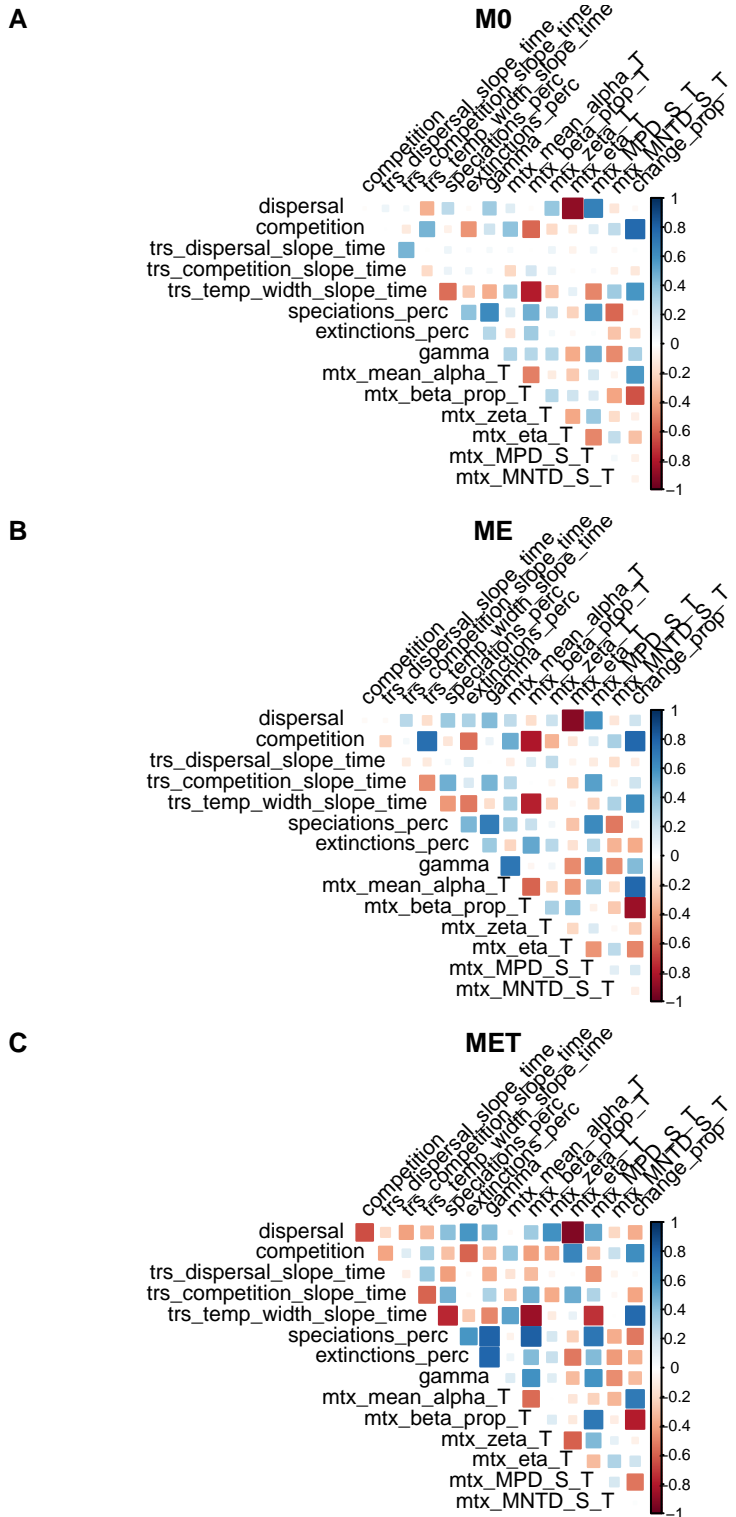


Figure 41: Correlations for hand-picked summary statistics for M0 (A); ME (B) and MET (C).

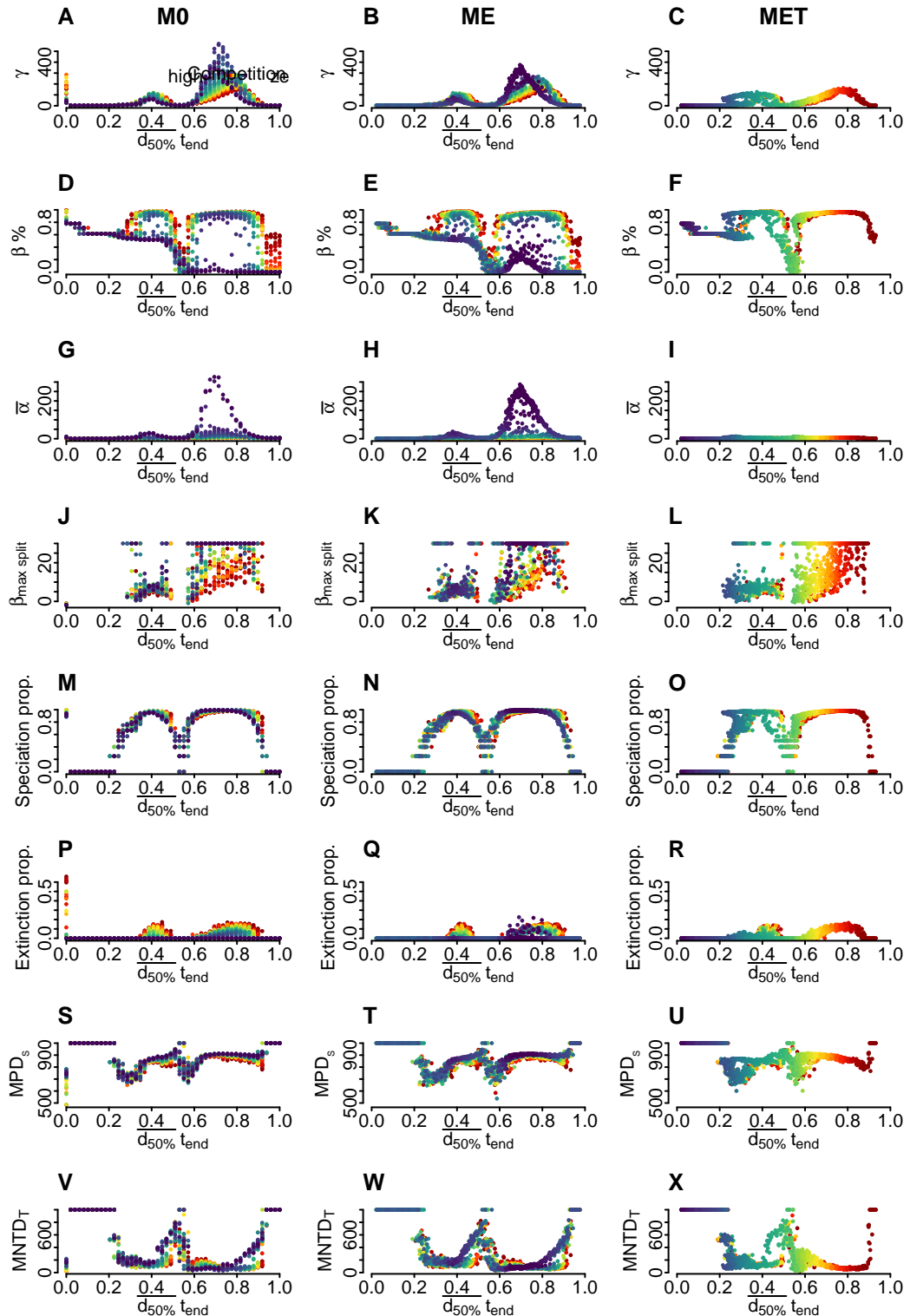


Figure 42: Comparison of M0, ME and MET for 8 summary statistics. Dispersal x axis plot the mean dispersal trait at the end of the simulation, rather than the initial dispersal parameter  $d$ . The same applies for the competition values that color the points

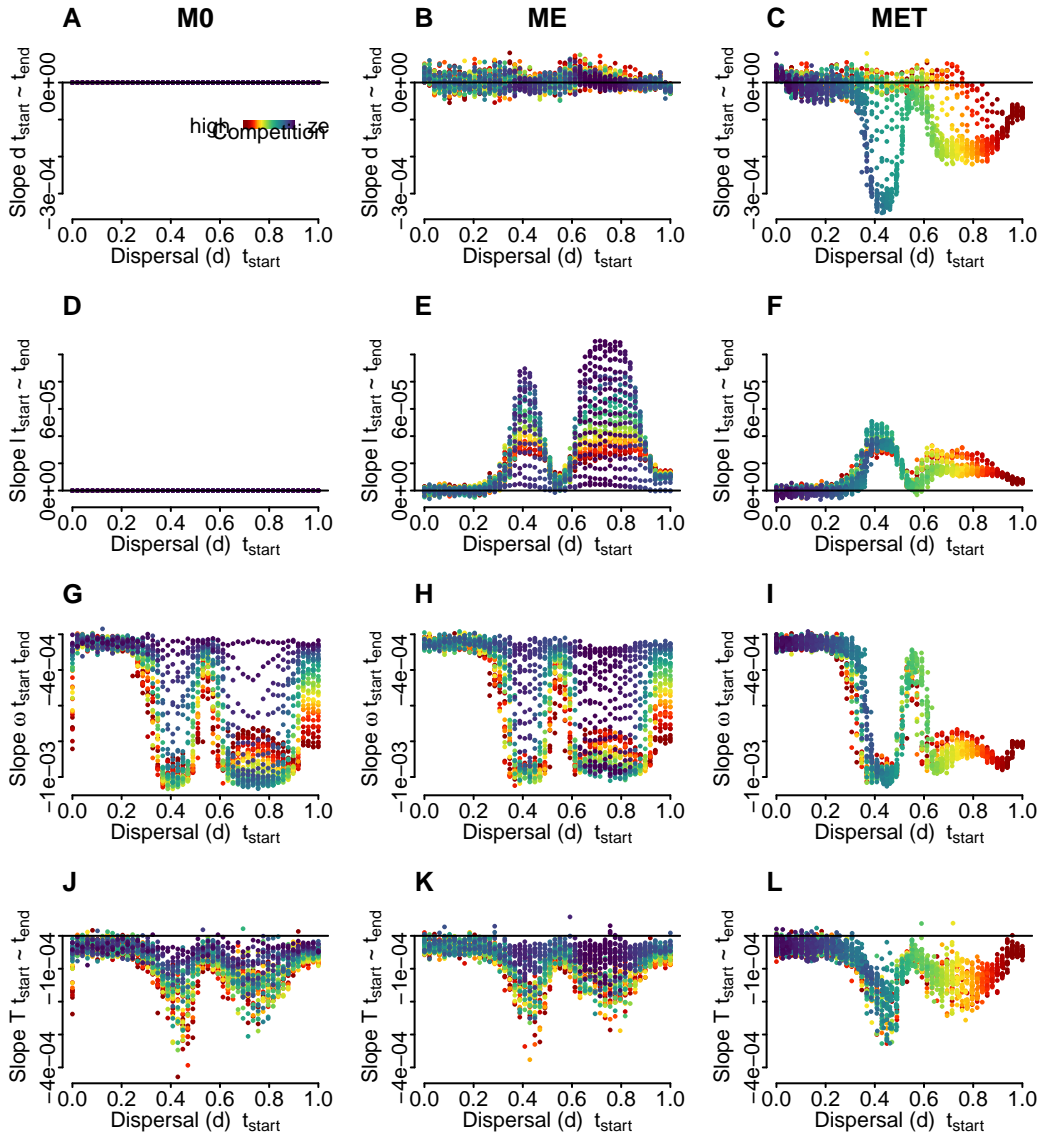


Figure 43: Slopes of trait change for M0, ME and MET (columns) between initial and final timestep, i.e. dispersal (A-C), tolerance to other species (D-F), thermal range (G-I), thermal optimum (J-L). The warmer the color the higher the competition.

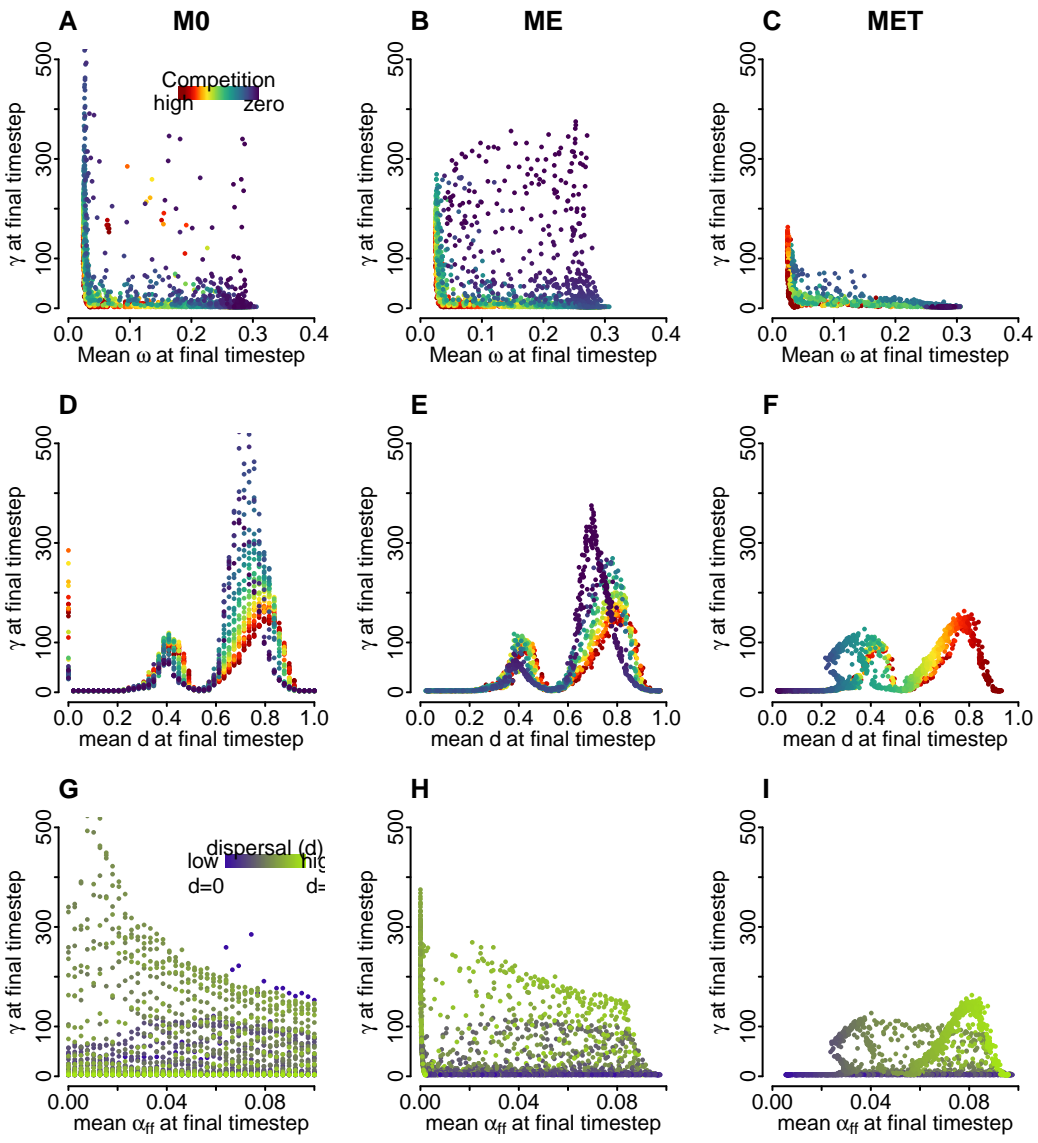


Figure 44: Final gamma richness at final timestep against different final mean parameter values (i.e. thermal range A-C, Dispersal D-F, Heterospecific interaction coefficient G-I) for Models MO, ME and MET on each column. Two color gradients are used, one for the strength of competition (A-F) and the other for the strength of dispersal (G-I).

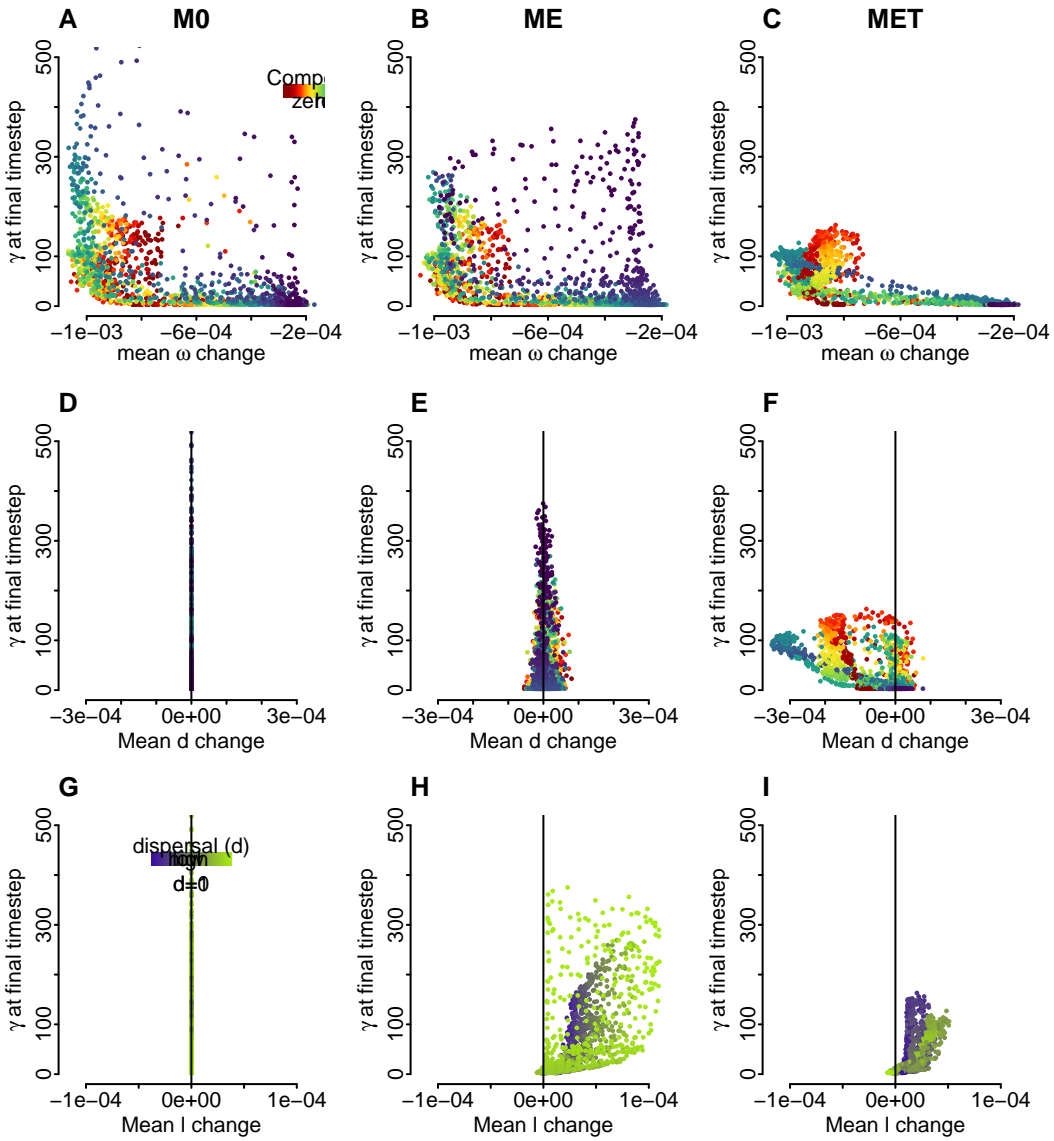


Figure 45: Final gamma richness at the last timestep plotted against the mean trait changes, which represent the slope between the initial and final trait values for all species. The mean trait is shown for thermal range A-C, dispersal D-F, and heterospecific interaction coefficient G-I for Models MO, ME, and MET in each column. Two color gradients are used, one for the strength of competition (A-F) and the other for the strength of dispersal (G-I).

plotted against final the mean competitive trait ( $l$ ) (i.e. tolerance to other species), thermal optimum ( $T$ ), and thermal range ( $\omega$ ) across Models MO, ME, and MET (Figure 46 Figure A-I). Further expanding on ecological theories, Figure Figure 47 delves into the theory of limiting similarity, illustrating how signals for species diversity are correlated with average population sizes linked through competitive exclusion. Lastly, Figure Figure 48 juxtaposes speciation versus extinction percentages with temporal stability in macroevolutionary events. This figure highlights the impact of interspecific competition on biodiversity outcomes and shows temporal invariability fo the macroevolutionary processes (Figure 48 D-F).

## Handpicked simulation

Examining a single simulation, specifically how trait changed though time for each species, enables us to closely investigate the implemented processes in action (Figure 50). For this we select a simulation with initial  $l=9.56$  and  $d=0.367$ , thus sampling initial value of  $l$  that leads to moderate competition and falls within connectivity regime  $\kappa_1$ . Moreover, in all simulations, island C remained occupied by only one species, serving as a control on biodiversity while island D is never occupied (Figure 51). As implemented,  $l$  and  $d$  did not change though time for M0 (Figure 50 I,M). Note the single black isolated line that corresponds to single species in island C (Figure 50 E,F,G,J,K,O).

All models exhibit rapid niche specialization around 1 Ma, characterized by a decrease in  $\alpha$  and the increase in variability of  $T$ . The inclusion of trait evolution (i.e. ME and MET) illustrates the swift in the evolution of tolerance to other species' traits ( $l$ ) in the presence of other species. Note isolated species in island C, with clearly lower final  $l$  than species present in the species rich islands A and B (Figure 50 J,K). Note that this tolerance is less pronounced when a trade-off between  $d$  and  $l$  exists. Furthermore, ME and MET simulations reveal a less abrupt decrease in niche width, though thermal range, compared to M0, as the latter only allows for species to escape competition in this form (i.e. no  $l$  or  $d$  evolution). In MET simulations, the trade-off deviates  $d$  evolution from a more neutral case, i.e. ME. Spatial patterns diverge among the models, with biodiversity hotspots shifting towards the center of the island - at this specific simulation (Figure 51 A,B,C) while the frequency of local extinctions consistently rises during periods of increased environmental variability (i.e. 2.5-0 Ma), impacting  $\alpha$  diversity but without any global extinction (Figure 51 G,H,I).

The described cycle is depicted at Figure 49, where a flowchart illustrates eco-evolutionary dynamics observed in M0, ME, and MET, which are relevant to biodiversity. All processes are strongly influenced by dispersal and landscape structure. Changes in diversity influence heterospecific competition. Subsequently, a transition occurs towards niche specialization, suggesting that species evolve to occupy specific ecological niches as they compete, such as a decrease in thermal range ( $\omega$ ). This specialization may lead to a reduction in species' geographical range (i.e. local extinctions). If global extinction happens, diversity is negatively impacted (red arrow Figure 49). Conversely, if extinction is averted, the flow progresses to isolation, suggesting that species may become isolated in particular habitats or environments.

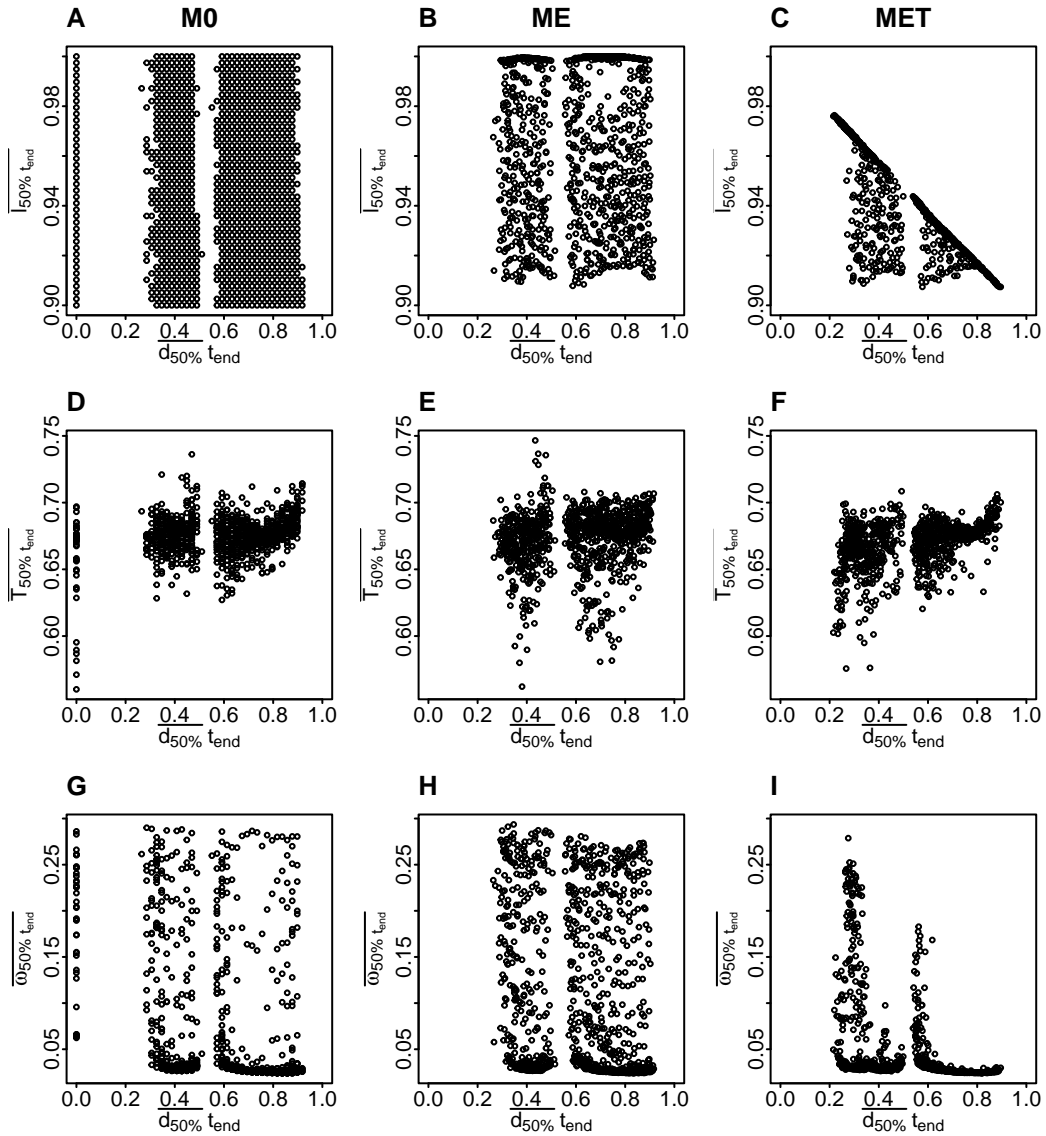


Figure 46: Final mean traits at last timestep are plotted against the mean trait changes. The mean trait is shown for tolerance to other species A-C, thermal optimum D-F, and thermal range G-I for Models MO, ME, and MET in each column.

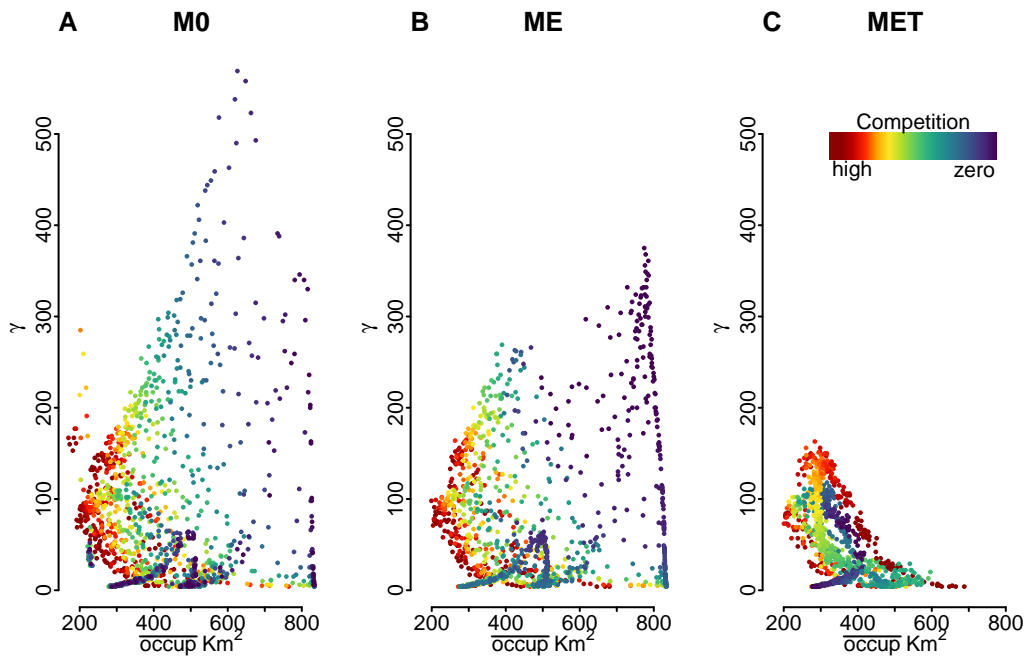


Figure 47: The theory of limiting similarity predicts that as species diversity increases, the average occupation decreases due to the need for coexisting species to be sufficiently different to coexist, resulting in lower occupation, as well as population sizes, when higher competition is present.

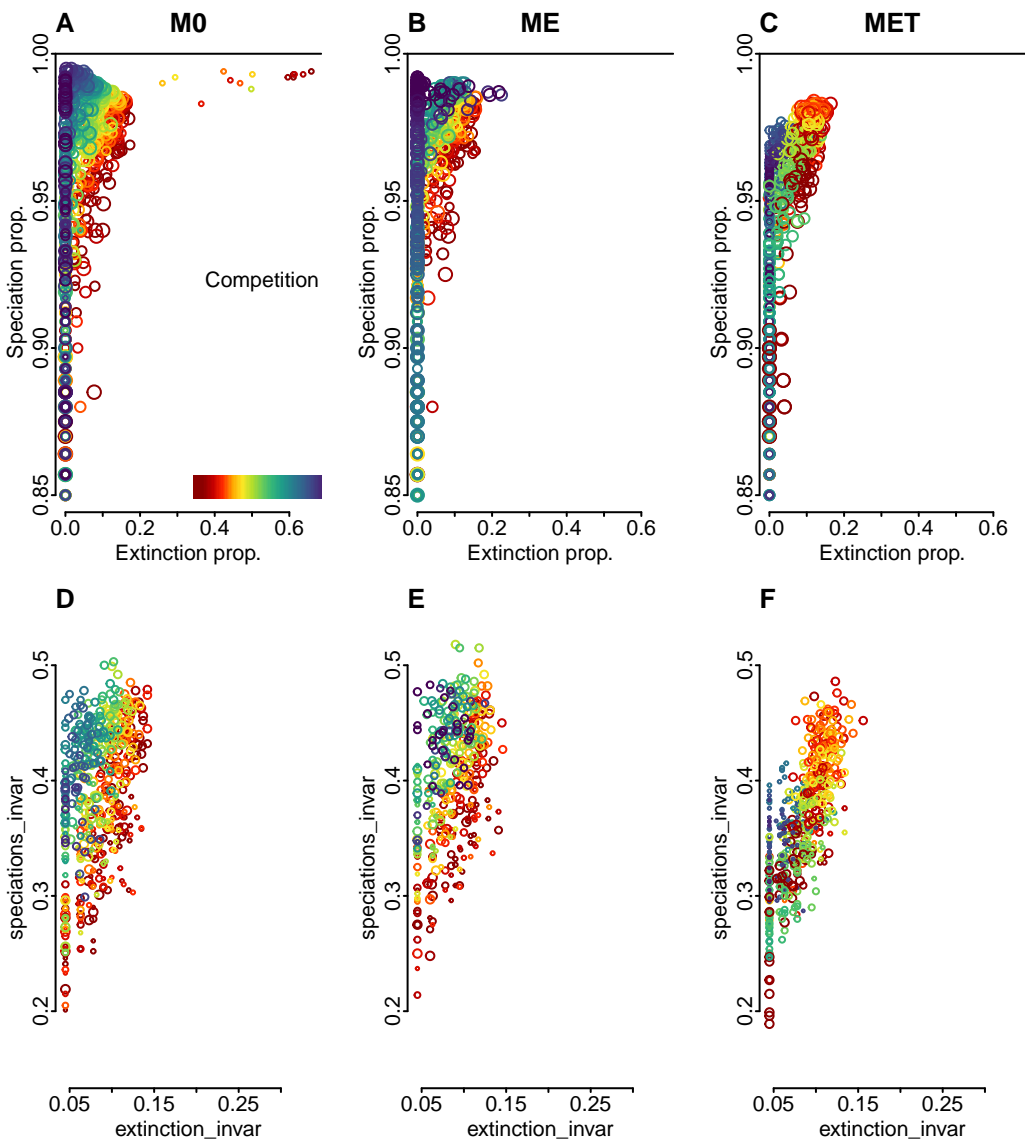


Figure 48: Speciation versus extinction percentage (A-C) and temporal invariability (i.e. temporal stability of macroevolutionary events) (D-F). Circles size are relative to mean dispersal trait at the final timestep. MET was the only model that show increased interspecific competition enhancing extinction and speciation.

From isolation, there arises potential for speciation through isolation fostering the emergence of new species (if they global extinction is avoided). If speciation unfolds, the flow completes a loop, contributing to diversity (blue arrow Figure 49). Overall, Figure 49 exemplifies the interconnectedness of ecological and evolutionary processes and the delicate balance between competition, niche specialization, geographical range changes, extinction, isolation, and speciation in shaping biodiversity dynamics. It highlights a cyclic pattern in a delicate balance where local extinction can stimulate renewed diversity.

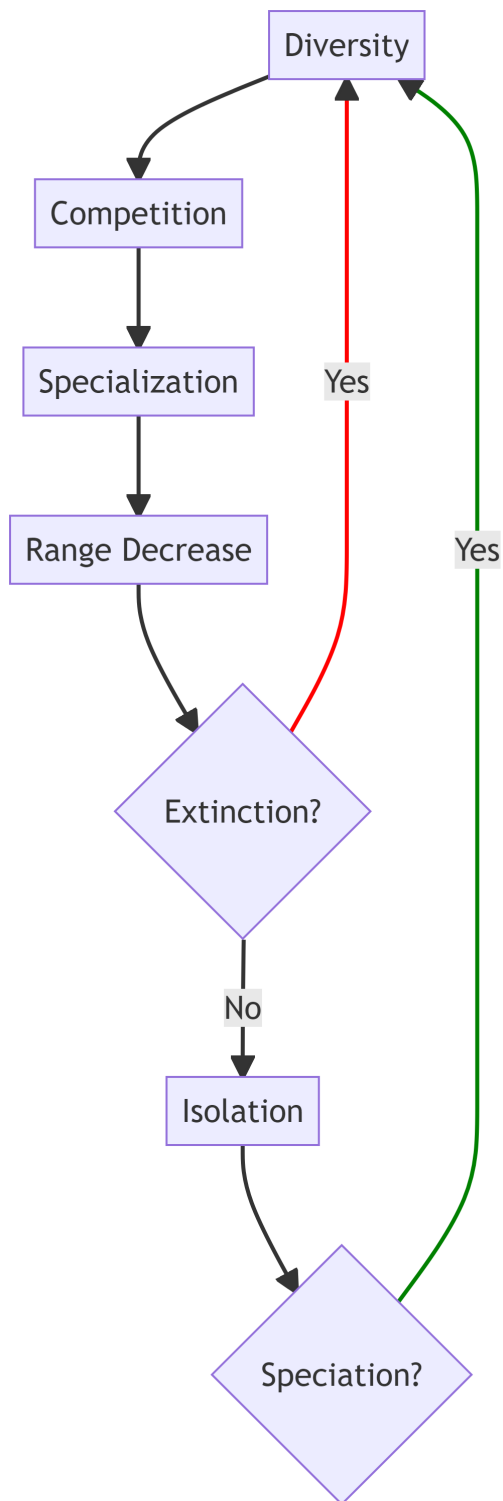


Figure 49: Flowchart of general eco-evolutionary dynamics in M0, ME, and MET, showing one simulated feedback loop relevant to biodiversity when competition is present and there is appropriate environmental structure and dispersal ability.

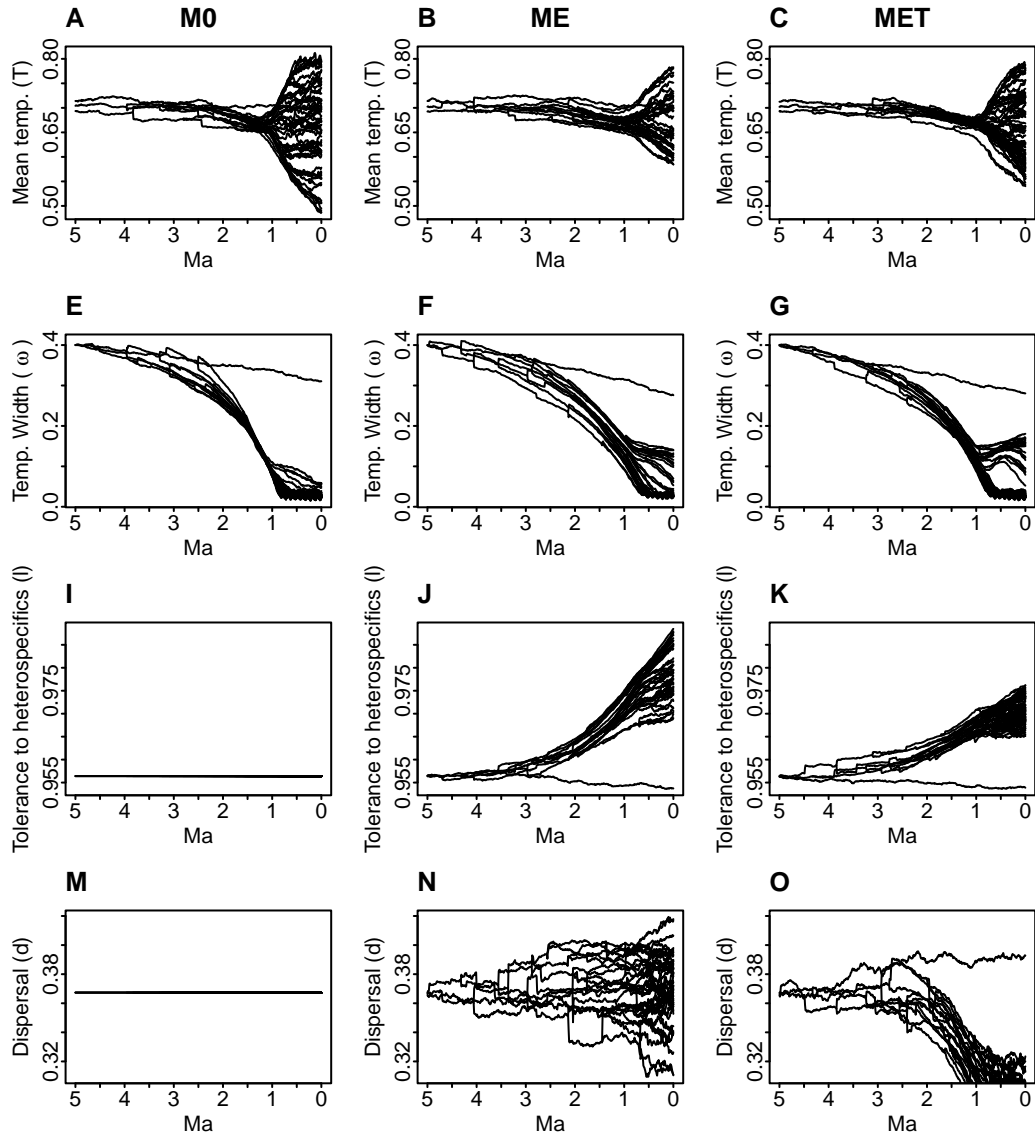


Figure 50: Trait change through time for a single simulation, i.e. config\_1119, with same initial parameters  $d=0.367$ ,  $l=0.956$  for M0, ME and MET, respectively with 63, 46 and 69 species alive at the final timestep.

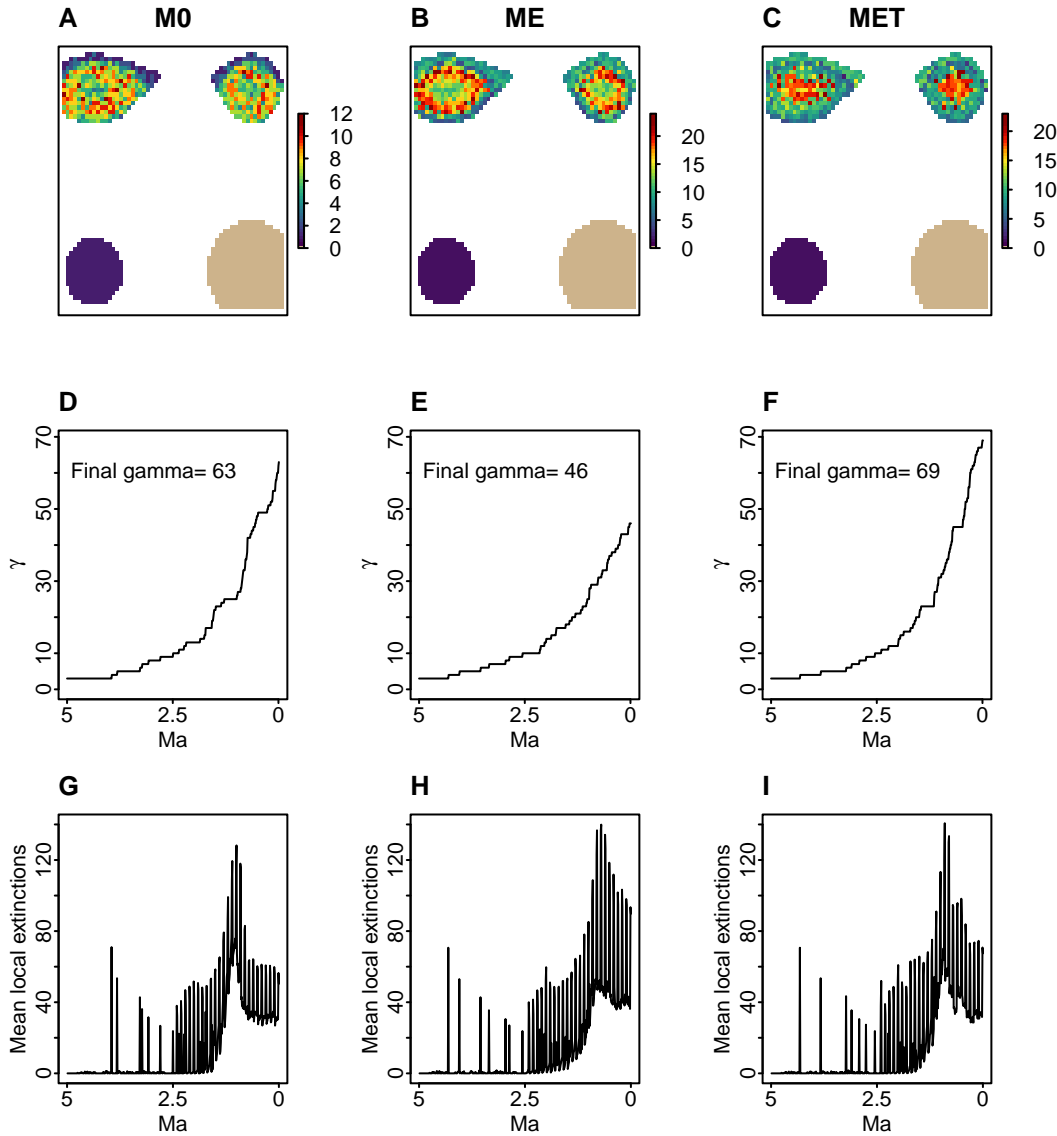


Figure 51: Trait change through time for a single simulation, with same initial parameters  $d=0.367$ ,  $l=0.956$  for ME and MET, respectively with 63, 46 and 69 species alive at the final timestep.

## References

- Bortolussi, N., E. Durand, M. Blum, and O. Francois. 2006. “apTreeshape: Statistical Analysis of Phylogenetic Tree Shape.” *Bioinformatics* 22 (3): 363–64. <https://doi.org/10.1093/bioinformatics/bti798>.
- Castiglione, Silvia, Carmela Serio, Martina Piccolo, Alessandro Mondanaro, Marina Melchionna, Mirko Di Febbraro, Gabriele Sansalone, Stephen Wroe, and Pasquale Raia. 2021. “The Influence of Domestication, Insularity and Sociality on the Tempo and Mode of Brain Size Evolution in Mammals.” *Biological Journal of the Linnean Society* 132 (1): 221–31. <https://doi.org/10.1093/biolinnean/blaa186>.
- Hagen, Oskar, Benjamin Flück, Fabian Fopp, Juliano S. Cabral, Florian Hartig, Mikael Pontarp, Thiago F. Rangel, and Loïc Pellissier. 2021. “Gen3sis: A General Engine for Eco-Evolutionary Simulations of the Processes That Shape Earth’s Biodiversity.” *PLoS Biology* 19 (7): e3001340. <https://doi.org/10.1371/journal.pbio.3001340>.
- Hoffmann, Ary A., and Carla M. Sgrò. 2011. “Climate Change and Evolutionary Adaptation.” *Nature* 470 (7335): 479–85. <https://doi.org/10.1038/nature09670>.
- Kembel, S. W., P. D. Cowan, M. R. Helmus, W. K. Cornwell, H. Morlon, D. D. Ackerly, S. P. Blomberg, and C. O. Webb. 2010. “Picante: R Tools for Integrating Phylogenies and Ecology.” *Bioinformatics* 26 (11): 1463–64. <https://doi.org/10.1093/bioinformatics/btq166>.
- Pillans, Brad, John Chappell, and Tim R. Naish. 1998. “A Review of the Milankovitch Climatic Beat: Template for Plio–Pleistocene Sea-Level Changes and Sequence Stratigraphy.” *Sedimentary Geology* 122 (1-4): 5–21. [https://doi.org/10.1016/S0037-0738\(98\)00095-5](https://doi.org/10.1016/S0037-0738(98)00095-5).
- Shepard, Christopher, Jon D. Pelletier, Marcel G. Schaap, and Craig Rasmussen. 2018. “Signatures of Obliquity and Eccentricity in Soil Chronosequences.” *Geophysical Research Letters* 45 (20): 11, 147–11, 153. <https://doi.org/10.1029/2018GL078583>.
- Vasconcelos, T. N. C., S. Alcantara, C. O. Andrino, F. Forest, M. Reginato, M. F. Simon, and J. R. Pirani. 2020. “Fast Diversification Through a Mosaic of Evolutionary Histories Characterizes the Endemic Flora of Ancient Neotropical Mountains.” *Proceedings of the Royal Society B: Biological Sciences* 287 (1923): 20192933. <https://doi.org/10.1098/rspb.2019.2933>.
- Westerhold, Thomas, Norbert Marwan, Anna Joy Drury, Diederik Liebrand, Claudia Agnini, Eleni Anagnostou, James S. K. Barnet, et al. 2020. “An Astronomically Dated Record of Earth’s Climate and Its Predictability over the Last 66 Million Years.” *Science* 369 (6509): 1383–87. <https://doi.org/10.1126/science.aba6853>.